

**Calcareous nannofossils in the S-Atlantic during the  
Middle to Late Miocene:**

**Coccolithophorid carbonate budgets, fine-fraction stable isotopes and their  
paleoceanographic implications**

**Dissertation**

**zur Erlangung des Doktorgrades der Naturwissenschaften**

**(Dr. rer. nat.)**

**am Fachbereich Geowissenschaften  
der Universität Bremen, Deutschland**

**Dissertation**

**Submitted for a degree of Doctor in Natural Sciences**

**(Dr. rer. nat.)**

**at the Department of Geosciences  
at Bremen University, Germany**

**Vorgelegt von**

**Regina Krammer, Dipl.Geol.**

**Bremen, 2005**

**Tag des Kolloquiums:**

**17. November 2005**

**Gutachter:**

1. Prof. Dr. R. Henrich
2. Prof. Dr. G. Bohrmann

**Prüfer:**

1. Prof. Dr. R. Rendle-Bühning
2. Prof. Dr. M. Schulz

---

...WENN ES NUR EINE EINZIGE WAHRHEIT GÄBE, KÖNNTE MAN  
NICHT HUNDERT BILDER ÜBER DASSELBE THEMA MALEN...

- PABLO PICASSO -



## General outline

This PhD thesis summarizes doctoral research, carried out between 2002 and 2005 at the Research Center Ocean Margins, University of Bremen, Germany. The central issue of the research deals with investigation of deep-sea sediments in the southeast Atlantic and its relation to climatic variations and associated changes in the paleoproductivity during the Middle to Late Miocene. The thesis opens with an introductory chapter (**chapter 1**), briefly reviewing climate conditions and paleoceanography in the Middle to Late Miocene, a description of coccolithophores, important carbonate producing haptophyte algae, with a focus on their ecology and biogeochemical importance. In addition to a short summary of previous studies, a brief description of methods that were applied to the samples is given. **Chapters 2-4** comprise three scientific papers of which I am a co-author. One paper is in press in an international peer-reviewed journal, one manuscript is submitted and one will be submitted soon. **Chapter 5** summarizes the results and provides perspectives for ongoing investigations.

To minimize duplication due to the organization of this thesis into a series of manuscripts, references have been removed from each paper and are cited in a single reference list at the end of this thesis (**Chapter 6**). My contribution to the individual manuscripts is as follows:

**Chapter 2.**                   **“Middle to Late Miocene fluctuations in the incipient Benguela Upwelling System revealed by calcareous nannofossil assemblages”**

**Authors:** Regina Krammer, Karl-Heinz Baumann, Rüdiger Henrich  
**Status:** in press           **Journal:** *Palaeogeography, Palaeoclimatology, Palaeoecology*

**Contribution:** sample preparation, analytical work (bulk geochemical measurements and SEM analysis), data processing, contribution to paleoceanographic interpretation, graphical presentation, and principal writing.

**Chapter 3.**                   **“ODP Site 1085 nannofossil assemblages and fine-fraction carbonate stable isotopes as indicators for Middle to Late Miocene Benguela Upwelling initiation”**

**Authors:** Regina Krammer, Karl-Heinz Baumann, Torsten Bickert, Rüdiger Henrich  
**Status:** submitted       **Journal:** *Marine Micropaleontology*

**Contribution:** sample preparation, analytical work, data processing, contribution to interpretation, graphical presentation, and principal writing.

**Chapter 4.**            **“Calcareous nannofossil assemblages and fine-fraction carbonate stable isotopes in the sub-Antarctic South Atlantic during the Middle to Late Miocene (ODP Site 1092)”**

**Authors:**            Regina Krammer, Karl-Heinz Baumann, Torsten Bickert, Rüdiger Henrich

**Status:**             in preparation

**Contribution:**     sample preparation, analytical work, data processing, contribution to interpretation, graphical presentation, and principal writing.

## Abstract

The Cenozoic is characterized by major changes in the global climate system from 'greenhouse' conditions in the Early Paleogene towards 'ice-house'-regime in the Neogene. The opening and closing of oceanic gateways and mountain uplift episodes are assumed to be the main factors inducing these global climate changes resulting in an intensification of circumpolar currents and thermal isolation of Antarctic waters from the subtropics. Repeated reductions of calcium carbonate contents, the so-called 'Carbonate Crash' events, characterize pelagic sediment sequences at the Middle to Late Miocene transition. Until today, little is known about the global variations in the carbonate sedimentation pattern during the transition from Middle to Late Miocene.

The main object of this study was to document and understand the role of coccolithophores as the main carbonate producers in relation to changes in ocean circulation and global climate during the Middle to Late Miocene. For this purpose ODP Sites 1085 (1713 m water depth), drilled on the continental margin off Namibia, and ODP Site 1092 (1974 m water depth), drilled on the northern slope of the Meteor Rise in the sub-Antarctic sector of the South Atlantic, were investigated. The distribution pattern of single coccolithophorid species, the nanoplankton assemblage composition and the preservation of coccoliths from the eastern South-Atlantic provided the basis for paleoceanographic studies. Additionally, the nanoplankton contribution to the bulk carbonate production as well as the stable isotopic composition of the coccolith carbonate were explored.

The data show that calcareous nannofossils constitute a significant part of the carbonate fraction throughout the investigated interval from 12.5 to 7.5 Ma at both sites. Many paleoceanographic signals are preserved in coccolithophorid assemblages, and thus, reflect spatial and temporal changes in surface-ocean circulation.

At Site 1085, highest numbers of nannofossils were observed during the intervals 9.9 to 9.7 Ma and 8.7 to 8.0 Ma. These elevated numbers of coccoliths may generally be linked to the initiation of the Benguela Upwelling system. The distribution patterns of *Reticulofenestra minuta* and *Reticulofenestra haqii*, two abundant species with opportunistic behaviour, also reflect the initiation of upwelling off SW-Africa at about 10 Ma. Diminished numbers of coccoliths during 9.6 to 9.0 Ma probably indicate time periods of weakened nannofossil productivity resulting in a decrease in nannofossil carbonate content. This decrease in calcareous nanoplankton productivity is one possible explanation for the 'Carbonate Crash' between 9.6 and 9.0 Ma. Therefore, a correlation between productivity in the initiated Benguela Upwelling and carbonate production by coccolithophores seems reasonable.

At Site 1092, analyses of calcareous nannofossils show a rise in productivity associated with changes in nutrient availability between 8.8 and 8.6 Ma, traceable in the distribution patterns of *Coccolithus pelagicus*, *R. haqii* and *R. minuta*.

Additionally, analyses on polyspecific nannofossil carbonate stable isotopes were performed to reconstruct environmental changes in surface waters and to discuss the question if changes in productivity were linked to changes in nannofossil carbonate contribution. The potential of nannofossil stable isotopes as indicators of conditions in the shallow mixed-layer was shown by comparing these records with those of co-existing planktic foraminifers. Based on the data set of Site 1085, nannofossil carbonate isotopes reflect surface-water hydrographic conditions of the late winter-early spring period when relatively cool, nutrient-rich subsurface water mass is entrained into surface waters by vertical mixing. In contrast, foraminiferal isotopes reflect the post-deep-mixing, relatively warmer (late spring to fall) stratified water masses. This seasonality effect on plankton production offers the possibility to quantify paleoseasonality in the investigated region. The data imply that seasonality became weaker at Site 1085 during 10.4 to 9.1 Ma, corresponding well with the initiation of the Benguela Upwelling system at about 10 Ma. At Site 1092, located on the Meteor Rise in the sub-Antarctic South Atlantic, the difference between coccolithophorid and foraminiferal isotopic records is smaller, compared to Site 1085. It seems possible, that paleoseasonality was not the dominating factor in this study area.

This study shows, that coccolithophores provide important paleoenvironmental informations. They are a useful tool to reconstruct paleoproductivity and changing surface-water conditions in the eastern South Atlantic during the Middle to Late Miocene.

## Zusammenfassung

Das Känozoikum ist charakterisiert durch wesentliche Änderungen im globalem Klimasystem von Treibhaus-Bedingungen im frühen Paläozän hin zu einem 'Kühlhaus'-ähnlichen System im Neogen. Sowohl die Öffnung und Schließung von Meereszugängen als auch Gebirgsbildungsereignisse gelten als Hauptfaktoren, die Änderungen im globalen Klima hervorriefen. Diese wiederum resultierten in einer Intensivierung der zirkumpolaren Strömungen und der thermalen Isolation von antarktischen Wassermassen. Wiederholte Zusammenbrüche im Karbonatgehalt, die sogenannten ‚Carbonate-Crash‘-Ereignisse, charakterisieren mittlere bis spätmiozäne Ablagerungen im pelagischen Ozean. Bis heute ist nur sehr wenig bekannt über die globalen Variationen in der Karbonatsedimentation während der Übergangsphase vom mittleren bis späten Miozän.

Hauptziel dieser Studie war das Verständnis und die Dokumentation der Rolle von Coccolithophoriden als Hauptproduzenten von biogenem Karbonat in Bezug auf die Änderungen in der Ozeanzirkulation und im globalen Klima während dieser Zeit. Zu diesem Zweck wurden Sedimente von den ODP Bohrkernen 1085 (in 1713 m Wassertiefe), am Kontinentalrand vor Namibia, und 1092 (in 1974 m Wassertiefe), am Nordrand des Meteorrückens im sub-antarktischen Bereich des Atlantiks, untersucht. Die Verbreitungsmuster von einzelnen Coccolithophoriden-Arten, die Nannoplankton-Vergesellschaftung und die Erhaltungszustände von Coccolithen aus dem Untersuchungsgebiet im östlichen Südatlantik dienten als Grundlage für paläo-ozeanografische Studien. Zusätzlich wurde der Beitrag der Coccolithophoriden an der Gesamtkarbonat-Produktion ermittelt, und die Zusammensetzung der stabilen Isotopen im Coccolithenkarbonat untersucht.

Die Daten zeigen, dass kalkiges Nannoplankton einen wichtigen Anteil der Karbonatfraktion während des gesamten Untersuchungszeitraumes (12.5 bis 7.5 Millionen Jahre vor heute) an beiden Lokationen ausmacht. Viele paläo-ozeanografische Signale sind in der Coccolithen-Zusammensetzung erhalten und ermöglichen somit eine Rekonstruktion der zeitlichen und räumlichen Veränderungen in der Oberflächen-Zirkulation.

In den Ablagerungen von Kern 1085 weisen höchste Nannofossilzahlen in den Intervallen 9.9 bis 9.7 Ma und 8.7 bis 8.0 Ma auf den Beginn des Benguela-Auftriebssystem hin. Das Verbreitungsmuster von *Reticulofenestra minuta* und *Reticulofenestra haqii*, zwei sehr häufig vorkommenden opportunistischen Arten, spiegelt ebenfalls das Einsetzen des Auftriebsgebietes vor SW-Afrika wider. Zurückgehende Zahlen von Coccolithen während des Intervalls von 9.6 bis 9.0 Ma kennzeichnen möglicherweise Perioden von eingeschränkter

Nannoplankton-Produktivität, die in einer Abnahme des nannofossilen Karbonatgehaltes resultieren. Dieser Rückgang in der Nannoplankton-Produktivität ist eine mögliche Erklärung für den Einbruch im Gesamtkarbonatgehaltes während des ‚Carbonate Crash‘-Ereignisses zwischen 9.6 und 9.0 Ma. Daraus folgernd scheint eine Korrelation zwischen Produktivität im beginnenden Benguela-Auftriebssystem und der Karbonatproduktion über Coccolithophoriden möglich.

In den Sedimenten von Bohrkern 1092 weisen Analysen of kalkigen Nannofossilien auf einen Anstieg in der Produktivität in Verbindung mit einer Änderung in der Nährstoffverfügbarkeit zwischen 8.8 und 8.6 Ma hin. Dies ist auch in den Verbreitungsmustern der Arten *Coccolithus pelagicus*, *R. haqii* und *R. minuta* nachvollziehbar.

Zusätzlich zu den mikropaläontologischen Untersuchungen wurde auch die Zusammensetzung der stabilen Isotopen am Nannoplankton-Karbonat analysiert, um Umweltänderungen im Oberflächenwasser zu rekonstruieren. Weiters sollte die Frage geklärt werden, ob Veränderungen in der Produktivität mit Wechsel in der Nannoplankton-Karbonat-Produktion zusammenhängen. Das Potential der stabilen Isotopen von Nannoplankton als Anzeiger für Bedingungen im Oberflächenwasser wurde anhand eines Vergleichs von Isotopendaten von Coccolithen und Foraminiferen aufgezeigt. Der Datensatz von ODP Kern 1085 zeigt, dass Isotopen von Coccolithen Oberflächenwasser-Bedingungen der späten Winter/frühen Frühlingsphase widerspiegeln, wenn relativ kühles, nährstoffreiches Wasser durch vertikales Mischen an die Oberfläche gelangt. Im Gegensatz dazu zeigen die Isotopenwerte von Foraminiferen eine spätere Phase (später Frühling bis Herbst) mit wärmerem Wasser in einer stratifizierten Wassersäule an. Dieser Saisonalitätseffekt in der Planktonproduktion ermöglicht eine Abschätzung und Rekonstruktion von Paläo-Saisonalität in der untersuchten Region. Die Daten zeigen eine Abschwächung dieser Saisonalität bei 1085 zwischen 10.4 und 9.1 Ma, was sehr gut mit dem Einsetzen des Benguela Auftriebssystems bei ca. 10 Ma korrespondiert. In den Sedimenten von 1092 ist der Unterschied zwischen Coccolithen- und Foraminiferenisotopen wesentlich geringer im Vergleich zu 1085. Es erscheint daher plausibel, dass Paläo-Saisonalität nicht den dominierenden Faktor in dieser Region darstellte.

Diese Studie zeigt, dass Coccolithophoriden wichtige Informationen über die Paläo-Umwelt liefern können. Sie stellen ein nützliches Werkzeug dar, um Paläo-Produktivität und Änderungen in den Bedingungen des Oberflächenwassers im östlichen Südatlantiks während des mittleren bis späten Miozäns zu rekonstruieren.

## Table of contents

<b>1.</b>	<b>Introduction</b>	<b>1</b>
1.1	Climate and Paleoceanography in the Miocene	1
1.2	Marine biota and the global biogeochemical cycles	4
1.3	Coccolithophore biology, ecology and their fossil record	7
1.3.1	Coccolith production	10
1.3.2	Function of coccoliths	11
1.4	Coccolithophorid-based geochemical proxies	12
1.4.1	Stable isotopes in coccolith calcite	12
1.5	Objectives of the study	13
1.5.1	Methods	15
<b>2.</b>	<b>Middle to Late Miocene fluctuations in the incipient Benguela</b>	
	<b>Upwelling System revealed by calcareous nannofossil assemblages</b>	<b>17</b>
2.1	Introduction	18
2.2	Regional setting and Oceanography	19
2.2.1	Modern oceanographic setting	19
2.2.2	The Benguela upwelling system since the Middle Miocene	20
2.3	Material and methods	21
2.3.1	Background of Site 1085	21
2.3.2	Samples and analysis	21
2.3.3	Quantification of calcareous nannofossils and its carbonate content	22
2.3.4	Stratigraphy	23
2.4	Results	25
2.4.1	Absolute numbers and relative abundances of calcareous nannofossils	25
2.4.2	Bulk sediment parameters, nannofossil carbonate and preservation	27
2.5	Discussion	30
2.5.1	Abundances and fluctuations in the calcareous nannofossil species record	30
2.5.2	Variations in productivity and palaeoceanographic implications for the Benguela system based on nannofossil carbonate estimates	31
2.6	Conclusion	34

<b>3.</b>	<b>ODP Site 1085 nannofossil assemblages and fine-fraction carbonate stable isotopes as indicators for Middle to Late Miocene Benguela Upwelling initiation</b>	<b>37</b>
3.1	Introduction	38
3.2	Material and methods	39
	3.2.1 Study area	39
	3.2.2 Sediment treatment	40
3.3	Results	42
3.4	Discussion	44
	3.4.1 Origin of interspecific isotopic variation in calcareous nannofossil carbonate	46
	3.4.2 Comparison of fine-fraction and foraminiferal stable isotopic records	47
	3.4.3 Comparison to fine-fraction isotope records of other sites	53
3.5	Conclusion	54
<b>4.</b>	<b>Calcareous nannofossil assemblages and fine-fraction carbonate stable isotopes in the sub-Antarctic South Atlantic during the Middle to Late Miocene (ODP Site 1092)</b>	<b>57</b>
4.1	Introduction	58
4.2	Material and methods	59
	4.2.1 Study area	59
	4.2.2 Sediment treatment	62
4.3	Results	62
	4.3.1 Absolute numbers of calcareous nannofossils and coccolith carbonate	62
	4.3.2 Stable isotopic record of fraction < 20 µm	63
4.4	Discussion	66
	4.4.1 Calcareous nannofossils and their paleoceanographic implications	66
	4.4.2 Fine-fraction stable isotopes	67
4.5	Conclusion	71
<b>5.</b>	<b>Conclusion and Perspectives</b>	<b>75</b>
<b>6.</b>	<b>References</b>	<b>77</b>
<b>7.</b>	<b>Acknowledgements</b>	<b>93</b>

# **Chapter 1**

## **Introduction**



## 1. Introduction

### 1.1 Climate and Paleoclimatology in the Miocene

The Cenozoic is characterized by a major change in global climate system from early Paleogene 'greenhouse' conditions towards the Neogene 'ice-house' regime, as inferred from globally compiled deep-sea foraminiferal oxygen isotope records (Fig. 1.1). The Middle Miocene (15 - 11 Ma) (Miller et al., 1987; Zachos et al., 2001) includes one of three major Cenozoic oxygen isotope shifts, generally interpreted to indicate the major expansion and permanent establishment of the East Antarctic Ice Sheet accompanied by some effect of deepwater cooling (Woodruff and Savin, 1989; Wright et al., 1992; Wright and Miller, 1996; Flower and Kennett, 1993, 1995). A combination of changes in atmospheric carbon dioxide concentration (Berner, 1994) and oceanic heat transport (D'Hondt and Arthur, 1996) in cause of horizontal and vertical tectonic movements like opening or closing of oceanic gateways and mountain uplift episodes are assumed to be main factors inducing these global climate changes. For example, the opening of the Tasmanian Gateway at about 30 Ma (Kennett et al al., 1974, 1975) and the Drake Passage at 29 Ma (Lawver and Gahagan, 2003) and the resulting intensification of circumpolar currents and thermal isolation of Antarctic waters from the subtropics have been invoked as a primary driving factor for the Cenozoic cooling and accumulation of ice on Antarctica (Barker and Burrell, 1977; Kennett, 1977). Although the Drake Passage is thought to have opened initially in the Oligocene (Lawver and Gahagan, 1998, 2003), Pagani et al. (2000) postulated that the initiation of unrestricted eastward flow across the Passage and strengthening of the Antarctic circumpolar current (ACC) occurred at ~15-14.5 Ma. Another major element, the glaciation of the northern hemisphere, plays an important role in the evolution of the global Cenozoic climate. Clark (1982) proposed that the Arctic Ocean has been permanently ice-covered since the beginning of the Late Miocene or even earlier (Wolf and Tiede, 1991). Wolf and Thiede (1991) established the Middle to Late Miocene onset of glaciation on Greenland. Data of ODP legs 151 and 162 demonstrated occurrences of glacial derived IRD in the Middle Miocene in the Nordic Sea (Thiede et al., 1998). In the Fram Strait, IRD can be dated to around 14 Ma (Wolf-Welling et al., 1996). IRD records from both the Iceland and Vøring plateaux suggest a significant intensification of glaciation at about 7.1 Ma, which reflects the onset of middle-sized glaciation in the northern hemisphere (Jansen and Sjøholm, 1991; Larsen et al., 1994; Fronval and Jansen, 1996). Finally, the closure of the Central American Seaway is considered to trigger the last cooling step in the Cenozoic climate change due to the intensification of the Gulf Stream which

introduced warm and saline waters to high northern latitudes favouring early Pliocene glaciation of the northern continents (Jansen and Sjøholm, 1991; Haug and Tiedemann, 1998).

The Miocene was a period of geochemical reorganization of the world ocean. At the end of the Middle Miocene cooling step a strong basin-to-basin asymmetry developed between North Atlantic and North Pacific, with the deep Atlantic collecting carbonate, while the accumulation of silica shifted to the North Pacific ('silica switch', Keller and Barron, 1983; Cortese et al., 2004). This large-scale geochemical change led to a major reorganization in the deep circulation of the ocean (Woodruff and Savin, 1989) and is proposed to assign the beginning of the modern ocean thermohaline circulation (e.g., Berger and Wefer, 1996).

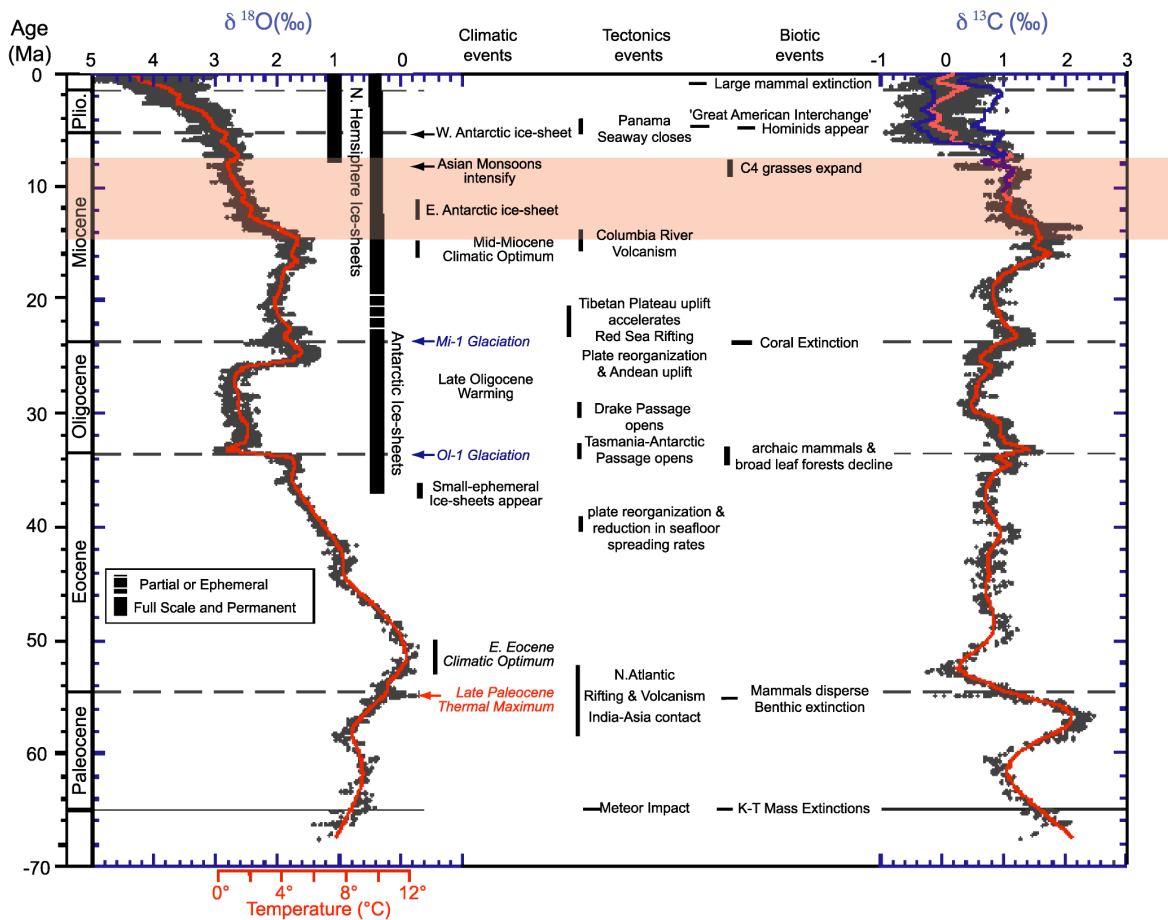


Fig. 1.1. Global deep-sea oxygen and carbon isotope record from the Paleocene to Holocene with some key tectonic and biotic events (from Zachos et al., 2001). With the carbon isotope record, separate curve fits were derived for the Atlantic (red) and Pacific (blue) above the Middle Miocene to illustrate the increase in basin-to-basin fractionation. The light red box indicates the time interval of this study.

At the transition from Middle to Late Miocene major changes in carbonate sedimentation in the eastern Equatorial Pacific (Lyle et al., 1995), western Equatorial Atlantic (King et al., 1997) and Caribbean Sea (Roth et al., 2000) occurred. These events, entitled the Miocene 'Carbonate Crash' (Lyle et al. 1995), have been ascribed to a drastic shoaling of the lysocline in the eastern Equatorial Pacific. These events have also been described in the southeast

Atlantic Ocean (e.g., Diester-Haass et al., 2004). The authors proposed an increase in the delivery of lithogenic matter from the Oranje River as principal cause of the 'Carbonate Crash' off southwest Africa since no clear evidence for carbonate dissolution was found.

Beside dilution and/or dissolution, the carbonate sedimentation is also influenced by changes in the ocean productivity. The efficiency of productivity in the ocean is linked to the advection of nutrient-rich water masses, whose distribution in the ocean is controlled by wind intensity and thermohaline circulation. For the Neogene, changes in the extent and intensity of productivity, as well as the type of production (changes from opal to carbonate) have been described in high-productivity areas such as the coastal upwelling off California (Lyle et al., 2000). These changes are considered to be related to the development of thermohaline circulation during the Miocene. The opening of the Drake Passage, first as a shallow, then later as a deep-water throughway, and the resulting formation of the Antarctic Circumpolar Current, are considered to be critical in the formation and spread of a cold, nutrient-rich Antarctic Intermediate Water (AAIW) (Pagani et al., 2000). The presence of AAIW below the warm Atlantic surface water is a prerequisite for the formation of gradients in the upper water column - such as the thermocline - that are necessary for the creation of high-productivity cells on the coasts or at oceanic fronts. The begin of upwelling off Namibia at about 10 Ma has been attributed to major influx of cold waters linked to ice-sheet expansion on Antarctica (Siesser, 1980; Diester-Haass et al., 1992). The aridification in southern Africa, as documented by Diekmann et al. (2003) at around 10 Ma, is nearly coincident with the first establishment of the trade-wind driven Benguela Upwelling system, probably as a consequence of the northward movement of the Intertropical Convergence Zone (Hay and Brock, 1992).

Therefore, the Middle Miocene cooling trend caused many major changes in the global climate system such as the invigoration of surface ocean circulation systems, the intensification of gyral circulation and increases in the strength of oceanic fronts (e.g., Kennett, 1977). Moreover, it has been suggested that the growth of the Antarctic ice-sheet changed the atmospheric circulation pattern driving ocean currents and upwelling (Hay and Brock, 1992). Further evidence for major changes in atmospheric circulation linked to ice-sheet expansion is documented by enhanced aridity in the Asian interior and the onset of the Indian and east Asian monsoons, about 9 - 8 Ma ago (Zhisheng et al., 2001). Generally, continental climates underwent major changes in the Middle Miocene. Increased aridity is inferred at this time for mid-latitude continental regions including Australia, Africa, North America and South America, and may have fostered the development of grasses and the consequent evolution of grassland adapted biota (Flower and Kennett, 1994).

## 1.2 Marine biota and the global biogeochemical cycles

The climate of the earth has undergone major changes over geologic time-scales driven by a complex interaction of tectonic processes, orbital parameters, changes in the strength of the sun, and internal response and feedback mechanisms. Since a possible greenhouse warming by increased release of carbon dioxide (CO<sub>2</sub>) by combustion of fossil fuels was proposed, the global carbon cycle is one of the most important topics in environmental sciences. For geologists this topic became even more relevant, because a close relation between atmospheric CO<sub>2</sub> contents and global temperature was detected in ice cores from Antarctica and Greenland (e.g., Barnola et al., 1987; Petit et al., 1999).

The oceans have played an important role in atmospheric changes due to their capability to store large amounts of heat and CO<sub>2</sub> (Fig. 1.2). Variations in glacial to interglacial CO<sub>2</sub> records seem to be coupled to changes in carbon exchange rates within the ocean (Broecker and Peng, 1986). Lower glacial CO<sub>2</sub> values appear to be tied to an enhanced transfer of carbon from the surface waters to the deep ocean by higher rates of photosynthesis and biological productivity ('biological pump', Berger et al., 1987). The cycle of organic carbon is of particular importance in this regard. The cycle of carbon in its inorganic, calcium carbonate (CaCO<sub>3</sub>) form also affects atmospheric CO<sub>2</sub>. It also plays an important role in regulating ocean chemistry and pH – a major factor in the viability of calcareous marine organisms. Although CaCO<sub>3</sub> precipitation occurs as cements and coatings in the marine environment, it is primarily associated with the activities of living organisms, such as corals, benthic shelly animals, plankton species such as coccolithophores and foraminifers, and pteropods, and where it takes place under direct metabolic control. Coccolithophores and planktic foraminifers form the largest part of the pelagic carbonate production, with lesser contribution due to pteropods and calcareous dinoflagellates (Milliman, 1993). The advent of carbonate biomineralization occurred around the time of the Precambrian – Cambrian boundary (Wood et al., 2002) when evolutionary innovation conferred on organisms the ability to precipitate carbonate structures. A second major development took place several hundred millions years later, with the Mesozoic proliferation of planktic calcifiers (Roth, 1987; Degens, 1989; Martin, 1995) and the establishment of the modern mode of carbonate cycling. Although benthic foraminifers and other bottom-dweller calcifiers evolved early in the Phanerozoic, it is not until the Mesozoic that a marked proliferation in coccolithophorid and planktic foraminiferal diversity and abundance is observed (Martin, 1995; Hart, 2003). At the Jurassic/Cretaceous boundary the first occurrence of nannofossil-generated pelagic carbonates were recorded, based on a switch from radiolaria-dominated siliceous sediments to nannofossil-dominated carbonates in the western Tethys (Baumgartner, 1987). Roth (1987)

proposed that nannoplankton originated in shelf environments and migrated later into oceanic habitats. This evolution of pelagic calcareous nannoplankton and planktic foraminifers in the Mesozoic caused a shift in global calcification from the continental shelves toward deeper oceans. This shift affected deep-ocean carbonate budgets, calcite compensation depths (CCDs), and geological carbonate turnover rates (Kennett, 1982; Bown, 1998). Zeebe and Westbroek (2003) conceptualised three distinct modes of marine carbonate cycles. (A) The geochemistry-ruled Precambrian mode of  $\text{CaCO}_3$  cycling resembles a carbonate ocean, in which biogenic precipitation of  $\text{CaCO}_3$  is essentially absent (called ‘Strangelove’-ocean). It is characterized by high-supersaturation and generally inorganic formation of carbonates. (B) Following the advent of biomineralization in the Cambrian, biologically controlled carbonate precipitation in shallow-water (neritic) environments became significant (the ‘Neritan’ ocean). (C) The Mesozoic shift towards widespread pelagic biomineralization finally led to a significant stabilization of the marine  $\text{CaCO}_3$  saturation state, termed the ‘Cretan’ ocean.

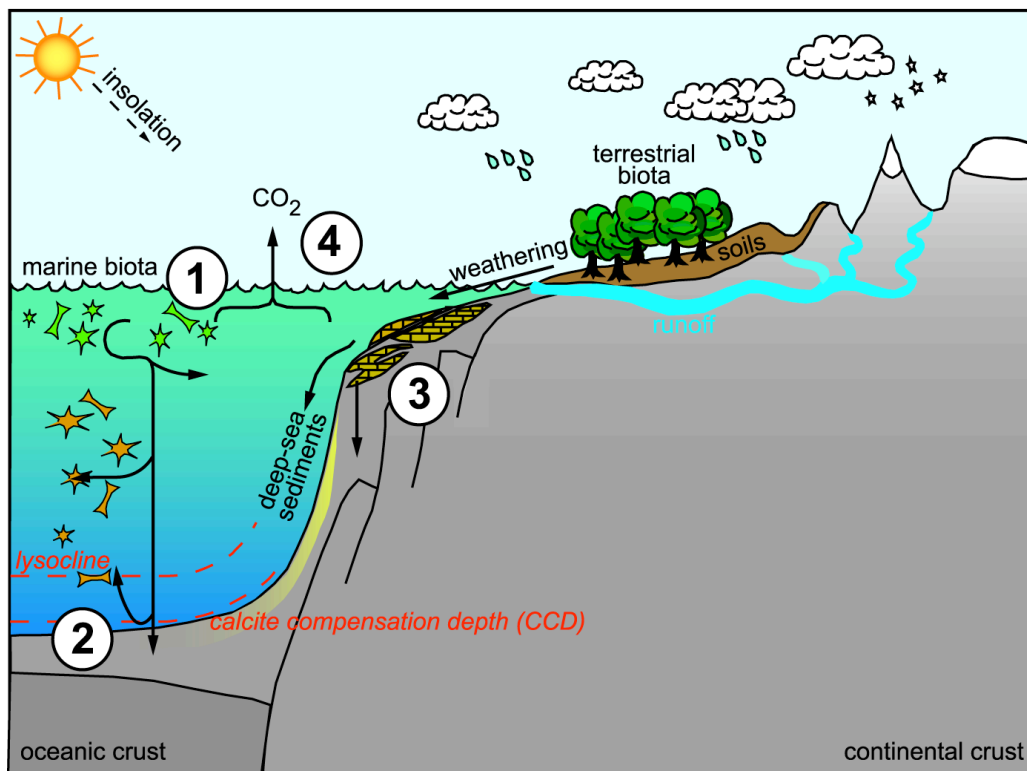
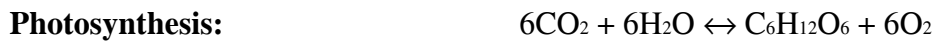


Fig. 1.2. The global biogeochemical cycling of calcium carbonate. #1. Precipitation of calcite and aragonite by coccolithophores, foraminifers, and pteropods in the open ocean. #2. Carbonate reaching deep-sea sediments will dissolve during early diagenesis, if the bottom water is under-saturated and/or the organic matter flux to the sediments is sufficiently high. #3. Precipitation of  $\text{CaCO}_3$  by corals and shelly animals, with a significant fraction as the aragonite polymorph and high-Mg calcite. #4. Precipitation of  $\text{CaCO}_3$  results in higher  $p\text{CO}_2$  at the surface, driving a net transfer of  $\text{CO}_2$  from the ocean to the atmosphere (modified from Ridgwell and Zeebe, 2005).

In this ‘Cretan’ ocean, the CaCO<sub>3</sub> production is entirely biologically controlled and to a large degree independent of the external supersaturation. Because in this ocean CaCO<sub>3</sub> production occurs in the open ocean, deep-sea accumulation and dissolution comes into play. The protagonists of this ‘Cretan’ ocean are CaCO<sub>3</sub> producing organisms such as planktic foraminifers and coccolithophores.

Coccolithophores play an important role in earth’s biogeochemical cycles, due to their great abundance, fast turnover rates, and their ability to carry out photosynthesis and calcification (Winter and Siesser, 1994; Bown, 1998). Coccolithophores may be small in size, but they occur in huge numbers in the surface layers of the oceans, sometimes in blooms with cell densities larger than a million cells per liter. These blooms can be traced even from satellites. It is obvious, the high reflectance in blooms of this size significantly alter the ocean albedo and reduce the capacity of the oceans to receive energy from solar radiation. The balance, that distinguish if coccolithophores, and especially the large blooms they form, act as a source or sink for atmospheric CO<sub>2</sub> is the ratio between calcification and photosynthesis.

The chemical reactions involved in the carbon and carbonate cycle are outlined in Fig. 1.3.



It is still accepted, that calcification of marine organisms act as a major source for CO<sub>2</sub>. Therefore all calcification by marine organisms is called the ‘carbonate pump’, that counteracts the ‘biological pump’ in which all organisms are combined that draw down CO<sub>2</sub> from the atmosphere by converting it during photosynthesis into organic matter. The assumption, that calcification is a source for CO<sub>2</sub>, is based on equations for inorganic carbonate precipitation, and might not be true for coccolithophores. Calcification and photosynthesis occur intracellular in coccolithophores, and theoretically it seems possible, that coccolithophore possess the ability, to supply their own CO<sub>2</sub> for photosynthesis via calcification. The aspect of an intracellular source of CO<sub>2</sub> for photosynthesis is of special interest, because several studies have shown, that phytoplankton growth can be limited by the availability of dissolved CO<sub>2</sub> in seawater (Raven, 1993; Riebesell et al., 1993). This effect especially controls organic and siliceous phytoplankton. Coccolithophores can detour this

limitation by producing their own CO<sub>2</sub> via bicarbonate consumption during calcification. Bicarbonate is the predominant form of dissolved CO<sub>2</sub> in seawater and therefore seems not to be limited at all. However, Nimer et al. (1997) have shown in culture studies, that coccolithophores might only use their intracellular CO<sub>2</sub> source under very limiting CO<sub>2</sub> conditions. In contrast, Rost and Riebesell (2004) have shown in a recent work, that calcification in coccolithophores appears not to be a prerequisite for efficient photosynthesis. Non-calcifying cells can photosynthesise as efficiently as, or even more efficiently than calcifying ones (Rost and Riebesell, 2004). Measurements of stable carbon isotope discrimination also indicate that *Emiliana huxleyi* can accumulate inorganic carbon but that calcification is not used directly to supply photosynthesis with carbon (Rost et al., 2002).

Beside organic and inorganic carbon, coccolithophores produce a third important compound. The emission of dimethyl sulphonioacetate (DMSP), a metabolic product, is also influencing the light reflectance. If converted into dimethyl sulphide (DMS), it promotes cloud condensation. Therefore, coccolithophores and cloud formation seem to be linked, in particular when a lot of DMS is released over a coccolithophorid bloom area (Westbroek et al., 1993).

Research on coccolithophores may increase our understanding of ocean and climate history. Based on the research of present-day processes, careful investigation of ancient oceans may lead to a better understanding of the past which in turn provides important clues to future scenarios.

### **1.3 Coccolithophore biology, ecology and their fossil record**

Coccolithophores are one of the main open-ocean carbonate producers. These marine, unicellular, flagellate algae belong to the class *Prymnesiophyceae* (Edwardsen et al., 2000) which also features non-calcifying organisms. Due to the possession of an exo-skeleton (coccosphere) composed of minute calcitic plates, the coccoliths, coccolithophores account for a major part of the fine-grained, pelagic sediments. These calcified remains are often referred to as calcareous nannofossils. Since the first appearance of these organisms in Late Triassic sediments (Di Nocera and Scandone, 1977; Jafar, 1983; Bralower et al., 1991), their geological record has been remarkably abundant and continuous. Beside their biostratigraphic importance, coccolithophores play a major role in unravelling paleoceanographic questions. They form a substantial component of the oceanic phytoplankton, and their remains in sediments reflect the physical and chemical characteristics of overlying water masses (summarised in Roth, 1994). Coccoliths records have been utilised as proxy indicators to reconstruct paleoenvironmental conditions.

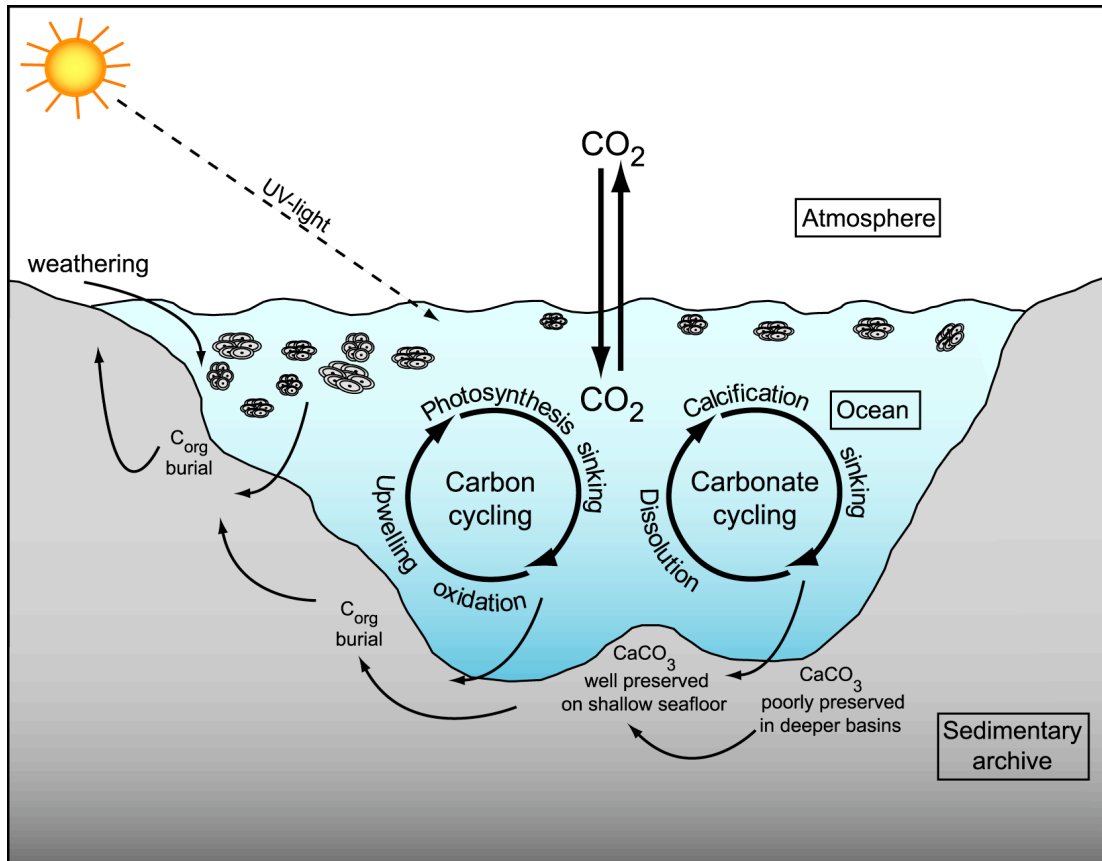


Fig.1.3. Schematic representation of the complex role of coccolithophores within the carbon cycle, modified from Baumann et al. (2004).

The position and fluctuations of frontal and current systems have been revealed in a number of studies (e.g., McIntyre et al., 1972; Okada and Wells, 1997; Flores et al., 1999; Findlay and Flores, 2000; Findlay and Giraudeau, 2002). Single species or the ratio between species groups have been applied to monitor variations in surface water productivity or nutri- and thermocline dynamics (e.g. Molino and McIntyre, 1990; Jordan et al., 1996; Kinkel et al., 2000; Baumann and Freitag, 2004).

Coccolithophores generally live in the photic zone where light levels are strong enough to carry out photosynthesis. Additionally, the horizontal and vertical distribution of coccolithophores is controlled by latitude, ocean currents, water masses along with their characteristic nutrient, salinity and temperature profiles, trace elements, and vitamins (Winter et al., 1994). A certain temperature dependence of coccolithophores has been noticed early and a rough biogeographic zonation scheme was set up by McIntyre and Bé (1967). The distribution of coccolithophores follows broad latitudinal belts or zones basically separated by frontal systems (Winter et al., 1994). These zonal boundaries are highly dynamic, seasonally variable and characterized by a specific species assemblage. The particular environments are dominated by characteristic assemblages which can be distinguished by their coccolith types

and coccosphere morphology (Young, 1994). Placolith-bearing species seem to be characteristic for upwelling areas (equatorial divergence and coastal upwelling) and high-latitudes. They include *Emiliana huxleyi*, *Gephyrocapsa* spp., *Reticulofenestra* spp., and *Umbellosphaera* spp. Their coccoliths are composed of a proximal and a distal shield joined by a central column. Umbelliform assemblages, composed of *Umbellosphaera* spp. and *Discosphaera tubifera*, bear coccoliths with large processes which flare distally to produce a double-layered coccospheres. They dominate oligotrophic mid-ocean environments. The floriform species form coccospheres with a dense asymmetrical mass of coccoliths surrounding a much smaller cell. These forms mainly characterize the deep photic zone assemblage in a stable water column of low- to mid-latitudes.

There are indications that temperature is not the only controlling factor for the biogeographic distribution of coccolithophores, most clearly demonstrated by the broad temperature range (1-31°C) that is tolerated by *Emiliana huxleyi* (McIntyre et al., 1970). Similar broad tolerances are observed for salinity (Winter et al., 1979; Hay and Honjo, 1989). It seems apparent, that nutrient availability due to the depth of the nutricline/thermocline, coupled with temperature and light intensity are the most important factors controlling the distribution pattern of coccolithophorids.

Coccolith assemblages preserved in sediments are fossil records of former coccolithophorid floras. Occurrences and abundances of coccolith species change substantially through geological time as a result of changing paleoceanographic conditions (McIntyre, 1967; McIntyre et al., 1970, 1972; Haq, 1980; Roth, 1989, 1994) and biological evolution of coccolithophores. The nanoplankton diversity records in the Cenozoic are closely correlated with climate change, increasing diversity associated with climate warming and decreasing diversity with cooling (Bown et al., 2004). Warm intervals supported high diversities of warm, K-selected taxa, such as discoasters, whereas cooling climates saw increases in meso- and eutrophic-adapted groups, such as the *Coccolithaceae*. Miocene diversities are not well correlated with paleoclimate trends but suggest that, while cooling proceeded at high latitudes, particularly associated with ice-sheet growth in Antarctica, warmer, oligotrophic habitats were sustained or expanded at low latitudes, supporting global high diversity (Bown et al., 2004).

When interpreting coccolith records the following points should be taken into consideration: A coccolith assemblage in sediments is not a complete record of the former living community. Biological, physical and chemical processes have changed the primary nanoplankton composition after death. These processes include grazing by zooplankton, sedimentation of coccoliths or transit from surface waters to the sediment (Samtleben et al., 1995), chemical

dissolution or selective preservation, and diagenetic effects (Berger and Roth, 1975; Steinmetz, 1994). The majority of coccoliths reaches the seafloor in faecal pellets of grazing zooplankton (Fig. 1.4), which accelerate the sinking rate of coccoliths and protect them from dissolution (Roth et al., 1975; Honjo, 1976; Samtleben and Bickert, 1990; Steinmetz, 1991).

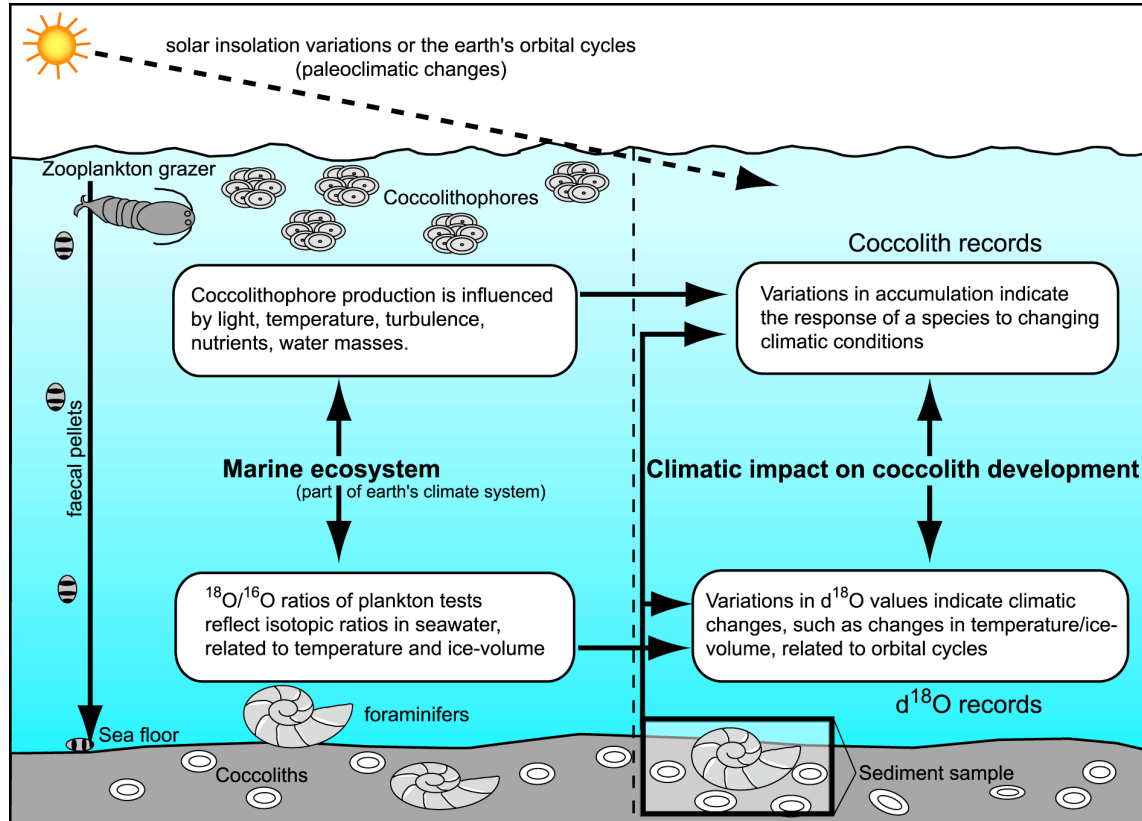


Fig.1.4. Generalized illustration of the ecosystem of living coccolithophorids and benthic foraminifers, and a correlation of the information about climatic changes by  $\delta^{18}\text{O}$  records and by coccolith accumulation records. Transport of coccoliths from the photic zone from Honjo (1976).

The accelerated sinking rates of the faecal pellets help to minimize lateral drift by ocean currents and ensure that a sediment assemblage on the seafloor has its origin in the overlying photic zone communities (McIntyre and Bé, 1967; Okada and Honjo, 1973; Baumann et al., 2000; Kinkel et al., 2000). Owing to selective dissolution, many delicate coccoliths, including nearly all holococcoliths and several heterococcoliths dissolve, and only coccoliths with robust crystals, e.g. *Calcidiscus*, *Reticulofenestra*, *Gephyrocapsa*, *Coccolithus*, *Discoaster*, *Helicosphaera*, are resistant to dissolution and preserved in sediments (e.g. Berger and Roth, 1975). Therefore, only a small portion of living coccolithophorid species has a substantial fossil record.

### 1.3.1 Coccolith production

In general, two morphologically distinct types of coccoliths are produced, the heterococcoliths and the holococcoliths, which are distinguished by their mode of formation

and the life-cycle stage during which they are produced (Bown, 1998). The heterococcoliths are formed intracellularly (Westbroek et al., 1989; Pienaar, 1994) and are constructed from radial arrays of variably-shaped crystal units. In contrast, holococcoliths are composed of a number of single equidimensional calcite crystallites of simple shape. Those forms are easily dissolved and therefore only rarely preserved in sediments. Haptophyte algae mainly reproduce asexually by binary fission (mitosis). Complex life-cycles with alternating phases with two or more distinct cell coverings have been observed (summarised by Billard, 1994). During the diploid stage, the haptophytes may be motile or non-motile. If calcification occurs, heterococcoliths are produced. Within the haploid stage, the cells are predominantly motile and may be covered by holococcoliths. In both stages, mitotic division is possible. However, the mechanisms that trigger the transition between life cycle stages are still poorly understood. In the last years, combination coccospheres, composed of holo- and heterococcoliths, have been detected (Cortés, 2000; Cros et al., 2000; Renaud and Klaas, 2001; Geisen et al., 2002). These combination cells are interpreted as the morphological expression of the state of phase transition (Geisen et al., 2002).

### 1.3.2 Function of coccoliths

There are various hypothesis about the usefulness of coccolith formation from biogeochemical and functional point of views. A number of studies emphasize, that coccolithophores may form coccoliths, to utilize the CO<sub>2</sub> from the calcification process for photosynthesis (Nimer et al., 1992; Sikes and Fabry, 1994; Nimer and Merrett, 1995). Coccolithophores would therefore be insensitive to CO<sub>2</sub> limitation. A number of coccolithophores do not produce calcitic scales at all and are only surrounded by a sphere of organic plates. This is sometimes observed even in species that usually calcify. It is not clear, whether this is due to different life cycles or other unknown reasons (Pienaar, 1994).

As to the function of the coccosphere, no definite explanation has been found so far. Coccoliths seem to have been adapted to perform a range of different functions, probably mainly the protection of the delicate cell wall from mechanical damage, microbial attack or chemical stock (Young, 1994). Furthermore, flotation and buoyancy of a cell, controlling the position within the water column necessary for enhanced nutrient uptake, may strongly depend on the shape of the coccosphere and the arrangement of the coccoliths. The latter may also have a light-regulating function. It has been proposed that coccoliths might reflect light from the cell, allowing coccolithophores to live higher in the water column, or refract light into the cell, enabling some species to live in the deep photic zone. Reflection of sunlight by coccoliths does not only alter the albedo of the surface ocean, and therefore makes

coccolithophore blooms visible to satellite sensors, it also increases the temperature of surface waters (Holligan et al., 1993).

#### 1.4 Coccolithophorid-based geochemical paleoproxies

Coccolithophores are the only marine organisms that provide indicators of paleoclimatic and paleoceanographic conditions from both the organic (molecular fossils or biomarkers) and inorganic ( $\text{CaCO}_3$ ) remains in the sediment. In the last decade, the alkenones, organic biomarkers produced by a small group of coccolithophores, have served as the basis for two important paleoproxies, the undersaturation ratio of alkenones ( $U_{37}^K$ ), which depends on temperature (Brassell et al., 1986), and the carbon isotopic fractionation,  $\epsilon_{\text{alkenones}}$ , used to reconstruct past atmospheric  $\text{CO}_2$  concentrations (Jasper and Hayes, 1990). In contrast, the use of coccoliths for elemental and stable isotopic analysis is a relatively recent paleoceanographic strategy. Stoll and Schrag (2000) have shown that the elemental chemistry of coccoliths can provide unique proxies for past variations in coccolith productivity. Culture studies also suggest the potential for new insights from coccolith stable isotope chemistry (e.g. Ziveri et al., 2003).

##### 1.4.1 Stable isotopes in coccolith calcite

Stable isotopic measurements in biogenic carbonates have been a key tool for paleoceanographic studies for nearly half a century. For all marine carbonates, the oxygen isotopic ratio depends on the temperature at which the carbonate precipitates as well as the isotopic composition of the seawater from which it forms. The carbon isotopic composition largely reflects the carbon isotopic composition of dissolved inorganic carbon (DIC) in the ocean, since the temperature effect on carbon isotopic fractionation is very small. Within the ocean, the spatial gradients in the carbon isotopic composition of DIC are controlled by biological productivity through the removal of isotopically light carbon in organic matter. The relative importance of different inputs of carbon to the ocean-atmosphere system (weathering, release of mantle carbon through volcanic  $\text{CO}_2$ , and release of methane hydrate) and relative removal rates of organic and inorganic carbon from the ocean, set the average carbon isotopic composition of DIC in the ocean. The carbon isotopic composition of marine carbonates can be used to identify past changes in productivity and ocean circulation (e.g., Broecker, 1971), while changes in the global average isotopic composition can be used to infer changes in the carbon cycle (e.g., Dickens, 2001).

In Early Cenozoic and Mesozoic sediments, where foraminifers were less common and core material was limited, coccolith-dominated bulk carbonate has been a standard phase for stable isotopic analyses (e.g., Bains et al., 1999). The reliability of these polyspecific bulk carbonate

records are still put into question, in part because cultures of coccolithophores show an especially wide range of ‘vital effects’ in oxygen and carbon isotopes (Dudley et al., 1986; Dudley and Goodney, 1979; Ziveri et al., 2003). Therefore, changes in the relative carbonate distribution of different species in sediments may cause significant changes in the isotopic ratios of the assemblage, potentially masking the signals of oceanic variability. Recently, Ziveri et al. (2003) provided species-specific correction factors for carbon and oxygen vital effects in coccoliths, although further experiments are still needed to confirm that these effects are constant for each species. New decanting, density stratified columns and microfiltering techniques (e.g., Stoll and Ziveri, 2002) were developed to separate more restricted (nearly monospecific) coccolith fractions from sediment. Although the methods are time-consuming, they might be the best approach for older sediments where species-specific ‘vital effects’ cannot be determined in culture.

The chemistry of calcite produced by coccolithophores offers the potential to extract information about past environmental and biological conditions, including: sea surface temperatures (alkenone undersaturation  $U_{37}^K$ , coccolith oxygen isotopic ratios), dissolved and atmospheric  $CO_2$  concentrations (carbon isotopic fractionation in biomarkers and  $\epsilon_{alkenone}$ ), coccolithophorid productivity (coccolith Sr/Ca) (Stoll and Schrag, 2000), and carbon cycling within the ocean and between other carbon reservoirs (coccolith carbon isotopes). Using multiple indicators all derived from the same organisms, is one of the greatest assets of coccolithophore-based geochemical proxies. Results from the current study have shown, that stable isotopic records of calcareous nannofossil carbonate provide useful information about paleoceanography during the Middle to late Miocene in the Southeast Atlantic. Continued calibration studies are still needed to further improve our understanding of these proxies and increase confidence in their paleoceanographic applications.

## **1.5 Objectives of the study**

The main objective of this thesis is to document and understand the role of calcareous nanoplankton as the main carbonate producer in relation to changes in ocean circulation and global climate in the Middle to Late Miocene. Knowledge of the distribution patterns of single species, the assemblage composition, and the preservation of coccoliths from the eastern South Atlantic provide the groundwork for paleoceanographic studies. Additionally, the nanoplankton contribution to the bulk carbonate production as well as the stable isotopic composition of the coccolith carbonate will be explored.

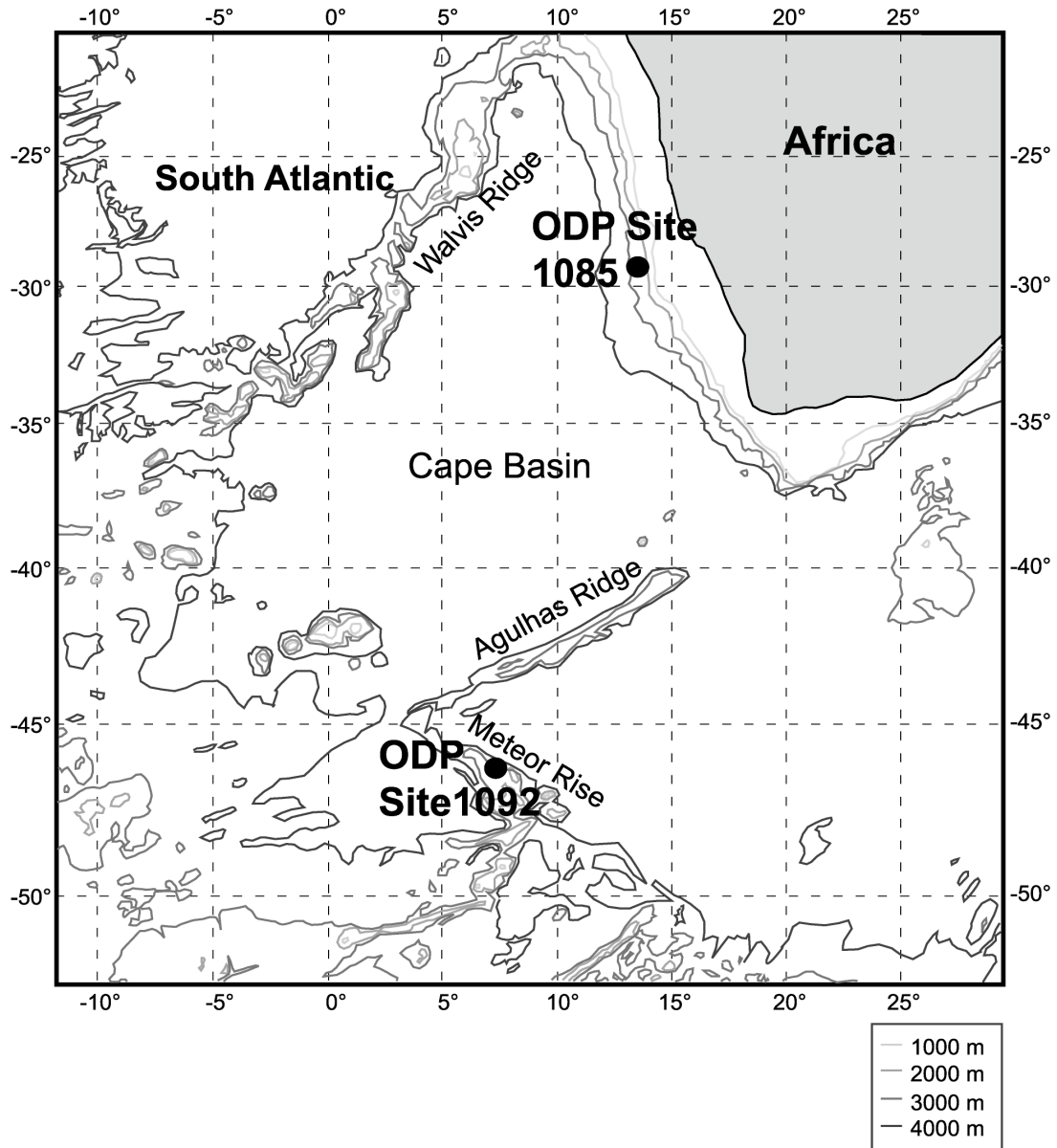


Fig. 1.5. Map of the study area and location of in the southeast Atlantic. Relevant topographic features and locations of studied drill sites (ODP Sites 1085 and 1092) are presented.

Therefore, the main questions are:

- Is it possible, to explain the Miocene ‘Carbonate Crash’ events in the southeast Atlantic by changes in the coccolithophorid species composition or in nannoplankton productivity?
- How are changes in the absolute numbers of coccolith species, in the nannofossil assemblages, and in the coccolith carbonate contribution linked to the development of the modern ocean circulation and climate events during the Middle to Late Miocene?
- Does the stable isotope record of the coccolith carbonate provide useful information about paleoceanographic changes in the studied region?

To answer these questions two ODP Sites in the South Atlantic, ODP Site 1085, drilled during Leg 175, and Site 1092, drilled during Leg 177 (Fig.1.5), have been investigated. The location and the analysed material are described in detail in the respective sections of the manuscripts.

### 1.5.1 Methods

The preparation of the sediment samples for the scanning electron microscope (SEM) generally followed the combined dilution/filtering technique described by Andruseit (1996). This method is described in particular in Chapter 2. Nannofossils in the bulk sediment were counted by scanning electron microscopy using a Zeiss DMS 940A at the Department for Sedimentology/Paleoceanography in Bremen. Counts and size measurements were converted into volume and mass contribution of each species using the approach of Young and Ziveri (2000) with given shape factors for various coccolith types, the average length of a species, and the density of calcite.

For stable isotope measurements, the sediment was first washed through a 20 µm-sieve to detach the nannofossils from juvenile foraminifera and their fragments. The clay fraction was separated using the Atterberg settling technique. The sample fractions were analysed using a Finnigan MAT 252 micromass-spectrometer coupled with a Finnigan automated carbonate device at the Department for Marine Geology in Bremen.

The flow-chart presented in Fig. 1.6 summarises all working steps.

The results of this thesis are presented in three manuscripts (chapters 2 through 4) of which the first one is already accepted by *Paleogeography, Paleoclimatology, Paleoecology*, the second manuscript is submitted to *Marine Micropaleontology*.

#### **Manuscript #1**

Krammer, R., Baumann, K.-H., and Henrich, R., 2005. Middle to Late Miocene fluctuations in the incipient Benguela Upwelling System revealed by calcareous nannofossil assemblages. *Palaeogeography, Palaeoclimatology, Palaeoecology*, in press.

#### **Manuscript #2**

Krammer, R., Baumann, K.-H., Bickert, T. and Henrich, R., ODP Site 1085 nannofossil assemblages and fine-fraction carbonate stable isotopes as indicators for Middle to Late Miocene Benguela Upwelling initiation. *Marine Micropaleontology*, submitted.

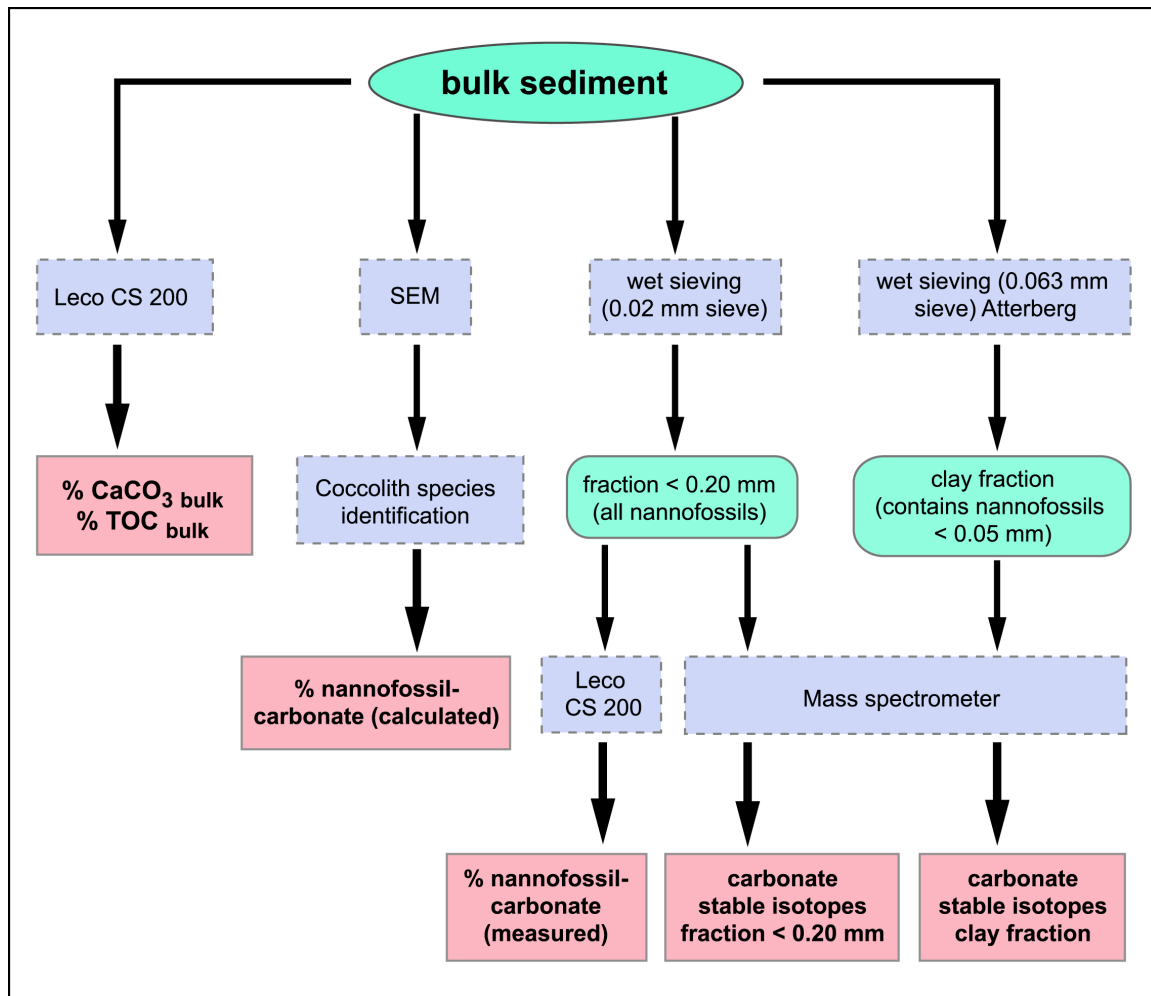


Fig. 1.6. Flow-chart of all methods performed.

### Manuscript #3

Krammer, R., Baumann, K.-H., Bickert, T. and Henrich, R., Calcareous nannofossil assemblages and fine-fraction carbonate stable isotopes in the sub-Antarctic South Atlantic during the Middle to Late Miocene (ODP Site 1092); manuscript in preparation.

All data and tables will be available at **PANGAEA** – Network for Geological and Environmental Data ([www.pangaea.de](http://www.pangaea.de)).

## **Chapter 2**

### **Manuscript 1:**

**Middle to Late Miocene fluctuations in the incipient  
Benguela Upwelling system revealed by calcareous  
nanofossil assemblages (ODP Site 1085)**



**Middle to Late Miocene fluctuations in the incipient Benguela Upwelling System  
revealed by calcareous nannofossil assemblages  
(ODP Site 1085A)**

Regina Krammer<sup>1</sup>, Karl-Heinz Baumann<sup>2</sup>, Rüdiger Henrich<sup>2</sup>

<sup>1</sup> *Research Center Ocean Margins, University of Bremen, Germany  
(krammer@uni-bremen.de)*

<sup>2</sup> *Department of Geosciences, University of Bremen, Germany*

*Palaeogeography, Palaeoclimatology, Palaeoecology, in press*

**Abstract**

Middle to Late Miocene calcareous nannofossil data of ODP Site 1085 from the eastern South Atlantic off Namibia were analysed to document spatial and temporal changes in surface-ocean circulation, upwelling initiation, and associated productivity.

Our data show that calcareous nannofossils constitute a significant part of the carbonate fraction throughout the investigated interval from 12.5 to 7.7 Million years (Ma). Highest numbers of calcareous nannofossils (up to  $38000 \times 10^6$  nannofossils g<sup>-1</sup> sediment) were observed during the intervals 9.9 to 9.7 and 8.7 to 8.0 Ma. These elevated numbers of calcareous nannofossils may generally be linked to the initiation of upwelling at about 10 Ma in the studied region. In contrast, diminished numbers of calcareous nannoplankton, as in the interval 9.6 to 9.0 Ma, probably characterise time intervals of weaker productivity resulting in a decrease of nannofossil carbonate contents in the sediments of Site 1085. This decrease in nannofossil production could be one possible explanation for the major CaCO<sub>3</sub> depression in between 9.6 and 9.0 Ma. Coccoliths of the genus *Reticulofenestra* are the most abundant taxa. Their occurrences are characterised by changes in the investigated time interval. In addition, *Coccolithus pelagicus*, *Calcidiscus leptoporus* and *Umbilicosphaera* spp. contribute a common part of the assemblage. Calcareous nannofossils account for more than half of the carbonate, with peak contribution up to 80 % at 8.8 Ma.

*Keywords:* calcareous nannoplankton; Namibia upwelling; paleoceanography; paleoecology; Miocene; South Atlantic

## **2.1 Introduction**

The Middle to Late Miocene is known as an interval of major changes in the climate system, such as the expansion of the Antarctic ice sheets, the cooling of surface and deep water masses, as well as the start both of Isthmus of Panama and Himalaya uplift (e.g., Zachos et al., 2001). These changing boundary conditions had significant impacts on ocean circulation, nutrient supply and, thus, on the productivity of the oceans. Previous investigations of the Miocene history of the upwelling off southwest Africa concluded that the onset of high productivity was at about 10 Ma (e.g., Siesser, 1980; Meyers et al., 1983) and postulated that the modern Benguela Current and related upwelling migrated progressively from south to north within the late Miocene and Pliocene (Diester-Haass et al., 1990). Subsequent investigations on lithologic changes reflected by light-dark sediment cycles corresponding glacial interglacial successions in Pliocene and Miocene times were interpreted as reflecting shifts in the course of the Benguela Current main flow (Diester-Haass et al., 1992) and/or changes in the nutrient content of the upwelled waters linked with global hydrography (Hay and Brock, 1992).

Within this time interval, several especially remarkable paleoceanographic events occurred which are summarized as the so-called ‘Carbonate Crash’. During about 12 to 9 Ma, several sharp drops in CaCO<sub>3</sub> accumulation happened, in particular in the equatorial latitudes of the Pacific and Indian Oceans (e.g. Peterson et al., 1992; Berger et al., 1993; Farrell et al., 1995; Lyle, 2003), in the equatorial Atlantic (King et al., 1997), and in the Caribbean Sea (Roth et al., 2000). Changes in deep-water circulation, shoaling of the calcite compensation depth (CCD), and shallow-deep fractionation were generally considered as possible causes, although the ‘Carbonate Crash’ remains poorly understood. Recently, this event has also been described in the southeast Atlantic Ocean (Diester-Haass et al., 2004). The authors proposed an increase in the delivery of lithogenic matter from the Oranje River as principal cause of the ‘Carbonate Crash’ off southwest Africa since no clear evidence for carbonate dissolution was found. However, their interpretations are mainly based on the sand-fraction, which is only about 2-3% of the total sediment, whereas the bulk of the material is rather fine-grained nannofossil ooze (Wefer, Berger, Richter et al., 1998). The most pronounced carbonate crash event VI from 9.6 – 9 Ma was linked to an overall increase in nutrient flux into the world’s oceans and therefore to the development of poorly ventilated intermediate to deep waters or at least an expansion of the oxygen minimum zone at the continental slope (Diester-Haass et al., 2004; Westerhold et al., *subm.*).

Although calcareous nannofossils are the main contributors to the carbonate depositional system, they have not been studied in detail for this time interval. This is surprising, since

calcareous nanoplankton is known as a sensitive indicator of environmental conditions because it directly depend on temperature, salinity, and nutrients, as well as the availability of sunlight (e.g., Giraudeau, 1992; Winter and Siesser, 1994). This plankton group responds to fluctuations in climate as well as changes in surface-water conditions. The potential of coccolithophores as paleoproxy for reconstructions of Quaternary surface-water conditions in the area off southwest Africa has already been shown by various authors. Core-top studies reveal a good correspondence of certain species and characteristic assemblages with oceanographic features of the overlying water masses (e.g., Giraudeau and Rogers, 1994; Baumann et al., 1999; Flores et al., 1999; Böckel and Baumann, 2004). In addition, shifts in species composition observed in several sediment cores were attributed to changes in upwelling intensity and eddy formation (Winter and Martin, 1990; Baumann and Freitag, 2004) or frontal movements (Flores et al., 1999).

In this study, we present Middle to Late Miocene calcareous nanofossil data from the eastern South Atlantic off Namibia. The studied ODP Site 1085 is located on the continental slope close to the mouth of the perennial Oranje River. The investigated time interval from 12.5 to 7.7 Ma is characterised by at least six ‘Carbonate Crash’ events (Westerhold et al., *subm.*), which are assumed to be caused either by dilution due to enhanced terrigenous input linked to sea level lowering or by dissolution due to enhanced inflow of corrosive Southern Component Water (SCW) during Miocene glacial events. Besides dilution and/or dissolution the ‘Carbonate Crash’ events could also be explained by changing coccolithophorid assemblages. To test this hypothesis, this site has been investigated for its calcareous nanofossil composition, absolute numbers and relative abundances, and their calcareous nanofossil carbonate content. This approach allows us to assess the significance of calcareous nanofossils in sediments where planktic foraminifera are scarce and, in addition, the comparison of this data helps us to reconstruct some of the environmental changes at the onset of the upwelling off southwest Africa.

## **2.2 Regional setting and Oceanography**

### **2.2.1 Modern oceanographic setting**

The Angola/Namibia system is one of the largest upwelling regions in the world. It extends over the West-African margin from South Africa to the Walvis Ridge, with productivity values  $\geq 180 \text{ g C/m}^2\text{yr}$  (Berger, 1989), characterized by organic-rich sediments. The modern oceanic upper-layer circulation in this area has been summarised in a number of reviews (e.g. Peterson and Stramma, 1991; Reid, 1996; Shannon and Nelson, 1996) so that only a brief summary is given here.

The recent surface water circulation in the Southeast Atlantic is dominated by the northward-directed Benguela Current (BC; Fig. 2.1) and the warmer, southward-flowing Angola Current (AC). The BC is forming a northeastern part of the anticyclonic South Atlantic gyre. Southerly and southeasterly trade winds in this region drive an offshore surface drift and cause coastal upwelling of cold, nutrient-rich water from depths of 200 to 300 m (Hart and Currie, 1960) over most of the continental shelf. Upwelling at present occurs in a number of cells south of about 18°S, with a major, in principle semipermanent cell at 27°S (Fig. 2.1; Shannon and Nelson, 1996). This upwelling leads to enhanced biological productivity off Namibia, evident from relatively high to moderate chlorophyll  $\alpha$  concentrations (Giraudeau and Rogers, 1994). The African coast along the upwelling area is a dry desert area; the only perennial river is the Oranje River.

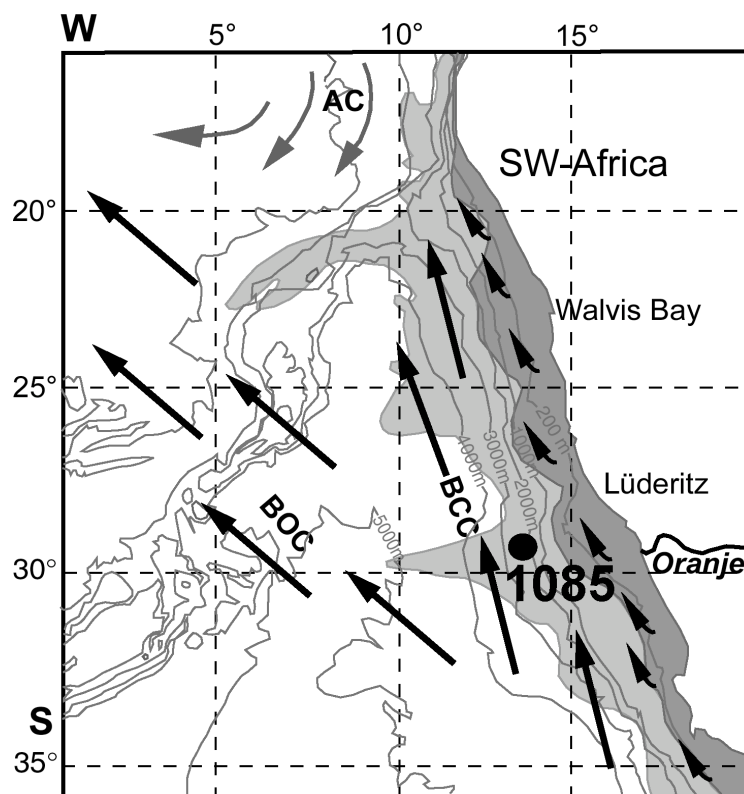


Fig. 2.1. Schematic modern surface current pattern off Southwest Africa. The black dot shows the location of the ODP Site 1085. Black arrows indicate relative cool currents of the Benguela Coastal Current (BCC) and the Benguela Oceanic Current (BOC). Grey arrows show the flow pattern of the warm Angola Current (AC). Dark shading indicates coastal upwelling, whereas light shading shows the extension of upwelling filaments into the mixing zone with oligotrophic open ocean waters (after Shannon and Nelson, 1996).

### 2.2.2 The Benguela upwelling system since the Middle Miocene

Former investigations of the Miocene history of the southwest African upwelling system have shown that the initiation of high productivity started at about 10 Ma (Siesser, 1980;

Meyers et al., 1983) and postulated that the Benguela Current (BC) has progressively strengthened since the Middle Miocene and related upwelling migrated progressively northward within the late Miocene and Pliocene (Diester-Haass, 1990, 1992). During Antarctic glacial periods the Benguela Current system has shifted northward reaching the Walvis Ridge, producing upwelling in the near-coastal areas, and turning west over the Walvis Ridge. In interglacial periods, however, the Benguela Current turned to the west within the Cape Basin. Pollen contents of sediments from Site 532 on the Walvis Ridge give evidence that the Namib Desert has existed since the late Miocene (van Zinderen Bakker, 1984). These earlier interpretations of the BC upwelling system suffered from poor temporal resolution, incomplete sediment sequences and information from only one location - DSDP Site 362/532 on Walvis Ridge (Bolli et al., 1978; Hay et al., 1984; Hay and Brock, 1992).

## **2.3 Material and methods**

### **2.3.1 Background of Site 1085A**

Sediment records obtained during ODP Leg 175 provided a new opportunity to study the history of upwelling in continuous and relatively undisturbed sediment sequences from multiple locations along the southwest African margin. ODP Site 1085A was drilled during this leg and is located at 29°22.45'S and 13°59.41'E in 1713 m water depth (Fig. 2.1). The Oranje River is discharging into the South Atlantic (Wefer, Berger, Richter et al., 1998), influencing Site 1085A. Today, Site 1085 is bathed primarily in the Upper Circumpolar Deep Water (UCDW) near the mixing zone with the North Atlantic Deep Water (NADW). The site penetrated the Middle Miocene and comprises a complete record of hemipelagic sediments down to 14 Ma, dominated by greenish-grey, foraminifera-bearing nannofossil ooze, diluted by various amounts of terrigenous silt and clay. The studied interval between 399 and 569 mbsf covers the Middle to Late Miocene, including the late Middle Miocene onset of the Benguela Current upwelling system and its associated elevated marine productivity (Diester-Haass et al., 2002).

### **2.3.2 Samples and analysis**

We set 2 g of each sample (318 samples with a resolution of about 15 ka) aside for carbon analysis, and the remaining material was washed through 20 µm sieves to detach calcareous nannofossils from adult and juvenile foraminifera. SEM observations of the fraction < 20 µm indicated that the calcareous particles in this fraction are almost exclusively composed of calcareous nannofossils. After separating the fraction < 2 µm (clay fraction) using Atterberg settling technique, scanning electron microscope (SEM) analysis of the clay showed that

calcareous nannofossils smaller than 5  $\mu\text{m}$  in size (i.e., *Reticulofenestra minuta* and *Reticulofenestra haqii*) make up the most important part of the calcareous clay.

The dried material was analysed for carbon content (total carbon; TC) using a LECO CS 200. To obtain the total organic carbon (TOC), the sediment was treated with 12.5% HCl, and the carbonate-free residue was rinsed, dried and measured with a LECO CS 200. The  $\text{CaCO}_3$  content was calculated after following equation:

$$\text{CaCO}_3 (\%) = (\text{TC} - \text{TOC}) \times 8.33$$

The carbonate content was measured on the bulk sediment, on the fraction  $< 20 \mu\text{m}$  and on the clay fraction.

### 2.3.3 Quantification of calcareous nannofossils and its carbonate content

For the preparation of calcareous nannofossil samples (80 samples), a combined dilution/filtering technique as introduced by Andruleit (1996) was used. A small amount of sediment (80 mg of dry bulk sediment) was weighed, brought into suspension, and splitted into subsamples. The final sample split was filtered onto polycarbonate membrane filters using a low-pressure vacuum pump. For calcareous nannofossil analysis with the SEM, a randomly chosen small section of the dried filter (approx.  $0.5 \text{ cm}^2$ ) was fixed on an aluminum stub and sputtered with gold/palladium. SEM examinations were carried out using a Zeiss DMS 940A at the University of Bremen. The numbers of up to 800 nannofossils per sample were counted on measured transects at a magnification of 3000x at 10 KV. All counted calcareous nannofossils were converted into numbers per gram dry sediment using the following equation:

$$Dc = (F \times C \times S) / (A \times W)$$

with  $Dc$  = nannofossil density (number of calcareous nannofossils/ $\text{g}_{\text{sediment}}$ ),  $F$  = filtration area ( $\text{mm}^2$ ),  $C$  = number of counted calcareous nannofossils,  $S$  = split factor,  $A$  = scanned filter area ( $\text{mm}^2$ ), and  $W$  = sediment weight (g).

Calcareous nannofossil numbers as calculated from the sediment were converted into nannofossil-carbonate contents on the basis of mean estimates of species masses. Using the mass equation of Young and Ziveri (2000) given shape factors of coccolith types ( $k_s$ ), the average length of a species ( $l$ ), and the density of calcite are considered. Nannoplankton carbonate mass can then be expressed as  $m = 2.7k_s l^3$  and the weight-balanced nannoplankton carbonate concentration as followed:

$$\text{Nannofossil carbonate (wt\%)} = \text{Nannofossil mass} \times Dc \times 10000.$$

The estimation of the shape factor is the greatest source of uncertainty in these calculations, but any biases in estimated volume contributions are consistent from sample to sample. However, the data given here seem reasonable in comparison to the total carbonate data, and, therefore, is expected to be a good approximation of the real nannofossil-carbonate content.

A good taxonomic overview of Neogene calcareous nannofossils is provided in Perch-Nielsen (1985). In general, the taxonomy follows the classification system of Young (1998), in addition, the taxonomy of the genus *Reticulofenestra* follows that outlined in Gibbs et al. (2005).

#### 2.3.4 Stratigraphy

Westerhold et al. (2005) developed an astronomically calibrated age model for the Miocene section of ODP Site 1085 that is used in this study. The age model was generated by orbital tuning of a high-resolution composite XRF-Fe intensity record of ODP Sites 1085 (see Fig. 2.2) to an Eccentricity-Tilt-Precession (ETP) target curve. Shipboard data of the biostratigraphic datums provided the preliminary age model for Site 1085 (Wefer, Berger, Richter, et al. 1998). The tuning procedure itself was done by correlating prominent features of the Fe record to the ETP target curve, whereby the record first was tuned in the 400-ka domain and then in the 100-ka domain. Because eccentricity modulates the signals derived from terrigenous material (magnetic susceptibility, XRF Fe record) in the Cape Basin, maxima in eccentricity correspond to maxima in the terrigenous signal. The tuning procedure gave an age control point for at least each eccentricity cycle. No lag between the tuning target and the lithologic signal has been assumed. The derived sedimentation rates range between 1.0 and 7.3 cm/ka. From 13.8 up to 11.7 Ma the sedimentation rates are well below 4 cm/ka, then they increase steadily to 7 cm/ka and remain at that value from 11.5 - 10.4 Ma, punctuated by a drop in sedimentation rates at 11.1 Ma. Thereafter rates decrease to an average value of 3 cm/ka till 6.5 Ma, interrupted by enhanced sedimentation rates at 9.9 Ma and around 7.6 Ma.

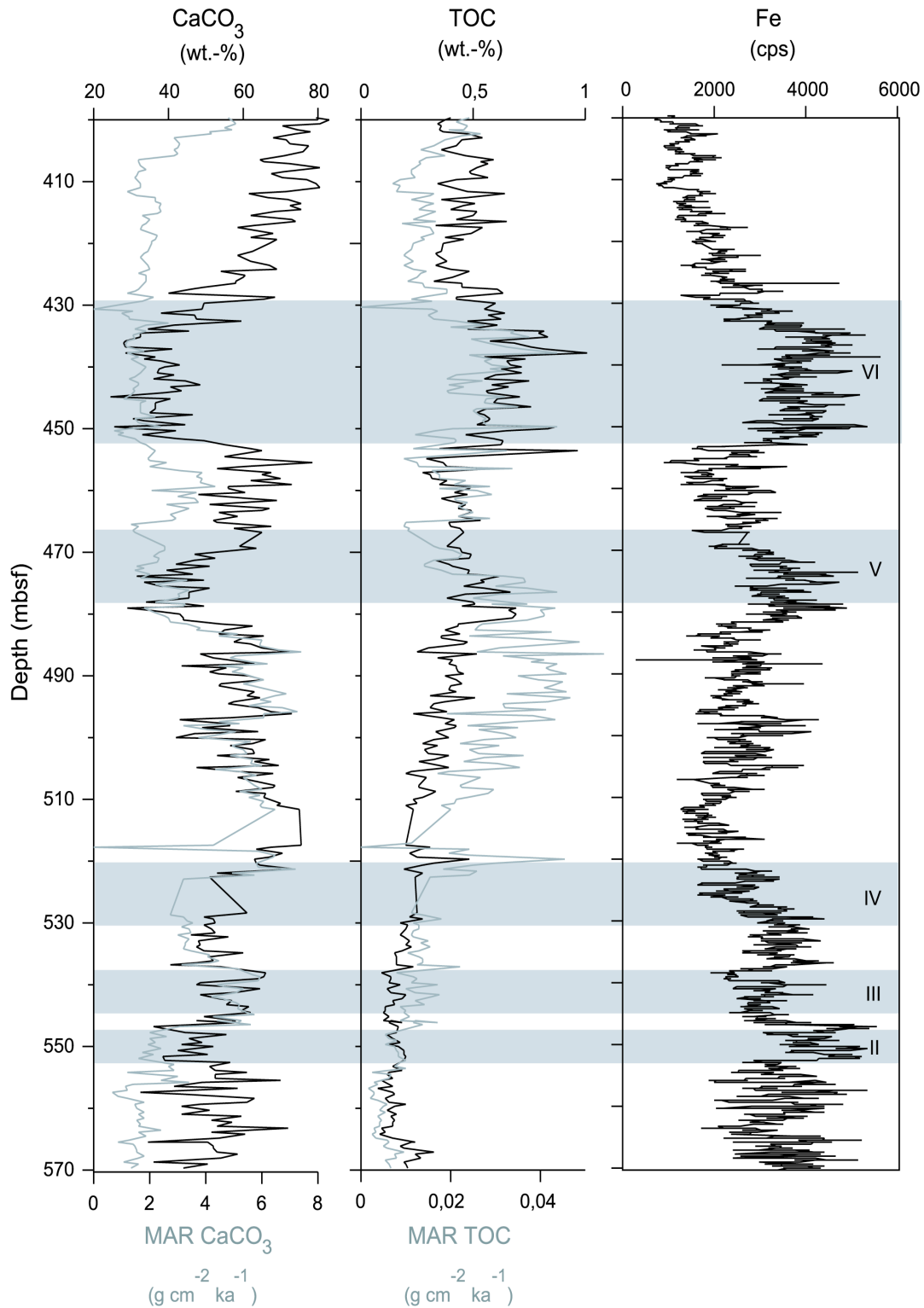


Fig.2.2. Bulk geochemical measurements (carbonate content, total organic carbon and Fe record) on samples of Site 1085 plotted against core depth (mbsf). Mass accumulation rates of carbonate and total organic carbon (MAR CaCO<sub>3</sub>, MAR TOC) with grey lines. Fe intensities in counts per second (cps) are from Westerhold et al. (2005). Grey shaded bars indicate intervals (II – IV) that are characterized by dramatic drops in carbonate content, the so called ‘Carbonate Crash’-events.

## 2.4 Results

### 2.4.1 Absolute numbers and relative abundances of calcareous nannofossils

Absolute calcareous nannofossil numbers range from  $5000 \times 10^6$  to  $38000 \times 10^6$  calcareous nannofossils per gram of sediment at Site 1085 (Fig. 2.3). Highest numbers of total calcareous nannofossils occur in the intervals 9.9 to 9.7 Ma and 8.7 to 8.0 Ma (Fig. 2.3).

The most abundant species are *Reticulofenestra minuta* (with highest values of  $24000 \times 10^6$  coccoliths  $g^{-1}$ ), followed by *Reticulofenestra haqii* (up to  $11000 \times 10^6$  coccoliths  $g^{-1}$ ), and *Coccolithus pelagicus* (up to  $2900 \times 10^6$  coccoliths  $g^{-1}$ ). In addition, *R. pseudumbilicus* (5-7  $\mu m$  in diameter, 'medium'), *R. pseudumbilicus* (> 7  $\mu m$  in diameter, 'large'), and *Calcidiscus leptoporus* make up a common part of the assemblage (see Fig. 2.3).

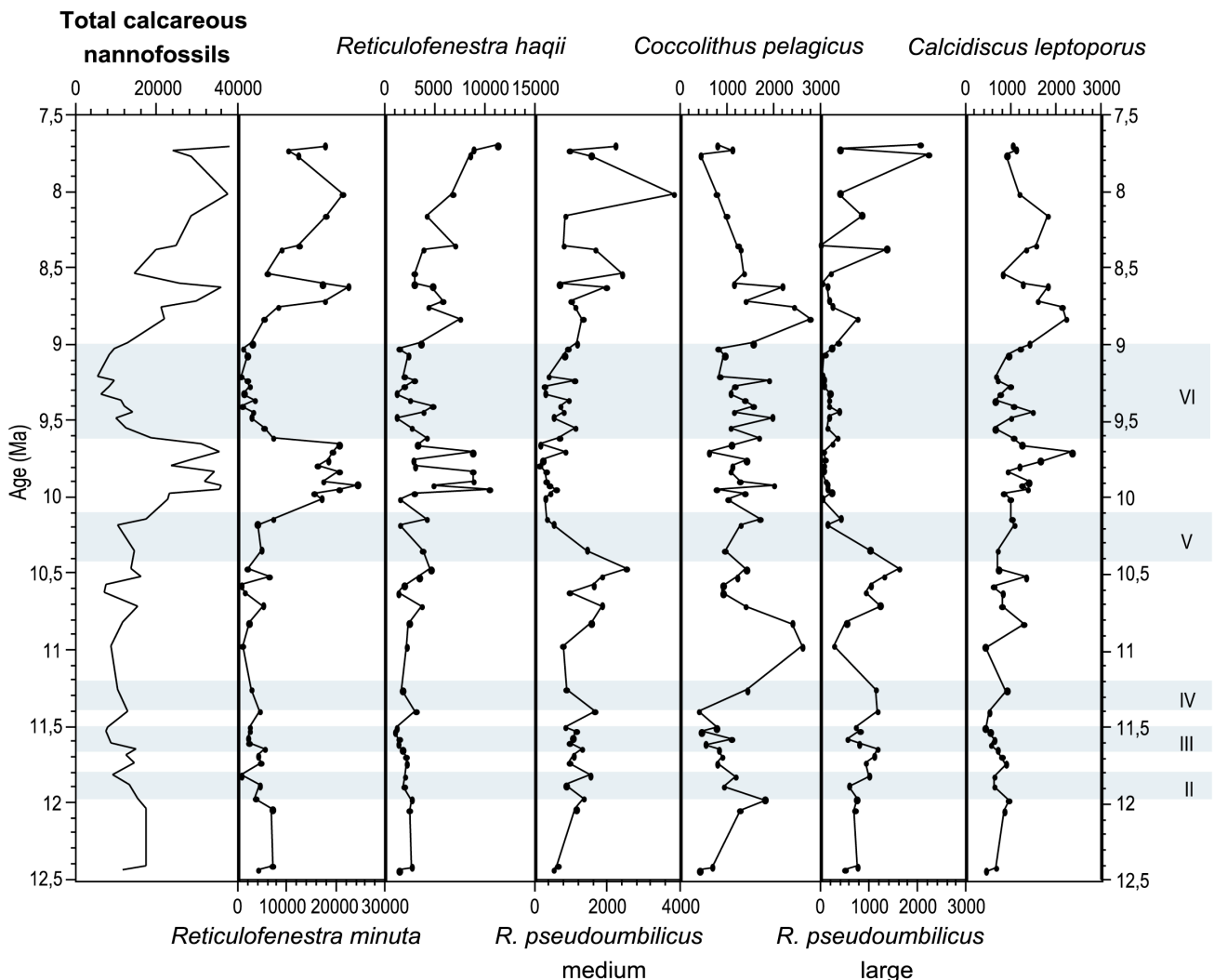


Fig. 2.3. Absolute numbers of the total nannofossils as well as of the most dominant species at Site 1085. Horizontal grey shaded bars (II-VI) indicate intervals that are characterized by dramatic drops in carbonate content.

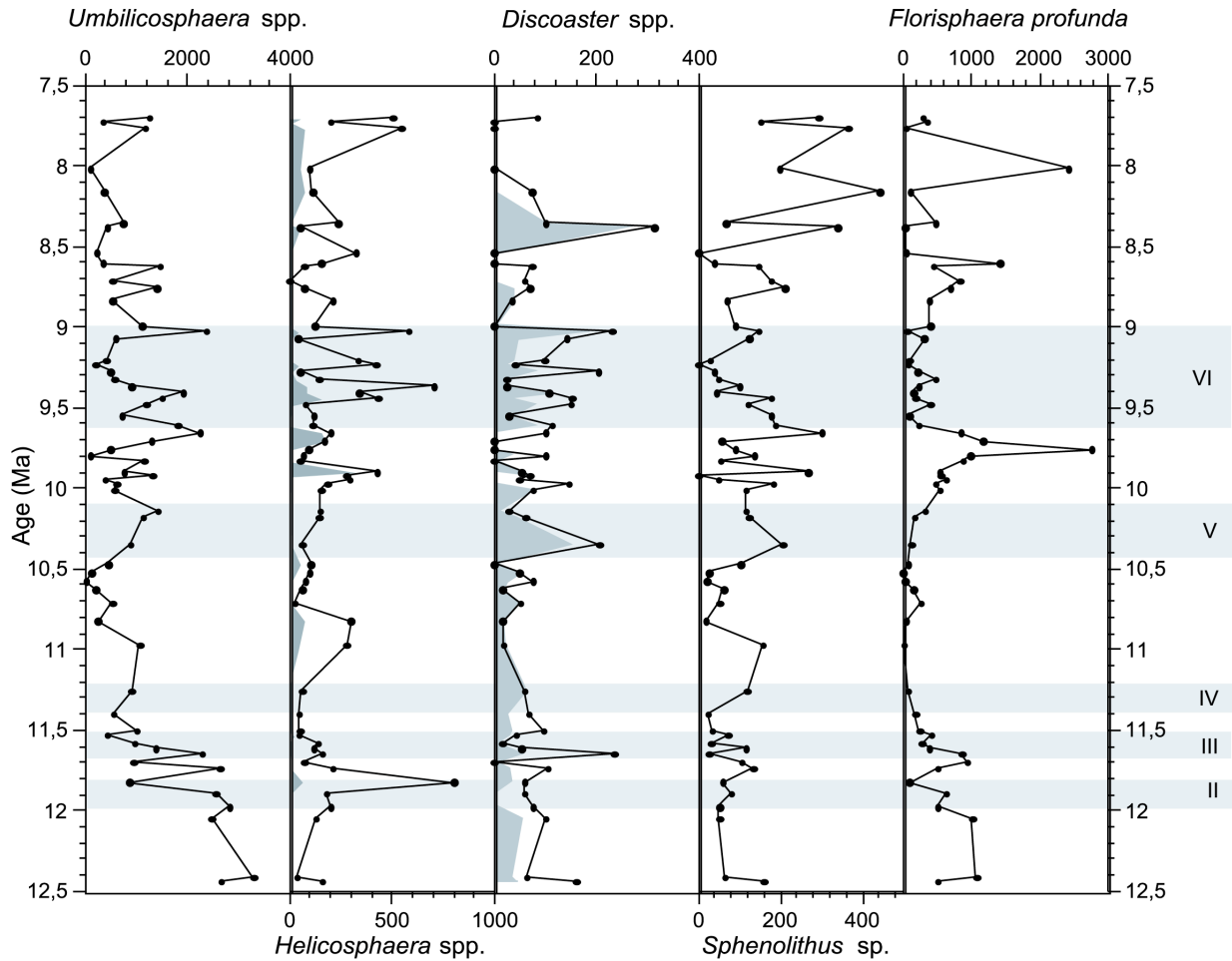


Fig.2.4. Absolute numbers of the common species at Site 1085. Horizontal grey shaded bars (II-VI) indicate intervals that are characterized by dramatic drops in carbonate content.

The deep-dwelling species *Florisphaera profunda* is constantly recorded during the entire time span (Fig. 2.4) with numbers lower than  $1 \times 10^9$  nannoliths  $g^{-1}$  (with exception of four values between  $1.1$  and  $2.7 \times 10^9$  nannoliths  $g^{-1}$ ). In general, the calcareous nannofossil flora is dominated by species of the genus *Reticulofenestra*, which usually comprise about 50% of the assemblage (Fig. 2.5). In addition, *C. pelagicus* and *C. leptoporus* make up an important part of the assemblage. Additionally, a number of other species are recorded in very low abundances (Fig. 2.4).

Although, beside the significant increase in both total calcareous nannofossil numbers and *R. minuta* content at 10.2 Ma, no drastic change in the assemblage composition occurred throughout the entire interval, some differences are recognizable in the species variations of both the high-carbonate intervals (e.g., 11.25 - 10.57 Ma and 8.83 - 8.38 Ma) and the low-carbonate interval from 9.6 to 9.0 Ma (see Fig. 2.9). In the low-carbonate interval the total calcareous nannofossil content and that of the species *R. minuta*, *R. haqii*, *R.*

*pseudoumbilicus*, *C. leptoporus*, and *F. profunda* show lowest values. In general, the group of reticulofenestrids reaches values between 40 and 70% of the assemblages. In comparison, during high-carbonate intervals, the content of reticulofenestrids reaches values up to 80% of the nannofossil assemblage.

The total nannofossil accumulation rate (expressed in numbers  $\text{cm}^{-2} \text{k}^{-1}$ , see Fig. 2.8) starts to increase at about 11 Ma, showing a decrease between 10.2 and 10.0 Ma, subsequently followed by a sharp increase in nannofossil accumulation at 10 Ma, corresponding with the accumulation rates of *R. minuta* and *R. haqii*. In comparison, the accumulation rates of *R. pseudoumbilicus* ('large' and 'medium'), *C. pelagicus*, and *C. leptoporus* start to increase 0.5 to 1 Ma earlier than the small placoliths. In the low-carbonate interval from 9.6 to 9.0 Ma, accumulation rates of all nannofossils show lowest values. These results agree with the postulated 'Carbonate Carsh' event IV (Westerhold et al., subm.). After 9.0 Ma a slightly stepwise increase in nannofossil accumulation rates is recognizable.

#### 2.4.2 Bulk sediment parameters, nannofossil carbonate and preservation

The entire interval from 12.5 to 7.5 Ma at Site 1085 is dominated by fine carbonate silt, indicating that calcareous nannofossils are the most important carbonate producers. The bulk carbonate contents range from 24.4 to 82.9 wt.-% (see Fig. 2.2 and 2.6), showing an inverse relationship to the total organic carbon (TOC) content. The  $\text{CaCO}_3$  content of the fraction  $< 20 \mu\text{m}$  varies between 77.9 wt.-% at 7.69 Ma and 25.9 wt.-% at 9.36 Ma. This record follows the pattern of bulk carbonate signal. The calculated nannofossil carbonate content ranges from 64.03 wt.-% at 8.62 Ma to 20.31 wt.-% at 11.5 Ma, with a mean of 31.9 wt.-% and is obviously linked to the bulk carbonate record (see Fig. 2.6). Carbonate mass accumulation rates (MAR  $\text{CaCO}_3$ ) range between 1 - 7  $\text{g cm}^{-2} \text{ka}^{-1}$ , showing highest values between 10.9 and 10.5 Ma, and a decrease down to 2  $\text{g cm}^{-2} \text{ka}^{-1}$  in the following interval from 10.4 to 10 Ma (see Fig. 2). Between 10.0 and 9.7 Ma the MAR  $\text{CaCO}_3$  increases again to values of about 4  $\text{g cm}^{-2} \text{ka}^{-1}$ , followed by a decrease at 9.6 Ma down to 2 - 3  $\text{g cm}^{-2} \text{ka}^{-1}$  for more than 1.5 Ma. After 7.9 Ma a stepwise increase to values of 4.5  $\text{g cm}^{-2} \text{ka}^{-1}$  is recorded. Total organic carbon mass accumulation rates (MAR TOC) are very low ( $< 0.05 \text{g cm}^{-2} \text{ka}^{-1}$ ) throughout the entire interval with slightly higher values from 10.8 to 10.4 Ma and 9.5 to 9 Ma (see Fig. 2.6). Mass accumulation rates of terrigenous matter (MAR terr., data from Kastanja et al., subm.) range from 1 to 6  $\text{g cm}^{-2} \text{ka}^{-1}$  and show highest values between 11 and 10.5 Ma (see Fig. 2.6). In the low-carbonate interval from 9.6 to 9.0 Ma, MAR terr. shows slightly higher values than before and after this interval. Biogenic opal at Site 1085 only represents a minor component, with concentrations between 0.3 and 1.3 wt.-%. Only very few nannofossil species

significantly contribute to the nannofossil carbonate content (Fig. 5) which are either massive or extremely abundant. Thus, the common species *C. pelagicus*, *C. leptoporus*, *R. pseudoumbilicus* ( $> 7 \mu\text{m}$ , ‘large’), and *R. pseudoumbilicus* (5-7  $\mu\text{m}$ , ‘medium’), which are rather big in contrast to most other coccolithophore species, are dominant with respect to carbonate throughout the investigated interval.

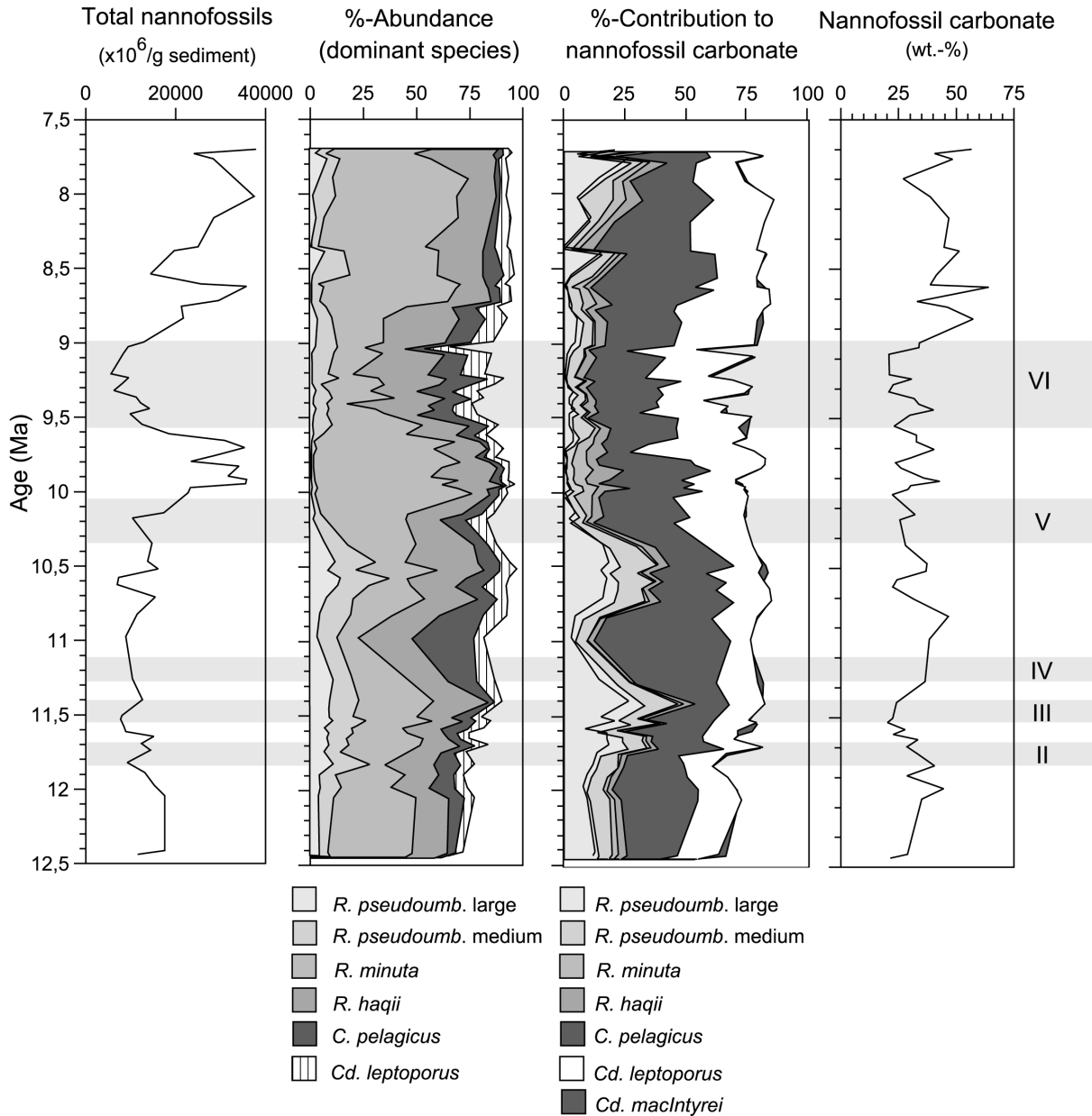


Fig.2.5. Absolute numbers of nannofossils, % - abundance of the dominant species, % - contribution of the dominant carbonate producers and absolute nannofossil carbonate content (wt.-%). The nanoplankton assemblage is clearly dominated by species of the genus *Reticulofenestra* which usually comprise more than 50 to 80% of the assemblage. Besides a few rather massive (or larger) species such as *C. leptoporus*, *C. pelagicus*, and *C. macIntyreii*, the numerically important reticulofenestrads likely produce a relatively high proportion of the nannofossil carbonate. Grey shaded bars indicate intervals that are characterized by dramatic drops in carbonate content.

Especially in the interval from 11.3 to 10.7 Ma *C. pelagicus* is the most important taxa in terms of carbonate contribution, although this species is not the most massive one. In the intervals 8.2 to 7.7, 10.7 to 10.2, and 12.3 to 11.3 Ma several species of the genus *Reticulofenestra* produce a relatively high proportion of the nannofossil carbonate (Fig. 2.5).

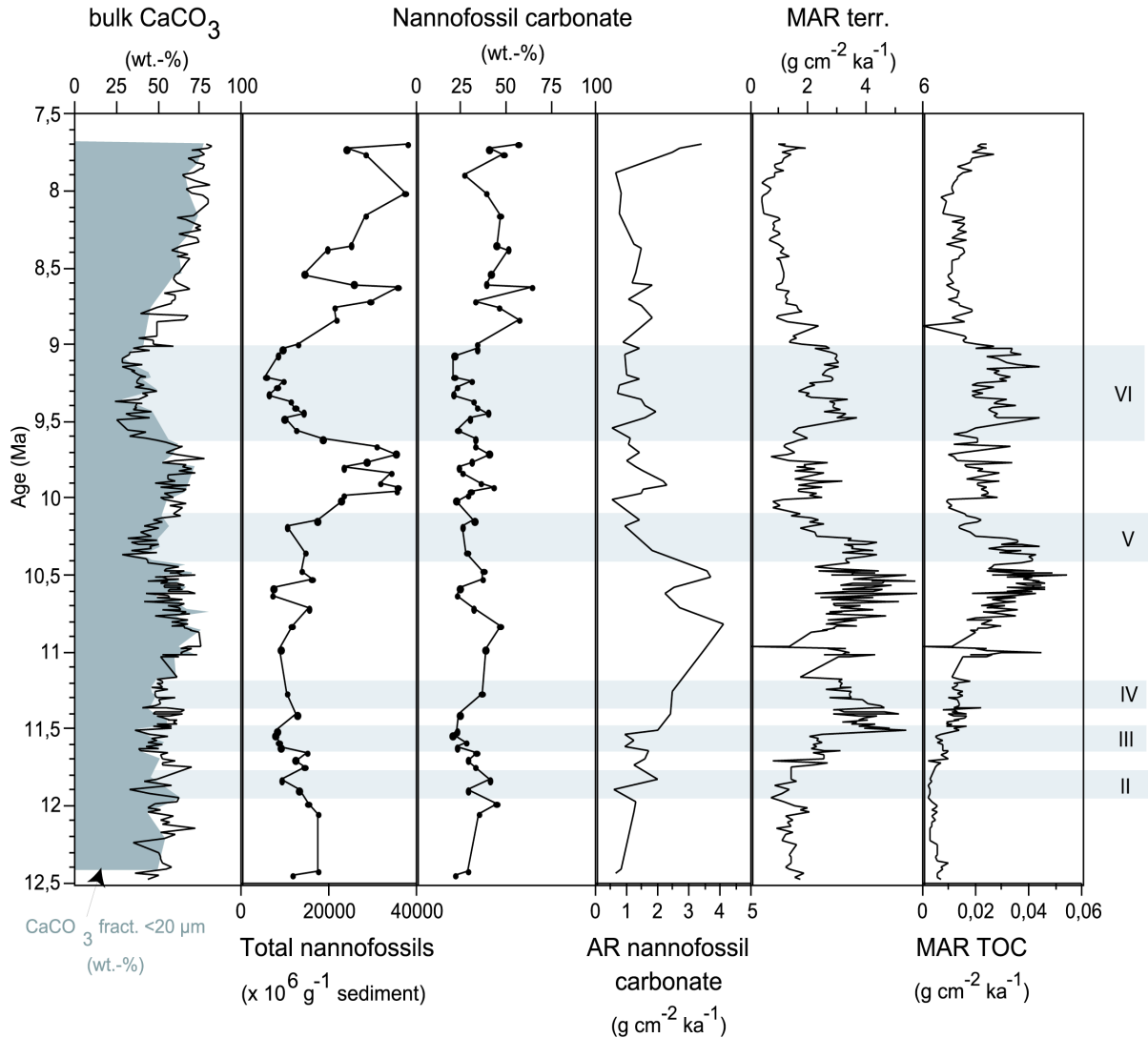


Fig. 2.6. Bulk carbonate content, carbonate content of the fraction  $< 20 \mu\text{m}$ , absolute numbers of total calcareous nannofossils and nannofossil carbonate mass contribution, accumulation rate of nannofossil carbonate, and mass accumulation rates both of terrigenous content (from Kastenja et al., subm.) and total organic carbon (TOC) in the investigated time interval of ODP Site 1085. Grey shaded bars indicate intervals that are characterized by dramatic drops in carbonate content.

Generally, calcareous nannofossils are well preserved throughout the entire interval studied. In most of the samples, even fragile specimens are present. However, a few drops in the absolute numbers, as well as a relative increase in massive and, therefore, more dissolution-resistant species such as *C. pelagicus* and *C. leptoporus*, could probably hint either towards weak carbonate dissolution or changes in the ecological conditions. However, the nannofossil

carbonate contents are never low enough to confirm more than very weak carbonate dissolution.

## 2.5 Discussion

### 2.5.1 Abundances and fluctuations in the calcareous nannofossil species record

In general, calcareous nannofossil assemblages found in the samples of Site 1085 are characterised by a moderate to relatively high species diversity and by abundant cosmopolitan forms, such as *R. minuta*, *R. haqii*, *R. pseudoumbilicus* (large and medium), or abundant temperate to subtropical species (e.g. *C. leptoporus*, *Helicosphaera* spp., *Umbilicosphaera* spp.). Species that have a preference to both cooler (*C. pelagicus*) and warmer temperate (e.g. *Discoaster* spp., *Sphenolithus* spp.) waters also occur in relatively high abundances.

Coccoliths of the genus *Reticulofenestra* are the most abundant taxa in samples of Site 1085 (see Fig. 3 and 4). Especially, the distribution patterns of *R. minuta* and *R. haqii* are of interest. Studies performed in modern assemblages show an opportunistic behaviour of ‘small placoliths’ (i.e. small reticulofenestrids, Okada and Honjo, 1973). Small reticulofenestrids increase their abundance during upwelling (Okada and Wells, 1997) and in periods of high fertility (Biekart, 1989). Negri and Villa (2000) have shown that these forms are – beside their biostratigraphic significance – important paleo-ecological and paleoceanographic indicators. Thus, the increase in the numbers of *R. minuta* and *R. haqii* from 10.1 to 9.7 Ma is suggested to indicate initial upwelling in this region, a finding that well corresponds to the studies of Siesser (1980) and Meyers et al. (1983).

*C. pelagicus* is well known as a modern cold-water species. Samtleben et al. (1995) have shown that its temperature-range includes even negative temperature values. The recent distribution of *C. pelagicus* is restricted to high latitudes where it is known from the North Atlantic and the Subarctic area (McIntyre and Bé, 1967; Okada and McIntyre, 1977; Samtleben et al., 1995; Baumann et al., 1999). Besides this small cold-water type found in subarctic environments, a large temperate form is known from upwelling regions (Baumann et al., 2000). This type is encountered here, which then is probably indicative for cool-temperate upwelling influenced condition in the studied region. The increase of *C. pelagicus* at about 11.9 Ma probably coincides with the initiation of upwelling at 12 Ma postulated by Diester-Haass et al. (2004).

Other species have a minor but consistent contribution to the assemblages in all of the samples, but they normally constitute less than 10% of the total assemblages. Their distribution often is more confused than the pattern of the prominent species (Fig. 2.4).

### 2.5.2 Variations in productivity and palaeoceanographic implications for the Benguela system based on nannofossil carbonate estimates

Carbonate contents at Sites 1085 show several decreases between 12.5 and 9 Ma (Westerhold et al., subm.). The deepest drop between 9.6 and 9 Ma is simultaneous with the ‘Carbonate Crash’ in the equatorial east Pacific Ocean (Lyle et al., 1995), whereas carbonate minima in the Caribbean occurred earlier – between 12 to 10 Ma (Roth et al., 2000). These lows in CaCO<sub>3</sub> contents and accumulation rates have been interpreted as times of increased carbonate dissolution and as a consequence of changes in deep water circulation (Roth et al., 2000).

Enhanced CaCO<sub>3</sub> dissolution should increase the benthic/planktic (B/P) foraminifera ratios. If the major depressions in CaCO<sub>3</sub> content between 12 and 9 Ma were due to carbonate dissolution, corresponding maxima in B/P ratios would be expected. Diester-Haass et al. (2004) have shown, that carbonate dissolution increased after the 9.6 to 9.0 Ma crash event until reaching maxima of up to 50% B/P between 8.5 and 7.5 Ma. However, they could not correlate changes in the B/P ratios (see Fig. 2.7) with the decreases in the carbonate content at Site 1085. Therefore, they concluded that dissolution is not the controlling factor in the CaCO<sub>3</sub> minima on the southwest African margin that correspond in time to the global ‘Carbonate Crash’. We therefore wondered whether changes in the productivity might have caused the decreases in carbonate content.

Calcareous nannofossils are the main carbonate producers. Our data show that nannofossils constitute a significant part of the carbonate content throughout the investigated interval at Site 1085. The most important contributors to the nannofossil carbonate are the relatively massive *C. pelagicus* and *C. leptoporus*, as well as the larger forms of reticulofenestrids (*R. pseudoumbilicus* ‘large’ and *R. pseudoumbilicus* ‘medium’). The calculated nannofossil carbonate content is obviously linked to the bulk carbonate record (Fig. 2.6) and is therefore indicative for the development of the productivity regime in this area. Highest absolute numbers of nannofossils as well as highest nannofossil accumulation rates in sediments at Site 1085 are observed during the intervals 10.1 to 9.7 Ma, 8.7 to 8.6 Ma, and 8.1 to 8.0 Ma.

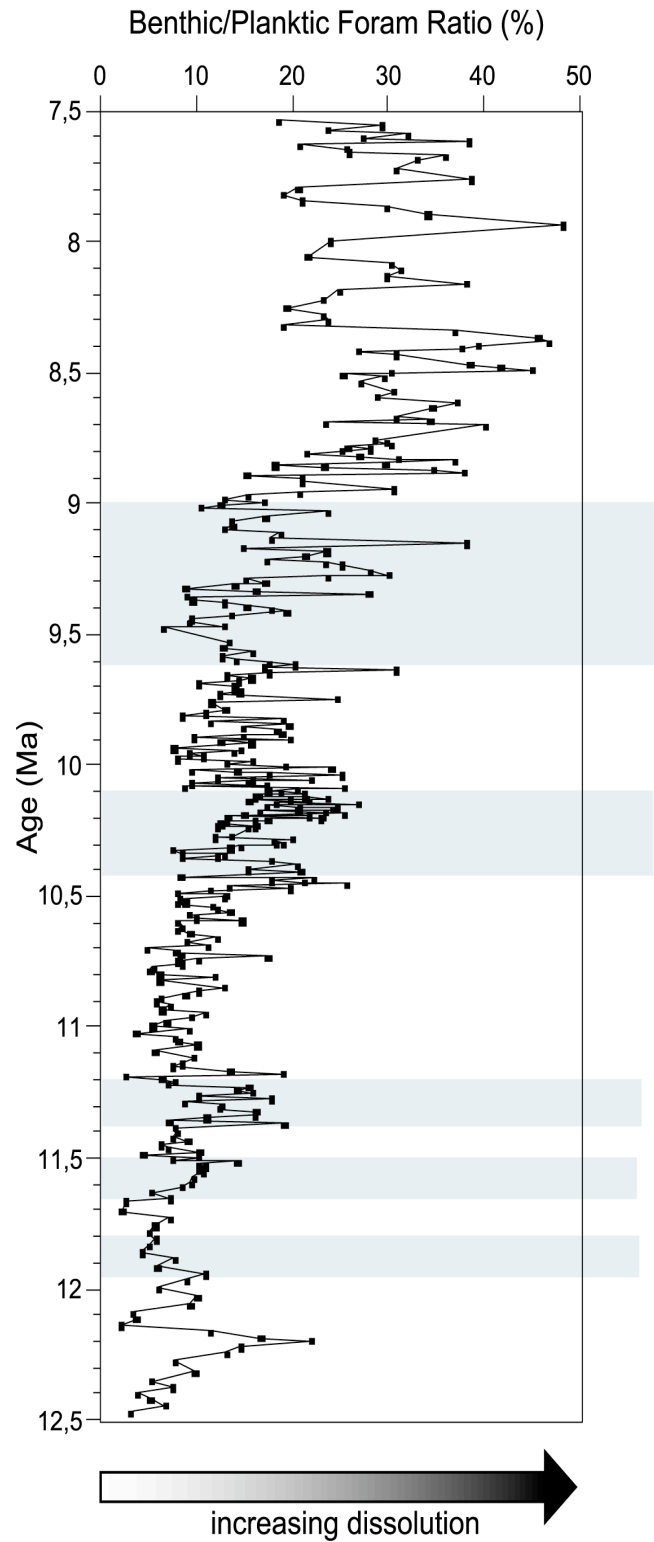


Fig. 2.7. Benthic/planktic foraminiferal ratio, expressed as the percent of benthic foraminifera in the total of benthic plus planktic foraminifera, in sediments of ODP Site 1085 (after Diester-Haass et al., 2004).

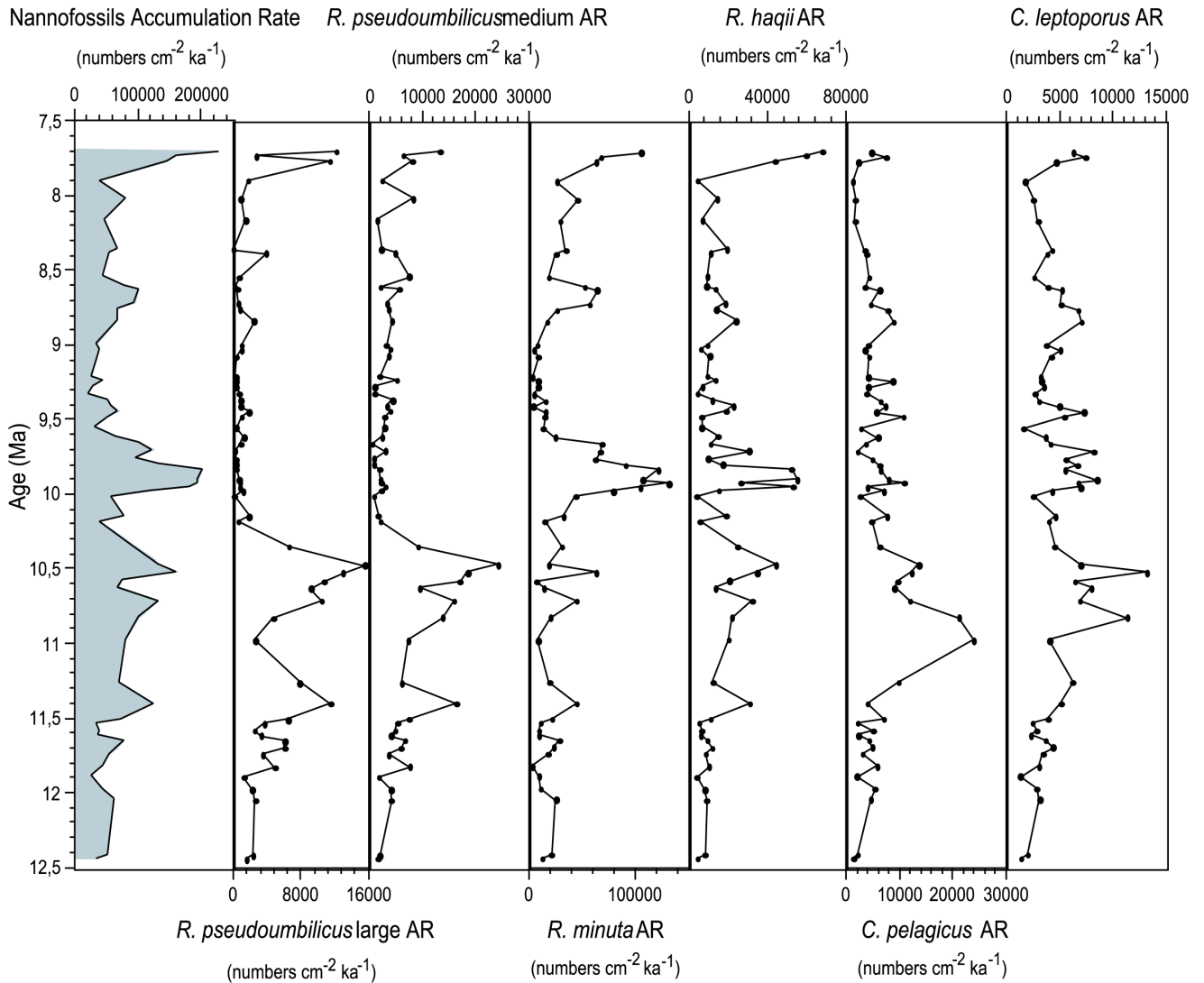


Fig. 2.8. Accumulation rates (all expressed in numbers  $\text{cm}^{-2}\text{ka}^{-1}$ ) of total nannofossils and the dominant species in sediments of ODP Site 1085.

Former studies have shown that highest contents of coccolithophorids were revealed in areas where oceanic and upwelled water mix compared to the oligotrophic ocean (e.g., Giraudeau, 1992; Giraudeau and Bailey, 1995). These nannofossils thrive preferentially well at the seaward edge of the upwelling centres (Shannon and Pillar, 1986; Wefer and Fischer, 1993) and may occasionally bloom in shallow waters of the inner and middle shelf during periods of relaxation of the upwelling process (Giraudeau and Bailey, 1995). Especially in the interval between 10.1 and 9.7 Ma nannofossils may generally be linked to the initiation of upwelling in the studied region. According to Diester-Haass et al. (2004), paleoproductivity, as reflected by total organic carbon, mass accumulation rates, the number of benthic foraminifers (NBF) and benthic foraminiferal accumulation rates (BFAR), began to increase at 12 Ma at Site 1085, coincident with the increase in terrigenous input. This would indicate

an earlier onset of upwelling as compared to the datum indicated by the nannofossil distribution at about 10 Ma.

In contrast, diminished numbers of calcareous nannofossils (Fig. 2.3 and 2.6) and lowest nannofossil accumulation rates (Fig. 2.8), as in the interval 9.6 to 9.0 Ma, probably characterise a time interval of weakened nannofossil productivity resulting in a decrease in the calcareous nannofossil content in the sediments. This decrease in nannofossil production could be one possible explanation for the major CaCO<sub>3</sub> depression in this interval. Diester-Haass et al. (2004) have shown, that during the time of the strongest decrease in carbonate concentration and highest pyrite content at 9.5 to 9.0 Ma, productivity was lower than prior to 10 - 9.5 Ma, as can be seen in lower CaCO<sub>3</sub> and TOC mass accumulation rates, lower numbers of benthic foraminifers and decreased benthic foraminiferal accumulation rates. Additionally, highest values in the accumulation rates of the terrigenous component (see Fig. 2.6) occur between 9.6 and 9.0 Ma, indicating a considerable increase in delivery of terrigenous matter by the Oranje River during this time interval, caused by a sea level regression that shifted the river mouth closer to the shelf edge (e.g., Haq et al., 1987).

In the time interval from 8.9 to 7.8 Ma, a stepwise increase of total nannofossil numbers and nannofossil accumulation rates is observed. That coincides with the recovery and gradual increase of the bulk carbonate values, ending up in highest values at about 7 Ma, followed by a period of high productivity - the so called 'biogenic bloom' period between 7 and 6 Ma (Farrell et al., 1995; Berger et al., 1993; Diester-Haass et al., 2004).

In general, the nannofossil distribution in the studied area seems to be probably related to the initiation of the Benguela Upwelling system. In addition, a correlation between increasing productivity and carbonate production by calcareous nanoplankton seems reasonable, although dilution by terrigenous materials played an important role in the interval from 9.6 to 9.0 Ma. Additionally, a very weak dissolution may have masked this connection.

## **2.6 Conclusion**

Calcareous nannofossils are a major component of Site 1085 sediments from the eastern South Atlantic off Namibia. As in many other parts of the world oceans, major oceanographic signals are preserved in nannofossil sediment assemblages, and thus, reflect spatial and temporal changes in surface-ocean circulation.

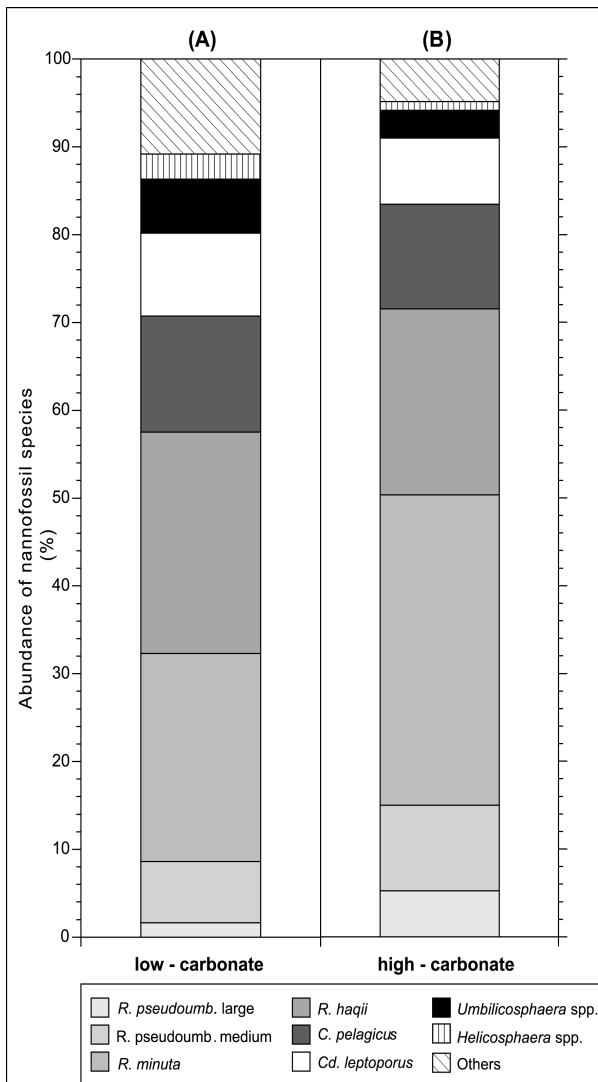


Fig. 2.9. Comparison of mean species composition in sediments of ODP Site 1085. (A) Variation in species composition in an interval (from 9.6 to 9.0 Ma) with low carbonate contents, (B) shows the species composition of two intervals (from 11.25 to 10.57 Ma and 8.8 to 8.38 Ma) with high carbonate contents.

The following conclusions and perspectives can be drawn from the present study.

- Analysis of calcareous nanofossils in sediment cores in these regions give useful information about the location of different water masses in the past, and consequently, about the paleoceanography in this area. The increasing of *R. minuta* and *R. haqii* from 10.1 to 9.7 Ma most probably indicates initiating upwelling in this region.
- Diminished numbers of calcareous nanofossils, such as in the interval 9.6 to 9.0 Ma, probably characterise time periods of weakened nanofossil productivity resulting in a decrease of nanofossil carbonate content. We therefore conclude that this decrease in calcareous nanoplankton production is one possible explanation for the ‘Carbonate Crash’ between 9.6 and 9.0 Ma.
- In the time interval from 8.9 to 7.8 Ma, a stepwise increase of total nanofossil numbers and nanofossil accumulation rates coincides with the recovery and graduate increase of the bulk carbonate values, ending up in highest values at about 7 Ma.

- A correlation between productivity in the initiated upwelling and carbonate production by nannofossils seems reasonable. Calcareous nannofossils account for more than half of the carbonate with peak contribution up to 65 wt.-%. The most important contributors are *C. pelagicus*, *C. leptoporus* and *R. pseudoumbilicus*.
- The initiation of the Benguela Upwelling system started at about 10 Ma based on nannofossil distribution patterns and nannofossil accumulation rates. This is a later onset as compared to carbon and coarse fraction data of Diester-Haass et al. (2004).

### **Acknowledgements**

We thank H. Heilmann, B. Kokisch, and R. Henning for laboratory assistance and M.-M. Kastanja and T. Bickert for their helpful suggestions in pre-reviewing the manuscript. Discussions with B. Beckmann, H. Paulsen, T. Westerhold, S. Steinke, and J. Schwarz greatly increased the quality of the initial manuscript. We gratefully acknowledge thoughtful comments from the reviewers Samantha Gibbs and José-Abel Flores. This research used samples provided by the Ocean Drilling Program (ODP). ODP is sponsored by the U.S. National Science Foundation (NSF) and participating countries under management of Joint Oceanographic Institutions (JOI), Inc. Funding for this research was provided by Deutsche Forschungsgemeinschaft (DFG) (Research Center for Ocean Margins, RCOM publication Nr. 0325).

# **Chapter 3**

## **Manuscript 2:**

**ODP Site 1085 nannofossil assemblages and fine-fraction carbonate stable isotopes as indicators  
for Middle to Late Miocene Upwelling initiation**



## **ODP Site 1085 nannofossil assemblages and fine-fraction carbonate stable isotopes as indicators for Middle to Late Miocene Benguela Upwelling initiation**

*Regina Krammer*<sup>1</sup>, *Karl-Heinz Baumann*<sup>2</sup>, *Torsten Bickert*<sup>2</sup>, *Rüdiger Henrich*<sup>2</sup>

<sup>1</sup> *Research Center Ocean Margins, University of Bremen, Germany*  
(*krammer@uni-bremen.de*)

<sup>2</sup> *Department of Geosciences, University of Bremen, Germany*

Submitted to *Marine Micropaleontology*

### **Abstract**

We compared Middle to Late Miocene calcareous nannofossil data with the isotopic records of the fraction smaller than 20  $\mu\text{m}$  (including all calcareous nannofossils) and of the clay fraction (including calcareous nannofossils  $< 5 \mu\text{m}$  in diameter) to decipher a possible influence of changing nannofossil assemblages on the carbonate isotopes. The studied site (ODP Site 1085) is located on the continental slope off Namibia in the eastern South Atlantic. To use nannofossil stable isotopes as a reliable proxy for paleoceanographic reconstruction of temperature and seawater chemistry, changes in nannofossil assemblages have to be taken into consideration. Our data show similar isotopic records for bulk nannofossil carbonate and the clay fraction carbonate despite different species compositions. This suggests a limited range of interspecific isotopic vital effects for the major Miocene nannofossil species even though some distinct offsets between these records are recognizable. These offsets in the isotopic signals can be explained by the contribution of nannofossils smaller than 5  $\mu\text{m}$ . There is evidence that isotopic fractionation becomes less sensitive at larger cell diameters. This would explain the positive shift in oxygen isotopes in the clay fraction in our data. Additionally, we demonstrate the potential of nannofossil stable isotopes as indicators of shallow mixed layer conditions by comparing their records with those of coexisting planktic foraminifers. In general, nannofossil carbonate stable isotopes are in good correspondence with those of deep-dwelling planktic foraminifers. Based on our data, we suggest that nannofossil carbonate isotopes reflect surface-water hydrographic conditions of the late winter-early spring period, when relatively cool, nutrient-rich subsurface water mass is entrained into surface waters by vertical mixing. In contrast, surface-dwelling planktic foraminifers reflect the post-deep-mixing, relatively warmer stratified surface waters. This

implies that paired analyses of nannofossil carbonate and surface-dwelling planktic foraminifers  $\delta^{18}\text{O}$  can be used to reconstruct paleoseasonality. The seasonal sea-surface  $\delta^{18}\text{O}$  amplitude ranges between  $-0.5$  and  $-2$  ‰, showing an decrease from 10.4 and 9.1 Ma. This indicates that seasonality became weaker during this interval, corresponding with the initiation of the Benguela Upwelling system at about 10 Ma.

*Keywords:* calcareous nannoplankton; fine-fraction stable isotopes; Namibia upwelling; Miocene; paleoceanography

### 3.1 Introduction

Today, one of the largest upwelling regions in the world is the Benguela Upwelling system, with productivity values  $\geq 180$  g C/m<sup>2</sup>yr (Berger, 1989). It extends along the West-African margin from South Africa to the Walvis Ridge, and is characterised by organic-rich sediments.

Southerly and southeasterly trade winds in this region drive an offshore surface drift and cause a coastal upwelling of cold, nutrient-rich water from depths of 200 to 300 m (Hart and Currie, 1960) over most of the continental shelf. Upwelling at present occurs in a number of cells south of about 18°S, with a major, in principle semi-permanent cell at 27°S (Fig. 3.1; Shannon and Nelson, 1996). This upwelling leads to enhanced biological productivity off Namibia, evident from relatively high to moderate chlorophyll  $\alpha$  concentrations (Giraudeau and Rogers, 1994). Today, the African coast along the upwelling area is occupied by the dry Namib Desert; the only perennial river is the Oranje River. High primary production in this region is driven by two different mechanisms: (1) SE trade winds and the cold northwest-flowing Benguela Current induce coastal upwelling along the continental shelf (Stramma and Peterson, 1989). (2) Another high productivity systems off SW-Africa is positioned at the Benguela-Angola front, where the northward directed Benguela Current mixes with the warmer, southward flowing Angola Current. In a recent study, Sarmiento et al. (2004) proposed that nutrient advection from the sub-Antarctic region plays an important role in these upwelling systems.

Previous studies dealing with the Miocene history of the southwest African upwelling system have shown that the initiation of high productivity started at about 10 Ma (Siesser, 1980; Meyers et al., 1983) and postulated that the Benguela Current (BC), and hence the upwelling area migrated progressively northward within the late Miocene and Pliocene

(Diester-Haass et al., 1990, 1992). These earlier interpretations of the BC upwelling system suffered from poor temporal resolution, incomplete sediment sequences and information from only one location (DSDP Site 362/532) on Walvis Ridge (Bolli et al., 1978; Hay et al., 1984; Hay and Brock, 1992). In the interval between 10.5 Ma to 5.4 Ma, upwelling was stronger during glacial periods over Walvis Ridge, whereas in interglacials it was weaker because the Benguela Current turned to the West within the Cape Basin and did not reach Walvis Ridge. In a recent paper, Diester-Haass et al. (2004) summarized some sedimentological and coarse fraction results of three sites (ODP Sites 1085, 1086, and 1087) drilled along the continental slope off SW Africa. The authors proposed an increase in paleoproductivity, reflected by TOC MAR (total organic carbon accumulation rate), NBF (numbers of benthic foraminifers) and BFAR (benthic foraminiferal accumulation rate), at about 12 Ma. However, these proxies record the increase of organic matter export and burial in this area. They do not explain what has happened in the surface waters and the photic zone at that time.

This is the central focus of this study. In particular, we address the following questions:

- Does the stable isotopic record of the Miocene nannofossil carbonate provide any valuable information about surface ocean environmental changes in the eastern South Atlantic during the investigated interval?
- How are changes in the nannofossil assemblages and in the nannofossil carbonate contribution linked to the increased primary production in the studied region during the Middle to Late Miocene?
- Is there any measure of a change in seasonality during the onset of Benguela Upwelling?

We address these questions by comparing Middle to Late Miocene calcareous nannofossil data with the isotopic records of the fraction smaller than 20  $\mu\text{m}$  (including all calcareous nannofossils) and the clay fraction (including calcareous nannofossils smaller than 5  $\mu\text{m}$  in diameter) during the Middle to Late Miocene climate transition.

## **3.2 Material and methods**

### **3.2.1 Study area**

Sediment records obtained during ODP Leg 175 provided a new opportunity to study the history of upwelling in continuous and relatively undisturbed sediment sequences from multiple locations along the southwest African margin. ODP Site 1085A was drilled during Leg 175 and is located at the SW-African continental margin (Fig. 3.1) at 29°22.45'S and

13°59.41'E in 1713 m water depth close to the Oranje River mouth. Site 1085A comprises a complete record of hemipelagic sediments down to 14 Ma.

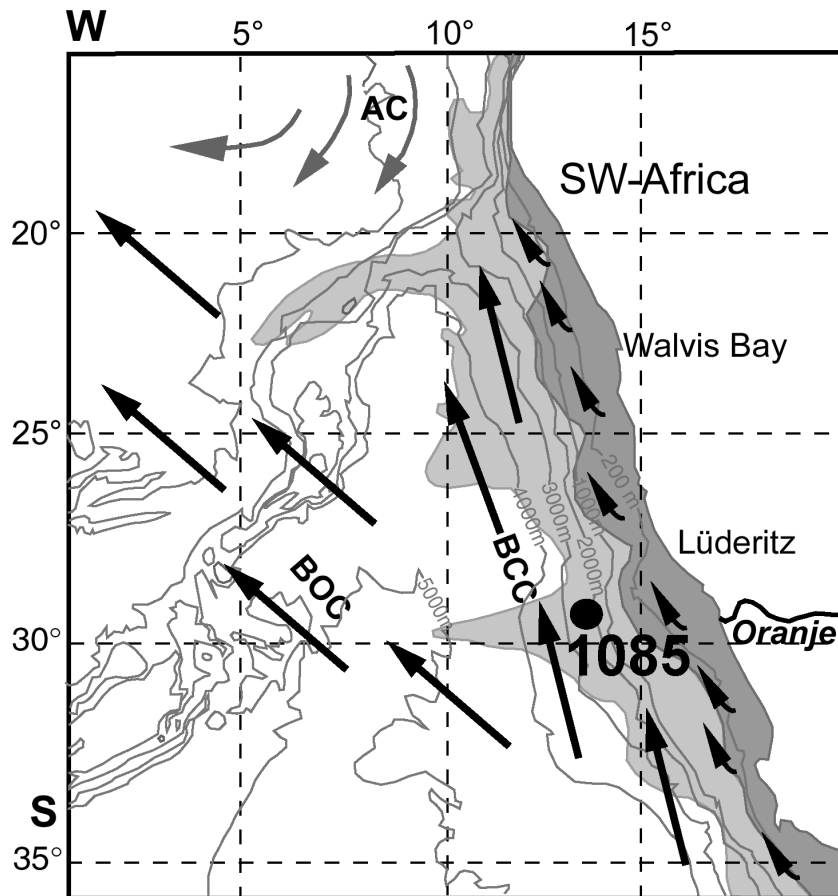


Fig. 3.1. Schematic surface current pattern off Southwest Africa and the location of ODP Site 1085. Black arrows indicate relative cool currents of the Benguela Coastal Current (BCC) and the Benguela Oceanic Current (BOC). Grey arrows show the flow pattern of the warm Angola Current (AC). Dark shading indicates coastal upwelling, whereas light shading shows the extension of upwelling filaments into the mixing zone with oligotrophic open ocean waters (after Shannon and Nelson 1996).

Sediments are dominated by greenish-grey, foraminifer-bearing nannofossil ooze, diluted by various amounts of silt and clay. The studied interval between 569 and 399 mbsf covers the Middle to Late Miocene (12.5 to 7.7 Ma), including the late Middle Miocene onset of the Benguela Current upwelling system and its associated elevated marine productivity (Diester-Haass et al., 2002, 2004). Sedimentation rates range from 3-7 cm/ka according to an astronomically calibrated age model, generated by orbital tuning of a high-resolution composite XRF-Fe intensity record of ODP Sites 1085 and 1087 (Westerhold et al., 2005).

### 3.2.2 Sediment treatment

We set 2 g of each freeze-dried bulk sample aside for carbon analysis, and the remaining material was washed through 20 µm-sieves to detach nannofossils from adult and juvenile

foraminifera (Fig. 3.2). SEM observations of the fraction < 20 µm indicated that the calcareous particles in this fraction are almost exclusively composed by calcareous nannofossils. After separating the fraction < 2 µm (clay fraction) using the Atterberg settling technique, SEM analysis of the clay showed, that nannofossils smaller than 5 µm (i.e., *Reticulofenestra minuta* and *Reticulofenestra haqii*) in diameter make up the most important part of the calcareous clay.

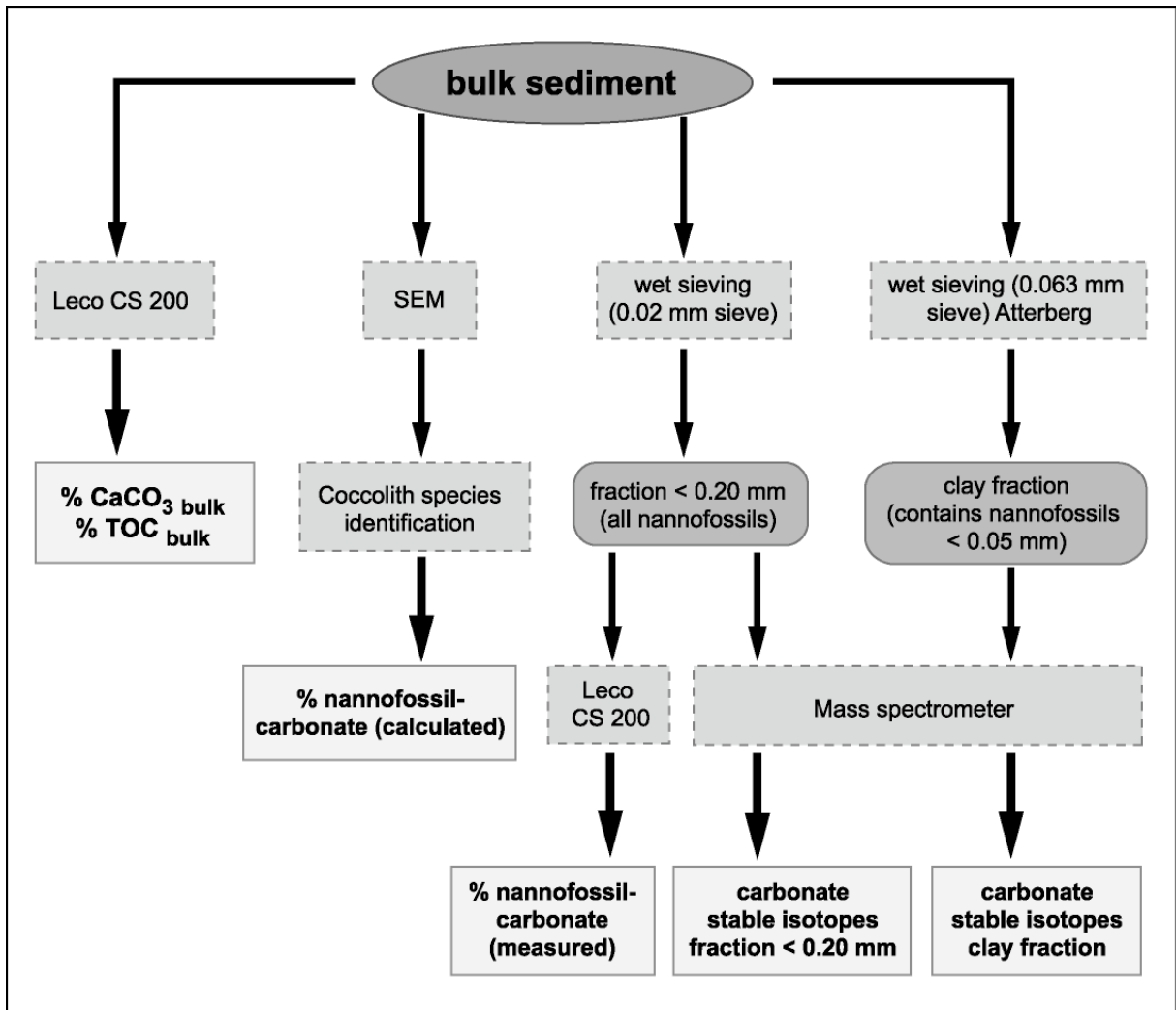


Fig. 3.2. Flow chart of methods and sample treatment.

Nannofossil assemblages in the bulk sediment were counted by scanning electron microscopy (SEM) using a Zeiss DMS 940A at the Department for Sedimentology/Paleoceanography in Bremen. Counts and size measurements were converted into volume and mass contribution of each species using the approach of Young and Ziveri (2000) with given shape factors for various coccolith types, the average length of a species, and the density of calcite.

For isotope measurements, the samples were analyzed using a Finnigan MAT 252 micromass-spectrometer coupled with a Finnigan automated carbonate device at the Department for Marine Geology in Bremen. The carbonate was reacted with orthophosphoric acid at 75°C. The reproducibility of the measurements, as referred to an internal carbonate standard (Solnhofen limestone), is  $\pm 0.07$  ‰ and  $\pm 0.05$  ‰ (1s over a one year period) for oxygen and carbon isotopes, respectively. The conversion to the VPDB-scale was performed using the international standard NIST 19.

### 3.3 Results

The entire interval from 12.5 to 7.7 Ma at Site 1085 is dominated by fine carbonate silt, therefore calcareous nannofossils are the most important carbonate producers. The calculated nannofossil carbonate content ranges from 64.03 wt.% at 8.62 Ma to 20.31 wt.% at 11.5 Ma, with a mean of 31.9 wt.% and is obviously linked to the bulk carbonate record (Krammer et al., in press, see Fig. 3.3). Only very few species significantly contribute to the bulk nannofossil carbonate content (Fig. 3.4, Krammer et al., 2005 in press) which are either massive or extremely abundant. Large species, such as *Coccolithus pelagicus*, *Calcidiscus leptoporus*, *Reticulofenestra pseudumbilicus* (> 7  $\mu\text{m}$ , ‘large’) and *Reticulofenestra pseudumbilicus* (5-7  $\mu\text{m}$ , ‘medium’), are most important contributors for carbonate. Nannofossil assemblage counts indicate that the most abundant taxa in samples of ODP Site 1085 belong to the genus *Reticulofenestra*. Especially, the distribution patterns of *Reticulofenestra minuta* and *Reticulofenestra haqii* are of interest, because they build most of the carbonate in the clay fraction.

Although the species contribution to the clay fraction and the fraction < 20  $\mu\text{m}$  are significantly different, these fractions have similar carbon and oxygen isotopic values. Only in some intervals the records differ by up to 2.5 ‰ (Fig. 3.4). In both fractions the calcareous nannofossil isotopic records are quite similar in trends and absolute values with exception of some intervals, which will be described in the following.

The isotopic records of the fraction < 20  $\mu\text{m}$  (see Fig. 3.4), including the bulk nannofossil carbonate dominated by *Coccolithus pelagicus* and *Calcidiscus leptoporus*, follow the overall trends of global ocean isotope records during the Middle to Late Miocene (Fig. 3.5; Zachos et al., 2001). In general,  $\delta^{13}\text{C}_{<20\mu\text{m}}$  starts with values of about 2 ‰ at 12.5 Ma, followed by a slight decrease until 10.4 Ma, with highest values of 2.3 ‰ at 11.4 Ma. In comparison, the  $\delta^{13}\text{C}$  record of the clay fraction starts with values of about 1.4 ‰ at 12.5 Ma, showing a negative shift of about 0.5 to 0.8 ‰ compared to the bulk nannofossil carbonate signal. This

offset between the two records is decreasing in the early Late Miocene. At 10.8 Ma the data of both the bulk nannofossil carbonate and the clay fraction show very similar values until 10.4 Ma. In the interval between 10.4 and 9.8 Ma the lowest values occur in the  $\delta^{13}\text{C}_{<20\mu\text{m}}$ .

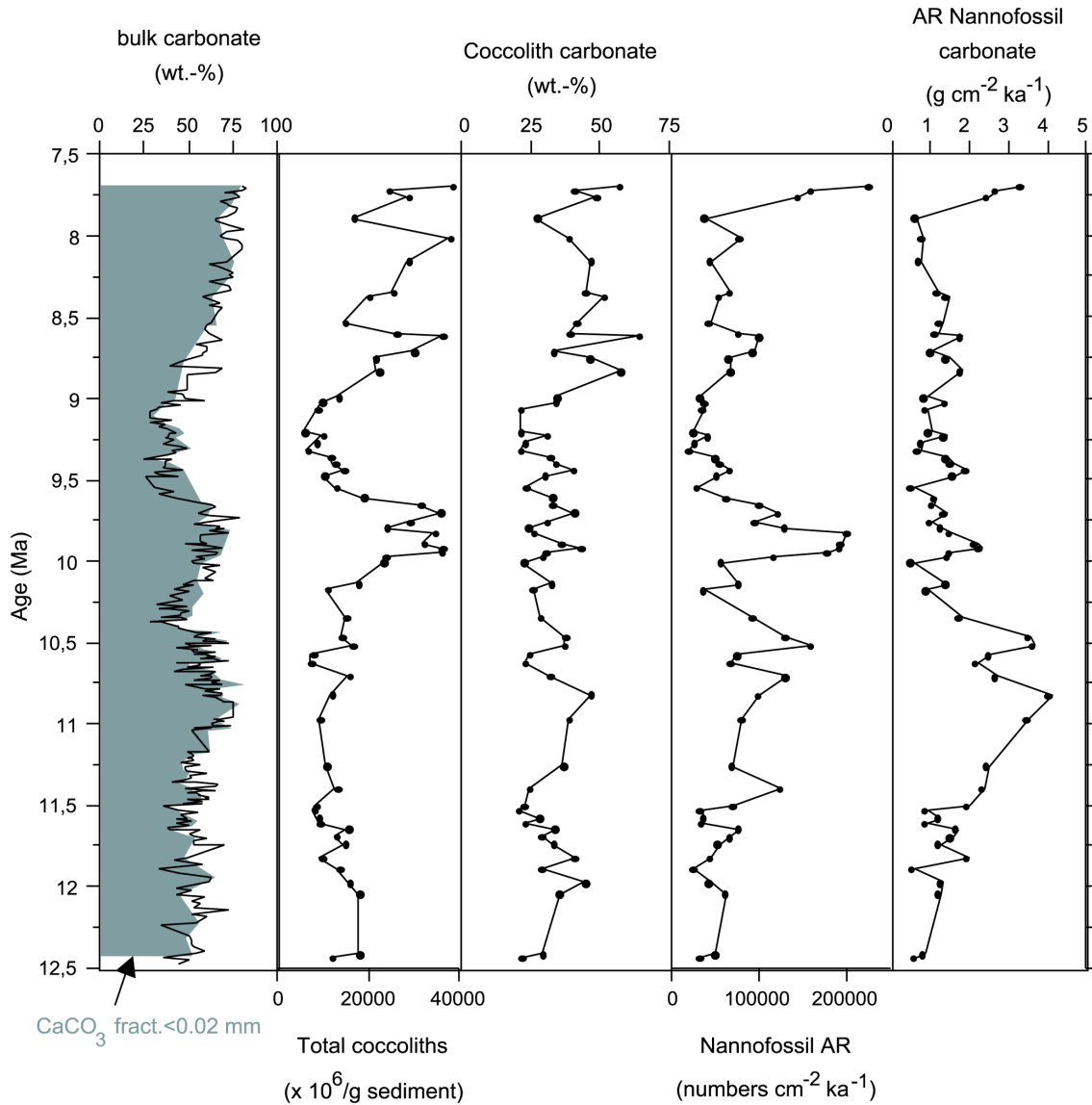


Fig. 3.3. Bulk carbonate content, CaCO<sub>3</sub> content of the fraction < 20 μm CaCO<sub>3</sub>, absolute numbers of the total nannofossil assemblage, calculated nannofossil carbonate mass contribution, nannofossil accumulation rate and accumulation rate of nannofossil carbonate (from Krammer et al., acc.).

Additionally, the carbon isotope record shows stronger amplitude variations compared to values below and above this interval. A positive shift in  $\delta^{13}\text{C}_{<20\mu\text{m}}$  is remarkable between 9.8 and 9.7 Ma reaching values of more than 1.5 ‰, followed by a stepwise decrease until 9.4 Ma. From 9.4 to 9.1 Ma another interval with slightly higher amplitudes occur. Upwards, the carbon isotopic record of the bulk nannofossil carbonate shows a continuous increase until 7.8 Ma with the highest value in  $\delta^{13}\text{C}_{<20\mu\text{m}}$  of 1.65 ‰. From 8.8 Ma to the end of the investigated

time span the carbon isotopes show a decreasing tendency. The clay carbon isotopes remain more or less constant from 9.8 to 9.0 Ma. From 9.0 Ma up to 7.7 Ma, the signals of the clay fraction become more depleted than the bulk nannofossil carbonate data.

In general, the  $\delta^{18}\text{O}$  records of the fraction  $< 20 \mu\text{m}$  exhibit a relatively constant or slightly decreasing trend throughout the investigated interval (Fig. 3.4), with values between 1.9 and  $-0.01 \text{‰}$ . The most depleted  $\delta^{18}\text{O}_{<20\mu\text{m}}$  values occur between 10.2 and 9 Ma, the highest oxygen isotopes are recorded from 11.6 to 11.3 Ma and 10.7 to 10.4 Ma. In comparison, the  $\delta^{18}\text{O}$  record of the clay fraction (Fig. 3.4) starts with values around 2.6 ‰ at 12.5 Ma, showing an offset of less than 1.5 ‰ in comparison to the bulk nannofossil carbonate signal. From 12.3 to 11.4 Ma the clay fraction values are decreasing; and the difference between these two records becomes smaller. Between 11.4 and 10.3 Ma, the  $\delta^{18}\text{O}_{\text{clay}}$  record shows almost identical values like the fraction  $< 20 \mu\text{m}$ , ranging between 0 and 1.5 ‰. In the following interval until 9.6 Ma, the  $\delta^{18}\text{O}_{\text{clay}}$  displays a positive shift up to highest values of 2.83 ‰. Between 9.6 and 9.0 Ma the  $\delta^{18}\text{O}_{\text{clay}}$  record shows similar values like the fraction  $< 20 \mu\text{m}$ , ranging between 0.4 and 1.7 ‰. From 9.0 Ma to the end of the investigated interval the oxygen isotopes reveal an offset of about 0.5 ‰ in comparison to the bulk nannofossil isotopic signal.

### 3.4 Discussion

Stable isotopic measurements in biogenic carbonates are a key tool for paleoceanographic studies. The oxygen isotopic ratio of marine biogenic carbonates is widely used to reconstruct the temperature of ancient oceans and to trace changes in oxygen isotope ratio of seawater. The carbon isotope ratio is used to reconstruct variations in the carbon isotopic composition of dissolved inorganic carbon in the ocean, which is controlled by organic matter production and respiration, but also by the exchange of carbon between different reservoirs. The paleoceanographic reconstructions of surface ocean conditions from stable isotopic measurements mostly rely on the analysis of planktonic foraminifers because individual species can be used which represent a certain habitat and which do have a small and limited range of isotopic vital effects. In sediments where planktonic foraminifers in the coarse fraction are sparse, bulk carbonate has also been used for stable isotopic analysis (e.g., Clarke and Jenkyns, 1999; Vonhof et al., 2000). However, interpretation of bulk carbonate isotopic data is critical, because bulk carbonate can be composed of shells secreted by different

planktonic organisms, such as juvenile foraminifers and their fragments as well as calcareous nannoplankton.

Calcareous nannofossils, tiny plates produced by coccolithophorid algae, are known as sensitive indicators of environmental conditions because they depend on temperature, salinity, and nutrients, as well as the availability of sunlight (e.g., Giraudeau, 1992; Winter and Siesser, 1994).

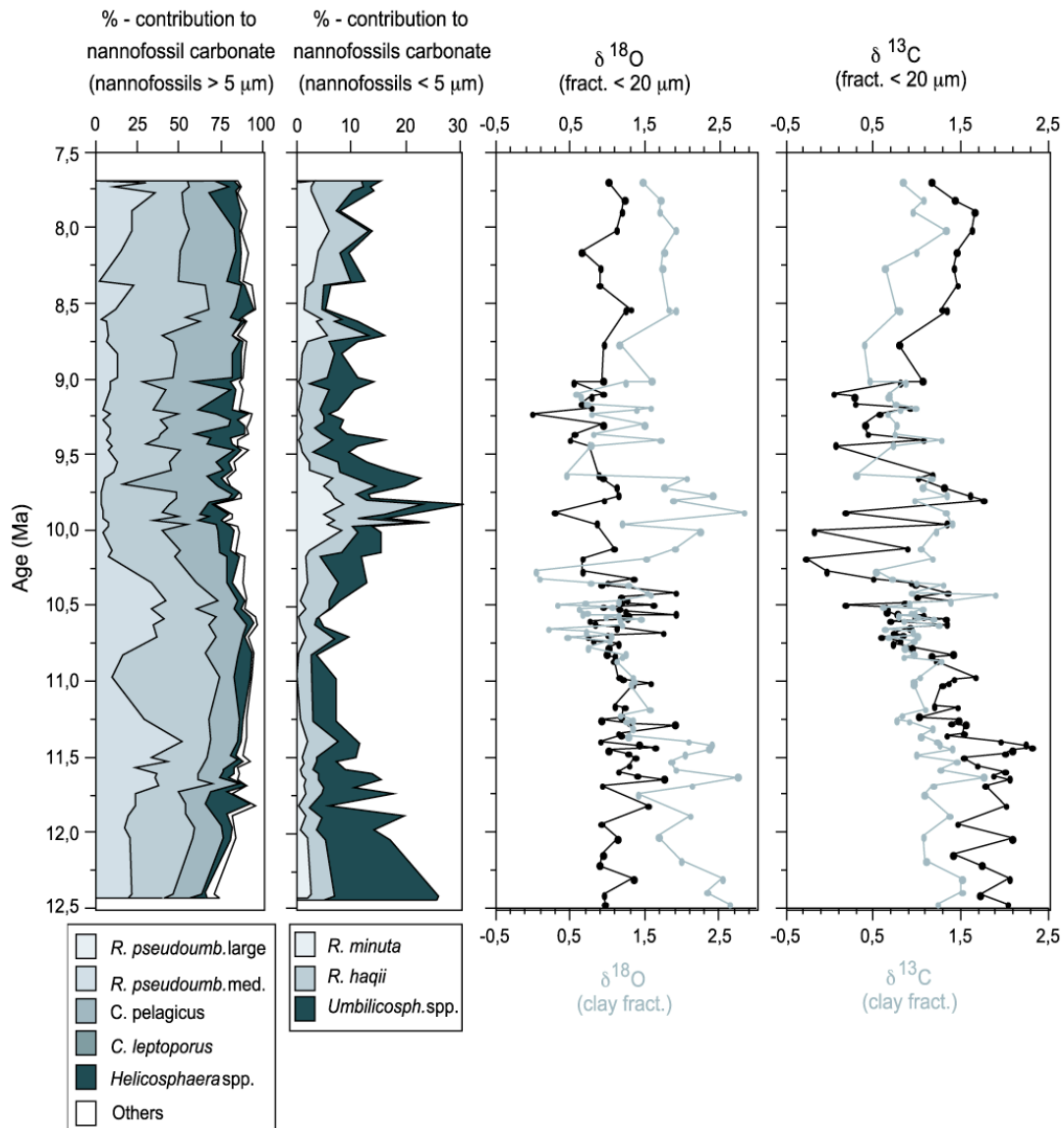


Fig. 3.4. %-contribution both of the dominant carbonate producers (nannofossils > 5 μm) and the smaller, but very abundant species (nannofossils < 5 μm in diameter), stable isotopic data (in ‰) of both the fraction < 20 μm and the clay fraction (in light grey).

This plankton group responds sensitively to fluctuations, in particular to changes in surface-water conditions. However, because coccoliths grown in culture experiments exhibit a nearly 5 permil array of interspecific vital effects in both oxygen (Dudley and Goodney, 1979; Dudley et al., 1980, 1986; Ziveri et al., 2003) and carbon isotopes (Ziveri et al., 2003),

changes in the relative carbonate contribution of different calcareous nannofossil species may cause significant variance in bulk carbonate isotopic records, partially masking signals of changing environmental conditions. Furthermore, changes in the nannofossil assemblages over longer time intervals may have considerable impact on the isotope record although the vital effect cannot be constrained for extinct species. Consequently, the validity of bulk carbonate isotopic results has been called into question for many records (e.g., Paull and Thierstein, 1987, 1990; Shackleton and Hall, 1997).

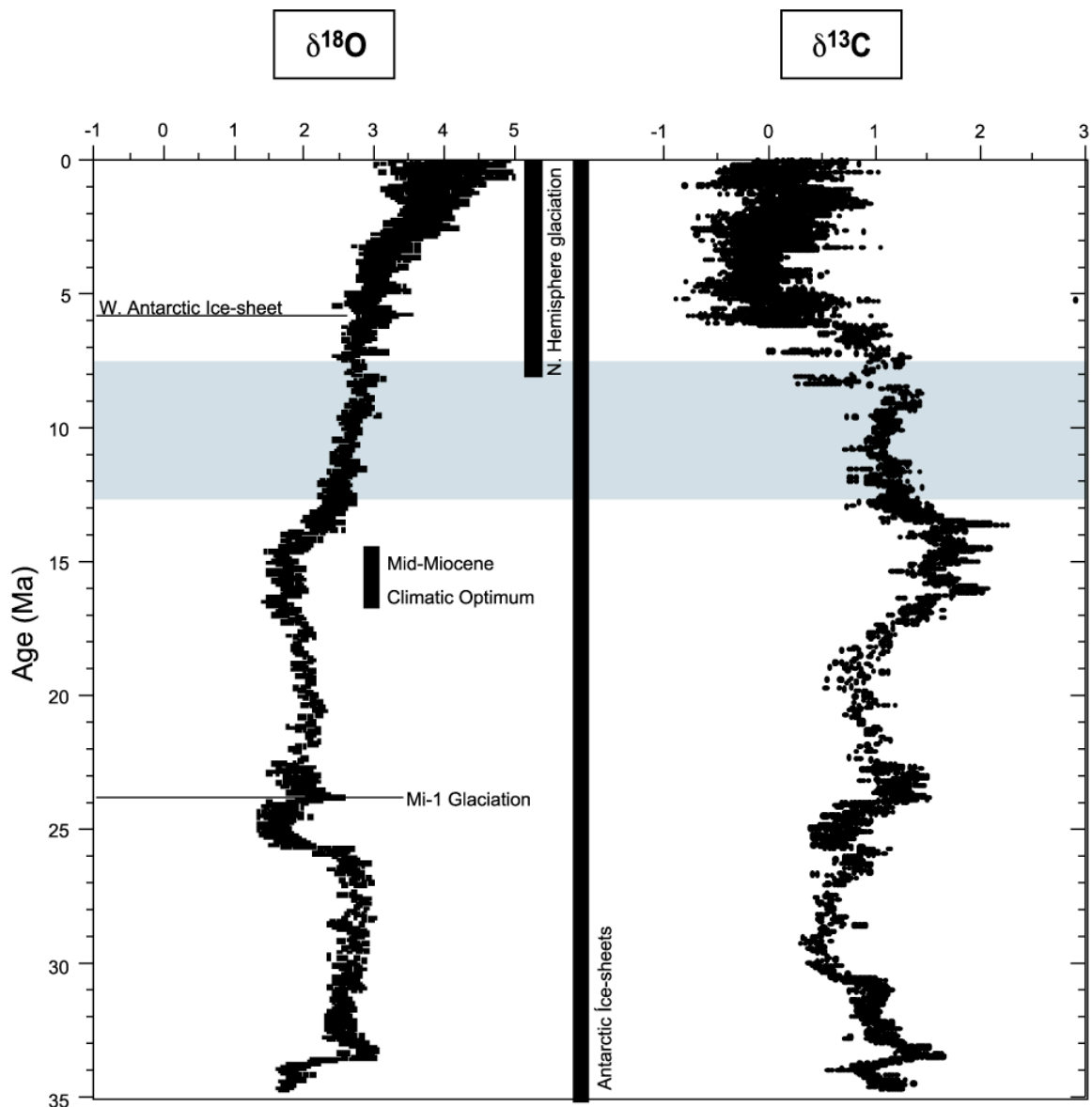


Fig. 3.5. Global deep-sea oxygen and carbon isotope records (in ‰) based on data from more than 40 DSDP and ODP Sites (after Zachos et al., 2001). Most of the data were derived from analyses of two common and long lived benthic foraminifers, *Cibicidoides* and *Nuttalides*. The light grey bar indicates the investigated interval of the present study.

### 3.4.1 Origin of interspecific isotopic variation in calcareous nannofossil carbonate

At ODP Site 1085, the isotopic data in both the bulk nannofossil carbonate and the clay fraction with different species composition, suggest a limited range of interspecific isotopic

vital effects in the major Miocene nannofossil species. In some intervals, for example in the time span between 10.28 and 9.6 Ma, the oxygen isotopes of the clay fraction (including all nannofossils < 5 µm in diameter, Fig. 3.4) show a positive shift up to highest values of 2.83 ‰ in comparison to bulk nannofossil isotope data. This offset in the isotopic signals might be explained by the contribution of nannofossils smaller than 5 µm (*Reticulofenestra minuta*, *Reticulofenestra haqii*, *Umbilicosphaera* spp.). When the fine nannofossil carbonate reaches 20 to 30 wt.% of the total nannofossil carbonate, the oxygen isotopic record of the clay fraction shows more enriched values. This is also recognizable in intervals from 12.5 to 11.9 Ma, from 11.7 to 11.4 Ma and 8.6 to 7.7 Ma. Different isotopic compositions in different species of calcareous nanoplankton may arise from different depth habitats within the water column or from species-specific vital effects in isotopic fractionation. Interspecific vital effects in modern coccolithophorids tend to produce positively correlated fractionations in carbon and oxygen isotopes in coccoliths (Paull and Thierstein, 1987; Ziveri et al., 2003) with increasing isotopic enrichment with smaller cell diameters. It seems possible, that isotopic fractionation becomes less sensitive to cell diameter at larger cell diameters (Ziveri et al., 2003; Stoll, 2005). This would explain the positive shift in oxygen isotopes in the clay fraction including all nannofossils < 5 µm in our data. The reason for the increase in *R. minuta* and *R. haqii* values from 10.1 to 9.7 Ma is most probably the initiation of upwelling in this region (Krammer et al., 2005 in press).

#### 3.4.2 Comparison of fine-fraction and foraminiferal stable isotope records

Isotopic records of surface- and deep-dwelling planktic foraminifera from Paulsen et al. (manuscript in preparation) are plotted along with data of the fraction < 20 µm and the clay fraction for Site 1085 in Fig. 3.6 and Fig. 3.7. Fine-fraction oxygen isotopic values are, in general, similar to those of deep-dwelling planktic foraminifera (*Globoquadrina dehiscens* and *Globorotalia conoidea*), in many cases they even overlap for most of the investigated interval (Fig. 3.6). In contrast, the surface-dwelling foraminifer *Globigerinoides trilobus* shows more depleted isotopic values with an offset of more than 1 ‰ in comparison to the nannofossil isotopic record. That coincides well with data from Ennyu et al. (2002) where an offset between *Globigerinoides* and fine-fraction isotopes of 1 to 1.5 ‰ was described. A similar relationship between < 63 µm-fraction and *Globigerinoides* isotopic trends for the Miocene is reported from Site 926 on the Ceara Rise, western equatorial Atlantic (Shackleton and Hall, 1997).

Carbon isotopic values of the fraction  $< 20 \mu\text{m}$  are, on average, depleted with respect to the corresponding surface-dwelling planktic foraminifers *Globigerinoides trilobus* and *Globigerina bulloides* throughout the Middle to Late Miocene at Site 1085 (Fig. 3.7). These results coincide with studies of Ennyu et al. (2002) which showed at ODP Site 516 (Rio Grande Rise, South Atlantic) and Site 608 (King's Trough, North Atlantic), that fine-fraction  $\delta^{13}\text{C}$  values are clearly more  $^{13}\text{C}$ -depleted than surface-dwelling planktic foraminifera.

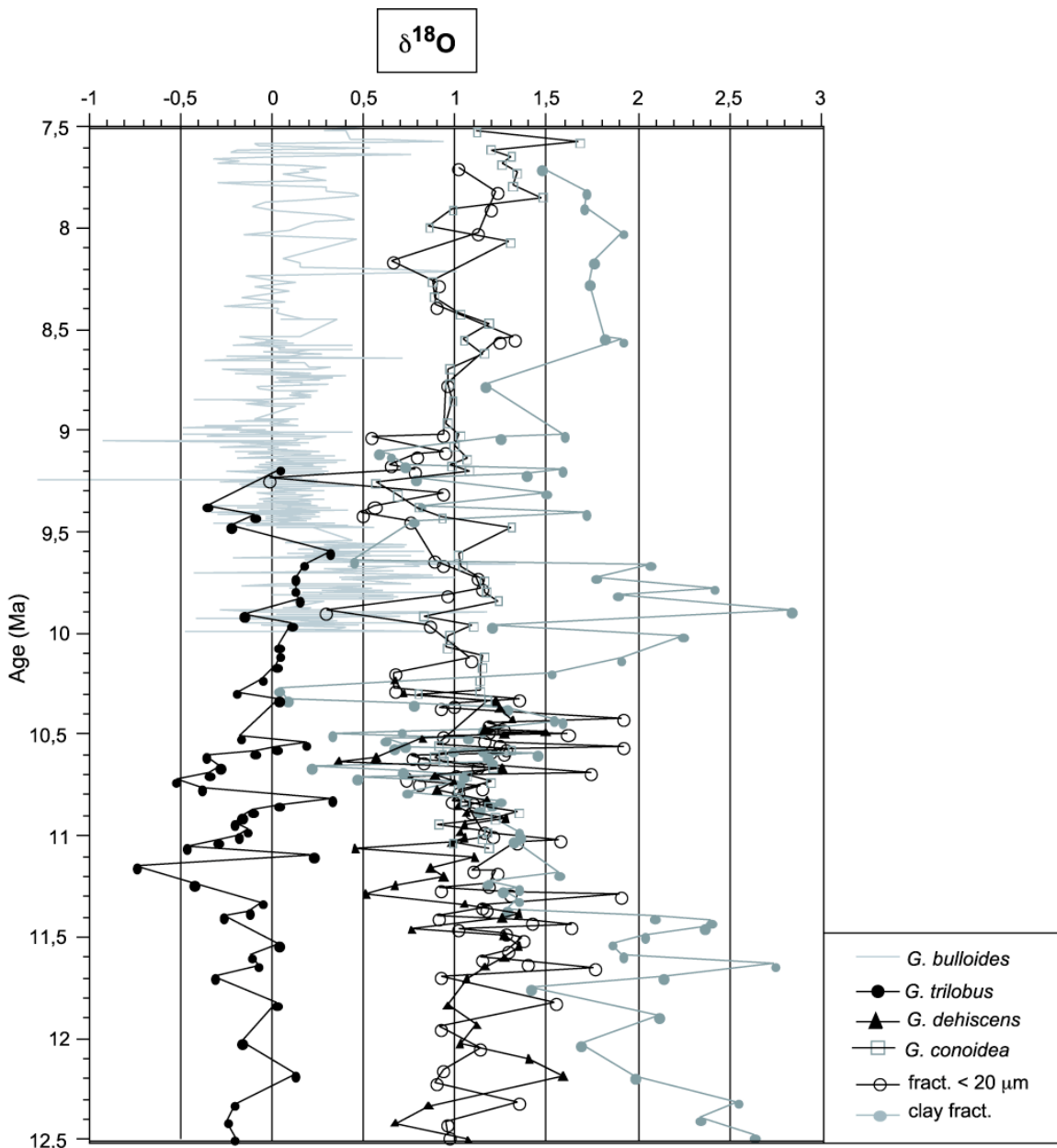


Fig. 3.6. Comparison of nannofossil and foraminiferal oxygen isotopic records (in ‰) from ODP Site 1085. Nannofossil carbonate data from the fraction  $< 20 \mu\text{m}$  and the clay fraction. Clay fraction is shown with grey line and small, solid circles; fraction  $< 20 \mu\text{m}$  with black line and circles. Values of *G. trilobus* are shown with large, black circles, *G. dehiscens* with triangles, *G. bulloides* with grey line, and *G. conoidea* with large squares (from Paulsen et al., manuscript in preparation).

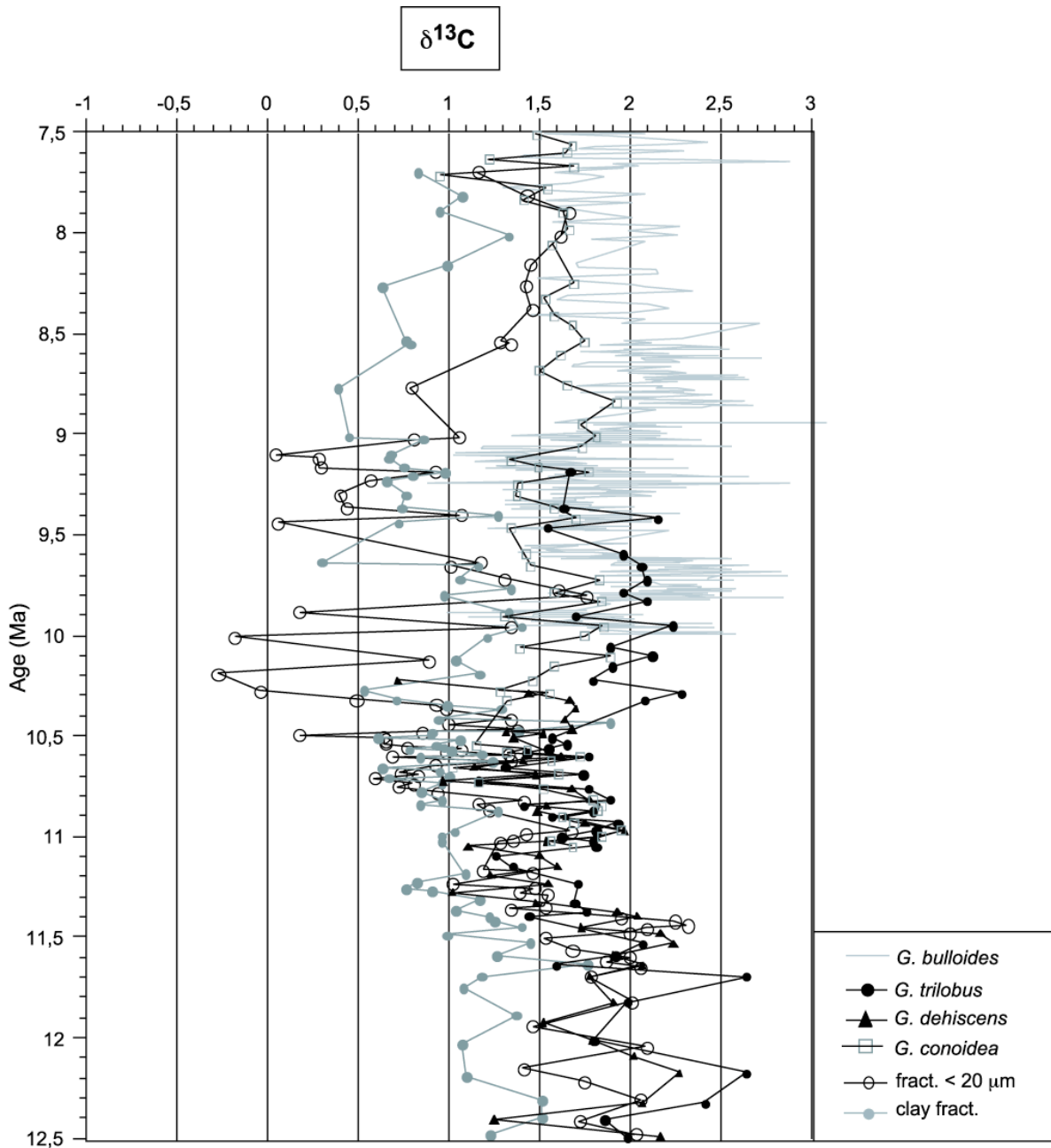


Fig. 3.7. Comparison of nannofossil and foraminiferal carbon isotopic records (in ‰) from ODP Site 1085. Nannofossil carbonate data from the fraction < 20  $\mu\text{m}$  and the clay fraction. Clay fraction is shown with grey line and small, solid circles; fraction < 20  $\mu\text{m}$  with black line and circles. Values of *G. trilobus* are shown with large, black circles, *G. dehiscens* with triangles, *G. bulloides* with grey line, and *G. conoidea* with large squares (from Paulsen et al., manuscript in preparation).

In contrast, deep-dwelling planktic foraminiferal (*Globoquadrina dehiscens* and *Globorotalia conoidea*)  $\delta^{13}\text{C}$  values are very similar to or slightly depleted relative to the corresponding  $\delta^{13}\text{C}$  values of the fraction < 20  $\mu\text{m}$ . It appears that the long-term trend in nannofossil carbonate  $\delta^{13}\text{C}$  is more similar to deep-dwelling foraminiferal species than to

surface-dwelling forms. The correlation between fraction < 20  $\mu\text{m}$  and planktic foraminiferal  $\delta^{13}\text{C}$  is better for *G. dehiscens* than *G. trilobus*.

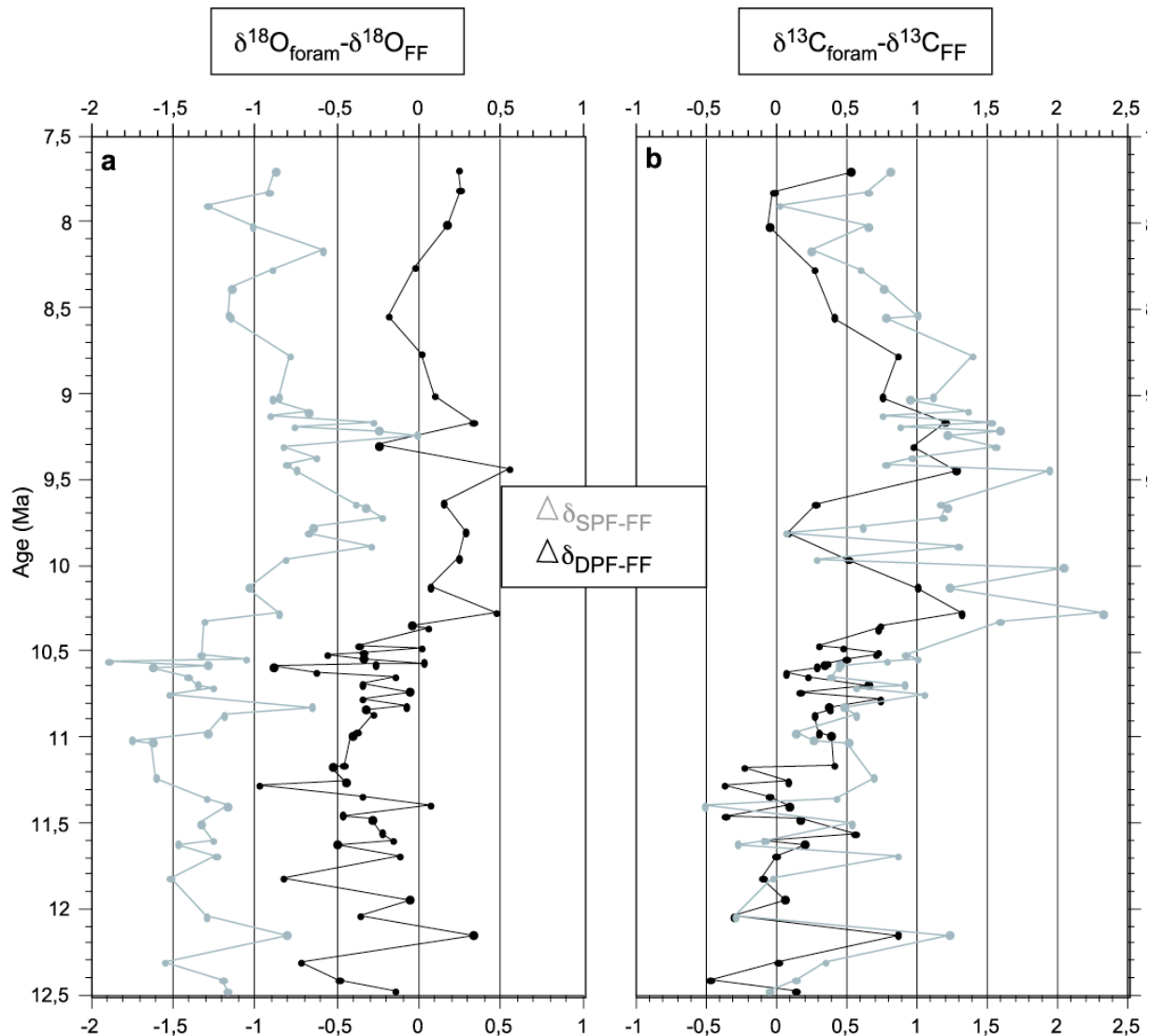


Fig. 3.8. Differences in oxygen (a) and carbon (b) isotopic values (in ‰) between foraminiferal species and nanofossil carbonate (fract. < 20  $\mu\text{m}$ ) at Site 1085. Grey lines show the difference between surface-dwelling foraminifera (*G. trilobus* and *G. bulloides*) and nanofossil carbonate, black lines show the difference between deep-dwelling foraminifera (*G. conoidea* and *G. dehiscens*) and nanofossil carbonate.

In conclusion, our data show that nanofossils show isotopic values more similar to deep-dwelling foraminifera than to surface-dwelling foraminifera. However, the water depth of coccolithophore growth is limited to within the photic zone (the upper ~ 150 m of the water column), and the depth of maximum production varies with latitude (Honjo, 1976; Okada and Honjo, 1973). Studies in the North Atlantic (Knappertsbusch and Brummer, 1995; Haidar et al., 2000; Haidar and Thierstein, 2001), in the Sargasso Sea (Michaels and Knap, 1996; Steinberg et al., 2001) and near Hawaii (Cortés et al., 2001) have shown, that the bulk of the coccolith assemblage accumulating on the sea floor represents taxa of the shallow mixed layer

or upper photic zone. The planktic foraminifer *Globigerinoides sacculifer* is regarded as a surface-dweller, and its isotopic composition has been used for reconstruction of Neogene sea-surface temperatures. Several experiments have shown that the depth habitat for the surface-dwelling planktic foraminifera *G. sacculifer* is very close to that of nanoplankters within the upper photic layer (e.g., Ravelo and Fairbanks, 1992; Deuser, 1986, 1987). The similar depth habitat implies that the depth of calcification is not a major factor accounting for the isotopic discrepancies between nannofossils and *G. sacculifer*. Therefore, the difference in isotope signals between *G. sacculifer* and nannofossils may reflect the difference in their particular season of growth.

Coccolithophore production occurs nearly year-round in the tropics to subpolar regions, but it is punctuated by strong seasonal fluctuations due to changing availability of nutrients associated with seasonal upwelling and/or deep mixing of surface waters. In general, coccolithophore cell density in subtropical to polar regions is highest in early spring when the seasonal thermocline is weakly developed and the upper water column is relatively cool and rich in nutrients (e.g. Haidar and Thierstein, 2001). The flux of planktic foraminifers shows strong species-specific seasonal fluctuations (e.g. Deuser and Ross, 1989). *G. sacculifer* flux increases during the later half of the spring bloom period towards the summer, and reaches highest level in the fall between October and November (Deuser, 1987; Deuser and Ross, 1989). Therefore, the isotopic composition of *Globigerinoides* may represent hydrographic features of warmer, nutrient-poor post-spring bloom surface waters. Ennyu et al. (2002) suggest that polyspecific coccolith stable isotopes reflect surface-water hydrographic conditions during upwelling season or the period of vertical mixing (late winter-early spring) when the surface waters are enriched in nutrients, whereas *Globigerinoides* reflect the post-deep-mixing, relatively warmer (late spring to fall) stratified surface waters.

Considering the seasonal differences in calcification of plankton,  $\delta^{18}\text{O}$  analysis of nannofossil carbonate and surface-dwelling planktic foraminifers (*G. bulloides* and *G. trilobus*) would allow the reconstruction of paleoseasonality. Based on absolute differences between  $\delta^{18}\text{O}$  of surface dwelling planktic foraminifera and nannofossil carbonate in the fract.  $< 20 \mu\text{m}$  ( $\Delta\delta^{18}\text{O}_{\text{SPF-FF}}$ ), the seasonal sea-surface  $\delta^{18}\text{O}$  amplitude shows values between  $-0.5$  and  $-2 \text{‰}$  (Fig. 3.8). Between 12.5 and 10.3 Ma, the  $\Delta\delta^{18}\text{O}_{\text{SPF-FF}}$  gradient exhibits highest values between 1.2 and 1.6 ‰. In the following interval from 10.1 to 9.0 Ma the  $\Delta\delta^{18}\text{O}_{\text{SPF-FF}}$  becomes stepwise smaller. This implies that seasonality became weaker during this interval. This would correspond with the strengthening of the Benguela Upwelling system at about 10.1 Ma

(e.g., Siesser, 1980; Meyers et al., 1983; Krammer et al., 2005 in press). After 9.0 Ma higher values of  $\Delta\delta^{18}\text{O}_{\text{SPF-FF}}$  indicate a more pronounced seasonality in this area. This coincides with the increased abundances of *R. minuta* and *R. haqii*, which are also assumed to indicate upwelling (Krammer et al., 2005 in press).

The similarity of isotopic values of nannofossil carbonate and deep-dwelling planktic foraminifera in the Miocene can also be explained by the seasonal calcification of dominant coccolithophores in the shallow mixed layer due to entrainment of subsurface water masses to the surface (Ennyu et al., 2002). Ortiz et al. (1996) have shown that deep-dwelling foraminiferal species, like for example *Globoquadrina hexagona*, calcify between ca. 250 and 600 m below sea surface. Since the water temperature and salinity are fairly stable in the permanent thermocline, showing no seasonal fluctuation (Levitus and Boyer, 1994; Levitus et al., 1994), the  $\delta^{18}\text{O}$  of deep-dwelling foraminifera should reflect the annual mean temperature of the permanent thermocline. In contrast, the oxygen isotopes of nannofossil carbonate show a ‘snapshot’ of the upper part of the permanent thermocline that crops out at the surface during the early spring deep-mixing period (Ennyu et al., 2002). Therefore, the properties of the ambient water in which the spring bloom coccolithophores calcify are more similar to relatively stable thermocline waters.

The offset between  $\delta^{18}\text{O}$  of *G. dehiscens* (and *G. conoidea*) and nannofossil carbonate ( $\Delta\delta^{18}\text{O}_{\text{DPF-FF}}$ ), therefore, may represent the temperature gradient between upper (subsurface waters beneath the seasonal thermocline) and lower (250-600m) depths of the permanent thermocline (Ennyu et al., 2002). At Site 1085, the  $\Delta\delta^{18}\text{O}_{\text{DPF-FF}}$  remains more or less consistent (with a range of about  $\sim 1\text{‰}$ , slightly following the pattern of  $\Delta\delta^{18}\text{O}_{\text{SPF-FF}}$ ) from 12.5 to 10.4 Ma (see Fig. 3.8), meaning that the vertical temperature gradient of the permanent thermocline was fairly stable during this time. From 10.4 Ma to the end of the investigated interval, some variations in the  $\Delta\delta^{18}\text{O}_{\text{DPF-FF}}$  gradient appear, implying variability in the temperature gradient of the permanent thermocline.

Nannofossil carbonate  $\delta^{13}\text{C}$  records are often regarded as a proxy for sea-surface  $\delta^{13}\text{C}_{\text{DIC}}$  (e.g., D’Hondt et al., 1998; Zachos et al., 1989; Vonhof et al., 2000). Ennyu et al. (2002) have shown, that the fine-fraction  $\delta^{13}\text{C}$  may represent the global trend of  $\delta^{13}\text{C}_{\text{DIC}}$  in the subsurface water mass that crops out during the late winter-early spring deep mixing, and is not representative of the annual mean sea surface.

$\Delta\delta^{13}\text{C}_{\text{SPF-FF}}$  gradients show values between  $-0.5$  to  $2.5$  ‰, from the Middle to Late Miocene at Site 1085 (Fig. 3.8). This  $\Delta\delta^{13}\text{C}_{\text{SPF-FF}}$  variability cannot be fully explained by seasonal fluctuations in the surface water  $\delta^{13}\text{C}$  of the dissolved inorganic carbon ( $\delta^{13}\text{C}_{\text{DIC}}$ ). Other factors, such as surface- to intermediate-water circulation, need to be considered for explaining the behaviour of the Middle to Late Miocene  $\delta^{13}\text{C}$  records of nannofossil carbonate. More analysis of nannofossil stable isotopes from different oceanographic settings is needed for a better understanding of factors that influence the nanoplankton isotopes.

Similar to the  $\Delta\delta^{18}\text{O}_{\text{DPF-FF}}$  gradient, which represents the temperature gradient between upper and lower depths of the permanent thermocline, the temporal record of the  $\Delta\delta^{13}\text{C}_{\text{DPF-FF}}$  gradient may indicate variability in the vertical  $\delta^{13}\text{C}_{\text{DIC}}$  gradient within the permanent thermocline (Ennyu et al., 2002). Until 10.5 Ma the  $\Delta\delta^{13}\text{C}_{\text{DPF-FF}}$  gradient shows relatively small variation (within  $\sim 1$  ‰), suggesting that the vertical  $\delta^{13}\text{C}_{\text{DIC}}$  gradient between upper and lower part of the permanent thermocline was relatively stable. In the intervals from 10.5 to 10 Ma and 9.6 to 8.7 Ma the gradient shows higher values, ranging between  $-0.5$  and  $1.3$  ‰. This may indicate a stronger variability in the vertical  $\delta^{13}\text{C}_{\text{DIC}}$  gradient within the permanent thermocline during these intervals.

### 3.4.3 Comparison to fine-fraction isotope records of other sites

Comparing our isotopic signals of ODP Site 1085 with fine fraction data from other sites in the North Atlantic, western South Atlantic, and South Pacific (Ennyu et al., 2002), the isotopic compositions of nannofossil carbonate closely correspond for the Middle to Late Miocene (Fig. 3.9). The  $\delta^{18}\text{O}$  record of Site 1085 exhibits values between  $1.9$  and  $-0.01$  ‰, showing an intermediate position between the values of Site 588 (S-Pacific) and Site 608 (N-Atlantic). Between 12.5 and 10.2 Ma,  $\delta^{18}\text{O}$  data of Site 1085 show more similarity with the record of Site 688 in the N-Atlantic. After 10.4 Ma, the values of Site 608 stay more or less stable until the end of the investigated interval, but values of Site 1085 decrease down to about  $0.5$  ‰, showing more similarity with Site 588 from the S-Pacific. The  $\delta^{13}\text{C}$  records of all investigated sites resemble one another before 10.4 Ma (Fig. 3.9), suggesting that the  $\delta^{13}\text{C}$  of dissolved inorganic carbon (DIC) in surface waters in which coccolithophores calcify was relatively uniform over the world ocean through the Middle to Late Miocene. In the interval from 10.4 to 9.0 Ma, the  $\delta^{13}\text{C}$  data at Site 1085, located in the eutrophic region off SW-Africa,

shows greater variations towards more negative values in comparison to Site 588 and 608 in the oligotrophic open oceans. This clearly indicates the upwelling of  $^{12}\text{C}$ - and nutrient-enriched sub-surface water masses and, therefore, confirms nicely the general observation of the onset of upwelling off Namibia at 10.4 Ma.

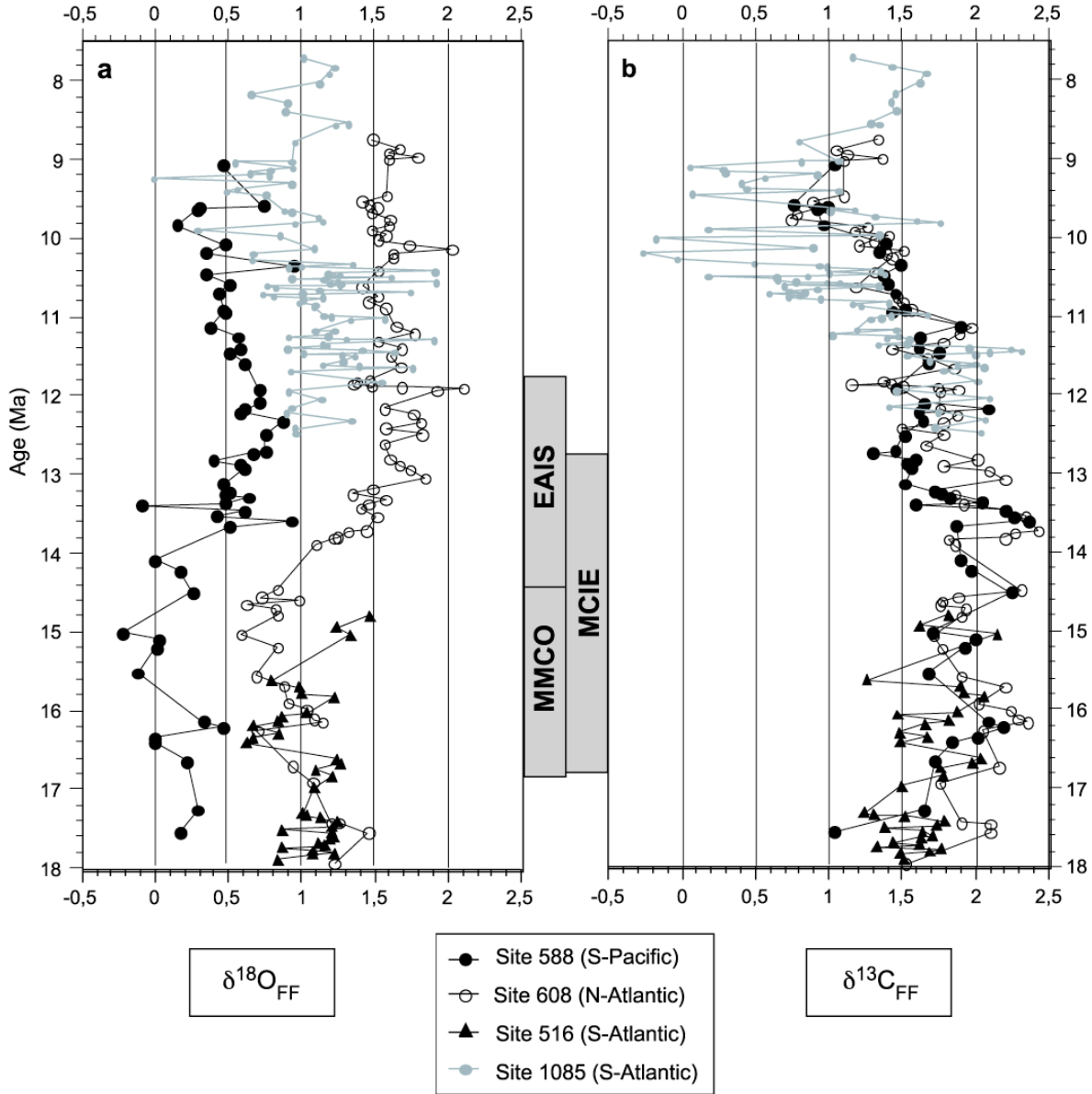


Fig. 3.9. Oxygen (a) and carbon (b) stable isotopic records (in ‰) of fine fraction carbonates from DSDP Sites 588, 608, and 516 (from Ennyu et al., 2002) and of the fraction < 20  $\mu\text{m}$  of ODP Site 1085 (our data). MMCO: Middle Miocene climatic optimum; EAIS: East Antarctic ice sheet event; MCIE: Monterey carbon isotope excursion.

### 3.5 Conclusion

We compared polyspecific nannofossil carbonate stable isotopes from the bulk nannofossil carbonate (fraction < 20  $\mu\text{m}$ ) and the clay fraction (including all nannofossils < 5  $\mu\text{m}$  in diameter), of ODP Site 1085 Middle to Late Miocene sediments (Fig. 3.4). The observed

offset in the isotopic signals can be explained by the contribution of nannofossils smaller than 5  $\mu\text{m}$ . Different isotopic compositions of different nanoplankton species may arise from different depth habitats within the water column or from species-specific vital effects in isotopic fractionation. Interspecific vital effects in modern coccolithophorids tend to produce positively correlated fractionations in carbon and oxygen isotopes in coccoliths (Paull and Thierstein, 1987; Ziveri et al., 2003) with increasing isotopic enrichment with smaller cell diameters. It seems possible, that isotopic fractionation becomes less sensitive to cell diameter at larger cell diameters. This would explain the positive shift in oxygen isotopes in the clay fraction in our data.

Additionally, we showed the potential of nannofossil stable isotopes as indicators of conditions in the shallow mixed layer by comparing these records with those of coexisting planktic foraminifera. To explain the origins of isotopic discrepancies between nannofossil carbonate and surface-dwelling planktic foraminifera, we used the conceptual framework developed by Ennyu et al. (2002). Based on our data, we suggest that nannofossil carbonate isotopes reflect surface-water hydrographic conditions of the late winter-early spring period when relatively cool, nutrient-rich subsurface water mass is entrained into surface waters by vertical mixing. In contrast, surface-dwelling planktic foraminifera reflect the post-deep-mixing, relatively warmer (late spring to fall) stratified surface waters. Therefore, we suggest that the isotopic offset between nannofossils and planktic foraminifera can be explained by the difference in the season of calcification.

This seasonality effect on plankton production offers the possibility to quantify paleoseasonality in the investigated region by performing paired analysis of nannofossil carbonate and surface-dwelling planktic foraminifera. The seasonal sea-surface  $\delta^{18}\text{O}$  amplitude ranges between  $-0.5$  and  $-2$  ‰, showing an decrease from 10.4 and 9.1 Ma. This implies that seasonality became weaker during this interval, corresponding with the initiation of the Benguela Upwelling system at about 10.1 Ma.

Comparing the nanoplankton stable isotopes with those of deep-dwelling planktic foraminifera, we can reconstruct the vertical variation in the upper and lower depths of the permanent thermocline. At Site 1085, the  $\Delta\delta^{18}\text{O}_{\text{DPF-FF}}$  gradient remains more or less the same from 12.5 to 10.4 Ma, meaning that the vertical temperature gradient of the permanent thermocline was fairly stable during this time. From 10.4 Ma to the end of the investigated interval, some variations in the  $\Delta\delta^{18}\text{O}_{\text{DPF-FF}}$  gradient appear, implying variability in the temperature gradient of the permanent thermocline.

Comparing to other fine-fraction isotopic records of oligotrophic regions, the  $\delta^{18}\text{O}$  values of Site 1085 show an intermediate position between the values of the South-Pacific and the North-Atlantic. The  $\delta^{13}\text{C}$  records of all sites resemble one another until 10.4 Ma. The onset of upwelling off Namibia at 10.4 Ma led to greater variations towards more negative values in the carbon isotopic record of Site 1085 in comparison to Site 588 and 608 in the oligotrophic open oceans.

### **Acknowledgements**

We thank H. Heilmann, B. Kokisch, and R. Henning for laboratory assistance. We are indebted to M. Segl and her team for carefully supervising the stable isotope analyses. Discussions with M.-M. Kastanja, B. Beckmann, H. Paulsen and T. Westerhold greatly increased the quality of the initial manuscript. We gratefully acknowledge thoughtful comments from the P. Ziveri to the first draft of this manuscript. This research used samples provided by the Ocean Drilling Program (ODP). Funding for this research was provided by Deutsche Forschungsgemeinschaft (DFG-Research Center Ocean Margins).

## **Chapter 4**

**Manuscript 3:**

**Calcareous nannofossil  
assemblages and fine-fraction carbonate stable isotopes in  
the sub-Antarctic South Atlantic during the Middle to  
Late Miocene (ODP Site 1092)**



**Calcareous nannofossil assemblages and fine-fraction carbonate stable isotopes in the sub-Antarctic South Atlantic during the Middle to Late Miocene (ODP Site 1092)**

Regina Krammer <sup>1</sup>, Karl-Heinz Baumann <sup>2</sup>, Torsten Bickert <sup>2</sup>, Rüdiger Henrich <sup>2</sup>

<sup>1</sup> *Research Center Ocean Margins, University of Bremen, Germany*  
(krammer@uni-bremen.de)

<sup>2</sup> *Department of Geosciences, University of Bremen, Germany*

Manuscript in preparation

**Abstract**

To use nannofossil stable isotopes as a reliable proxy for paleoceanographic reconstructions of temperature and seawater chemistry, changes in nannofossil assemblages have to be taken into consideration. Therefore, we compared Middle to Late Miocene calcareous nannofossil data with the isotopic records of the fraction smaller than 20 µm (including all calcareous nannofossils) to decipher a possible influence of changing nannofossil assemblages on the carbonate isotopes. The studied site (ODP Site 1092) in the Southern Ocean is located on the northern slope of the Meteor Rise at a water depth of 1974 m. Variations in the Southern Ocean were important because paleoceanographic and tectonic changes during the Cenozoic resulted in the formation of the Antarctic Circumpolar current and the thermal isolation of the Antarctic continent.

Our data show, that calcareous nannofossils are the major carbonate producers of Site 1092 sediments. This plankton group gives useful information about water masses and paleoceanographic developments in this region. The isotopic record of the fine-fraction at Site 1092 shows similarities with the contribution of coccolith carbonate produced by *R. pseudoumbilicus* ('large' and 'medium'). A comparison of fine-fraction stable isotopes with those of co-existing planktic foraminifers approved the assumption that fine-fraction isotopes represent conditions of the shallow mixed-layer. The similar values in  $\delta^{18}\text{O}$  of both foraminifers and coccoliths indicate that paleoseasonality played a subordinate role at this location. Comparing our signals of ODP Site 1092 with fine-fraction data of Site 1085 (Krammer et al., *subm.*) in the Benguela Upwelling system off SW-Africa, the  $\delta^{18}\text{O}$  record of 1092 shows a distinct offset towards heavier values due to difference in latitude and thus

temperature between these two locations. The difference in  $\delta^{18}\text{O}$  exhibits a slightly increasing trend during the entire interval probably associated with the expansion and establishment of the East Antarctic ice sheets and related cooling. The carbon isotopic records of both sites show more similarities suggesting that  $\delta^{13}\text{C}$  of dissolved inorganic carbon in surface waters was relatively uniform during the Middle to Late Miocene in the South Atlantic.

*Keywords:* calcareous nannoplankton; fine-fraction stable isotopes; South Atlantic; Miocene; paleoceanography; paleoecology

#### **4.1 Introduction**

To understand past climate changes, suitable deep-sea records from appropriate regions of the ocean are necessary. One of these key areas is the high-latitude Southern Hemisphere, because processes occurring in the Southern Ocean have played an important role in Earth's climate system throughout the Cenozoic (Gersonde and Hodell, 2002). Leg 177 of the Ocean Drilling Program (ODP) was the first scientific drilling campaign to specifically investigate a north - south transect across the Antarctic Circumpolar Current (ACC) using modern coring techniques. The location of this transect was appropriate for resolving global-scale ocean circulation changes because it crosses each of the major surface frontal boundaries of the ACC between 41 and 53°S (Gersonde and Hodell, 2002).

Cenozoic evolution in the Southern Ocean topography was important because ocean gateway configurations during this time resulted in the formation of the Antarctic Circumpolar Current and the thermal isolation of the Antarctic continent. During the course of the Miocene, the Tasmanian Gateway (Kennett et al., 1974, 1975) and the Drake Passage (Lawver and Gahagan, 2003) opened to deep water passages, which led to the establishment of the Circum-Antarctic Current, thermally isolating Antarctica and finally causing the establishment of Antarctic ice sheets (Kennett and Shackleton, 1976; Lawver et al., 1992; Woodruff and Savin, 1989; Zachos et al., 2001). The onset of the Antarctic Circumpolar Current (ACC) promoted thermal isolation and glaciation of the Antarctic continent during the late Oligocene and early Miocene (Pagani et al., 2000) influencing intermediate-, deep-, and bottom-water formation in the Southern Ocean. Cooling prevailed during the Oligocene and the Oligocene/Miocene transition (Miller et al., 1991; Wright and Miller, 1993). In the Early Miocene, temperatures appeared to have warmed, followed by a return to glacial conditions in the Middle Miocene (Zachos et al., 1994). Ice-rafted detritus (IRD) indicates that there was a relatively stable and permanent ice sheet on Antarctica since the latest

Miocene (Kennett and Hodell, 1993). The opening of the Drake Passage, first as a shallow, then later as a deep-water throughway, and the resulting formation of the Antarctic Circumpolar Current, are considered to be critical in the formation and spread of a cold, nutrient-rich Antarctic Intermediate Water (AAIW) (Pagani et al., 2000). This AAIW is a prerequisite for the formation of gradients in the upper water column - such as the thermocline - that are necessary for the creation of high-productivity cells on the coasts or at oceanic fronts.

Therefore, we focus in the current study on following questions:

- Do changes in ocean circulation and climate conditions influence the production of calcareous nanoplankton in the shallow water masses at ODP Site 1092?
- How do fine-fraction stable isotopes represent changes in the shallow paleohydrography for the Middle to Late Miocene in this region?

The studied ODP Site 1092, which comprises a complete Middle to Late Miocene marine sedimentary record, is located on the northern slope of Meteor Rise in the southeast Atlantic at a water depth of 1974 m (Gersonde et al., 1999), close to the Sub-Antarctic Front (SAF) where the formation of AAIW takes place. In the current study, we compare Middle to Late Miocene calcareous nannofossil data with the isotopic records of the fraction smaller than 20  $\mu\text{m}$  (including all calcareous nannofossils) to decipher a possible influence of changing environmental conditions on nannofossil assemblages and their carbon and oxygen isotope composition. In addition, these data help us to reconstruct some of the environmental changes in surface ocean stratification and productivity in the Middle to Late Miocene of the sub-Antarctic South Atlantic.

## **4.2 Material and methods**

### **4.2.1 Study area**

Ocean Drilling Site 1092 ( $46^{\circ}24.70'S$ ,  $07^{\circ}04.79'E$ ) was drilled during Leg 177 on the northern slope of Meteor Rise in the southeast Atlantic at a water depth of 1974 m (Fig. 4.1). Today, this site is located approximately  $3^{\circ}$  north of the present-day Polar Front in the Polar Front Zone (PFZ) which is bounded by the Sub-Antarctic Front (SAF) to the north and the Polar Front (PF) to the south. The PFZ separates cold, nutrient-rich Antarctic surface water to the south from warmer, less nutrient-rich Sub-Antarctic Surface Water to the north. The average width of the PFZ in the South Atlantic is 670 km, centered at  $45^{\circ}S$  (Lutjeharms, 1985). Today, there is a transition within the PFZ from mixed siliceous-calcareous sediments near the SAF to more siliceous (diatomaceous) sediments accumulating south of the PF. The shallow location of Site 1092 (Fig. 4.2) is above the regional calcite lysocline and lies today

within the mixing zone of Circumpolar Deep Water (CDW) and North Atlantic Deep Water (NADW) (Hodell and Ciesielski, 1990). The primary objective for drilling at Site 1092 was to recover a carbonate-bearing, Late Neogene sediment sequence to improve and complement the existing record at Site 704 (Leg 114), located only 34 nmi to the southeast.

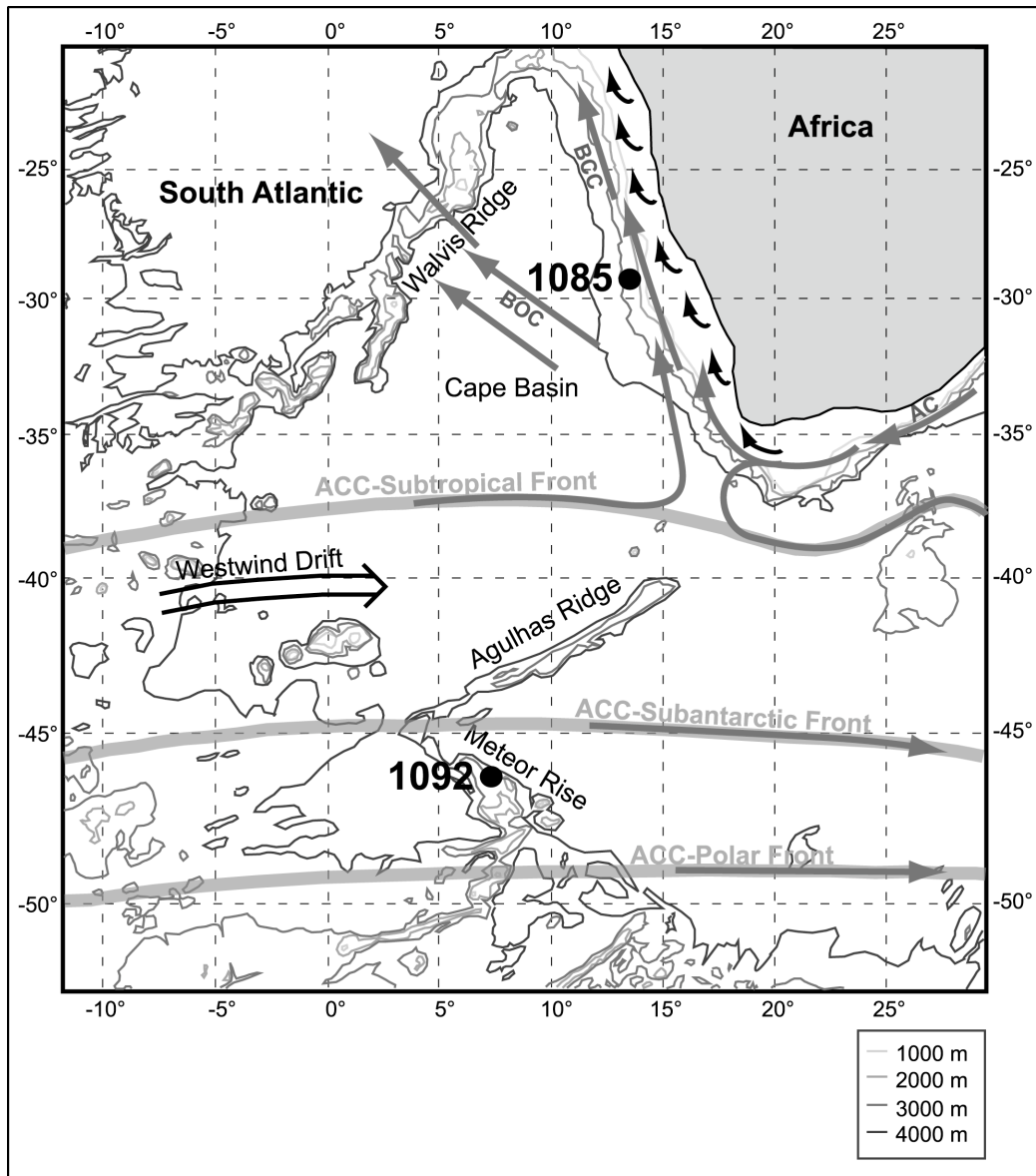


Fig. 4.1. Location of ODP Sites 1085 and 1092 in the southeastern Atlantic sector of the Southern Ocean drilled during Leg 175 and 177. The schematic illustration of the modern current system shows the frontal system of the Antarctic Circumpolar Current (ACC) (from Hodell et al. 2002, modified). Grey arrows show the flow pattern of Agulhas Current (AC), Benguela Oceanic Current (BOC), and Benguela Coastal Current (BCC). Black arrows indicate coastal upwelling off SW-Africa (modified from Shannon and Nelson, 1996).

The sediments of Site 1092 consist of pale brown-green to pure white nannofossil oozes with mixtures of diatom and foraminifer oozes and muds (Gersonde et al., 1999). The sedimentary section was sub-divided into two subunits. In sub-unit IA the sedimentary column consists of alternation of nannofossils, foraminifers, diatoms, mud and rarely dropstones. Carbonate content fluctuates between 17 and 95 wt.%. In subunit Ib nannofossils

are the predominant lithologic component and are replaced by diatoms or foraminifers in only a few intervals. Carbonate content is well over 80 wt.%. Below 112 mcd nannofossil ooze is the only major lithologic type with minor admixtures of diatoms and foraminifera.

Site 1085A was drilled during Leg 175 and is located at the SW-African continental margin (Fig. 4.1) at 29°22.45'S and 13°59.41'E in 1713 m water depth. The Oranje River is discharging into the South Atlantic (Wefer, Berger, Richter et al., 1998), influencing Site 1085. In present days, Site 1085 is bathed primarily in the Upper Circumpolar Deep Water (UCDW) near the mixing zone with the North Atlantic Deep Water (NADW). The site comprises a complete record of hemipelagic sediments down to 14 Ma, dominated by foraminifera-bearing nannofossil ooze.

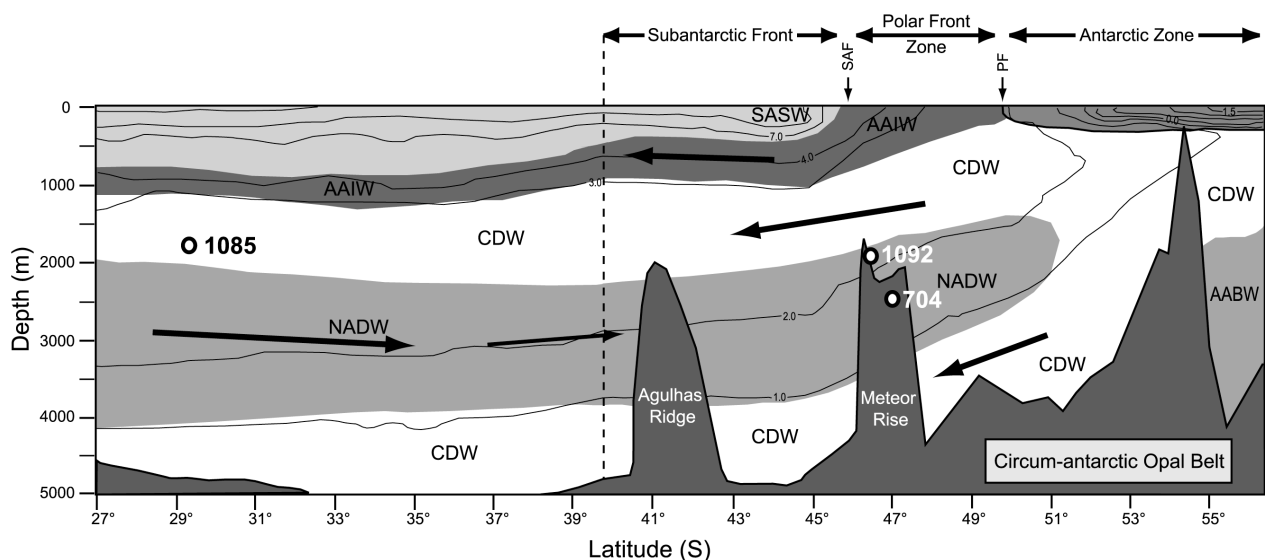


Fig.4.2. Schematic vertical distribution of water masses and potential temperature (°C) on a north-south transect across the frontal system of the Antarctic Circumpolar Current in the southeastern Southern Atlantic. The location of ODP Sites 1092, 1085, and 704 on the Meteor Rise are indicated. SASW, sub-Antarctic Surface Water; AAIW, Antarctic Intermediate Water; CDW, Circumpolar Deep Water; NADW, North Atlantic Deep Water; AABW, Antarctic Bottom Water; SAF, sub-Antarctic Front; PF, Polar Front (modified from Gersonde et al., 1999).

Multisensor track (MST) and color reflectance data collected from holes 1092A-D were used to construct an initial shipboard composite section for Site 1092 down to 188 mbsf (base of Core 177-1092A-18H). Aboard the ship, it was already noticed that much distortion occurred within individual cores. Based on X-ray fluorescence (XRF) scanning of half cores, Paulsen et al. (subm.) developed a revised composite depth section for Site 1092.

A first age model was developed by Censarek and Gersonde (2002) based on diatom biostratigraphy supported by shipboard paleomagnetic data. In this study we use the age model of Paulsen et al. (subm.) which is a combination of a model of magnetostratigraphy (Evans and Channell, 2003; Evans et al., 2004) and of a benthic oxygen isotope stratigraphy.

#### 4.2.2 Sediment treatment

We set 2 g of each freeze-dried bulk sample aside for carbon analysis, and the remaining material was washed through 20  $\mu\text{m}$ -sieves to detach nannofossils from adult and juvenile foraminifers. SEM observations of the fraction  $< 20 \mu\text{m}$  indicated that the calcareous particles in this fraction are almost exclusively composed of calcareous nannofossils. For isotope measurements, the fraction  $< 20 \mu\text{m}$  (83 samples of Site 1092) was analyzed using a Finnigan MAT 252 micromass-spectrometer coupled with a Finnigan automated carbonate device at the Department for Marine Geology in Bremen. The carbonate was reacted with orthophosphoric acid at 75°C. The reproducibility of the measurements, as referred to an internal carbonate standard (Solnhofen limestone), is  $\pm 0.07 \text{‰}$  and  $\pm 0.05 \text{‰}$  ( $1\sigma$  over a one year period) for oxygen and carbon isotopes, respectively. The conversion to the VPDB-scale was performed using the international standard NIST 19.

Nannofossil assemblages in the bulk sediment were counted by scanning electron microscopy (SEM) using a Zeiss DMS 940A at the Department for Sedimentology/Paleoceanography in Bremen. Counts and size measurements were converted into volume and mass contribution of each species using the approach of Young and Ziveri (2000) with given shape factors for various coccolith types, the average length of a species, and the density of calcite. A good taxonomic overview of Neogene calcareous nannofossils is provided in Perch-Nielsen (1985). In general, the taxonomy follows the classification system of Young (1998), in addition, the taxonomy of the genus *Reticulofenestra* follows that outlined in Gibbs et al. (2005).

### 4.3 Results

#### 4.3.1 Absolute numbers of calcareous nannofossils and coccolith carbonate

Absolute calcareous nannofossil numbers range from  $7000 \times 10^6$  to  $15000 \times 10^6$  calcareous nannofossils per gram sediment at Site 1092 (Fig. 4.3). Highest numbers of total calcareous nannofossils occur in the intervals 12.1 to 12.0 Ma, 11.5 to 11.0 Ma, and 9.0 to 8.6 Ma. The most abundant species are *Coccolithus pelagicus* (with highest values of  $5500 \times 10^6$  coccoliths/g sediment), followed by *Reticulofenestra pseudoumbilicus* ( $> 7 \mu\text{m}$  in diameter, ‘large’) with values up to  $5000 \times 10^6$  coccoliths/g sediment and *Reticulofenestra pseudoumbilicus* (5-7  $\mu\text{m}$  in diameter, ‘medium’). In addition, *Reticulofenestra haqii*, *Reticulofenestra minuta*, and *Calcidiscus leptoporus* make up a common part of the assemblage. The deep-dwelling species *Florisphaera profunda* is also recorded during the

entire time span, showing an increasing trend in the upper part if the investigated interval (from 9.1 Ma to the end of the record). In general, the calcareous nannofossil flora is dominated by species of the genus *Reticulofenestra*, which usually comprise between 45 and 80% of the assemblage (Fig. 4.4).

Although, no drastic change in the assemblage composition occurred throughout the investigated interval, some differences are recognizable in the species variations of Site 1092. Both forms of *Reticulofenestra pseudoumbilicus* ('medium' and 'large') show a similar pattern with highest values at 10.6 Ma, around 10.2 Ma and between 8.8 and 8.6 Ma (Fig. 4.3). In the last interval from 8.8 to 8.6 Ma, the small reticulofenestrids, like *R. minuta* and *R. haqii*, also show highest values. In comparison, the absolute numbers of *Coccolithus pelagicus* reach a maximum at 9.0 Ma, 0.2 Ma earlier than the highest values of the reticulofenestrids.

The entire interval from 12.6 to 7.6 Ma at Site 1092 is dominated by fine carbonate silt, therefore calcareous nannofossils are the most important carbonate producers. The bulk carbonate content ranges between 80 and 98 wt.% (from Westerhold, 2003) with strongest variations in the interval from 9.3 to 9.1 Ma. In this period the carbonate content drops down to 68 wt.% and is associated with higher Fe intensities (Westerhold, 2003). The calculated nannofossil carbonate content ranges from 92.6 wt.% at 9.03 Ma to 21.28 wt.% at 7.9 Ma (Fig. 4.4), with a mean of 38.5 wt.% and is obviously linked to the bulk carbonate content. Only very few nannofossil species contribute to the nannofossil carbonate content (Fig. 4.4) which are massive and abundant. The most important species in terms of carbonate production is *Coccolithus pelagicus* (up to 80 % contribution to nannofossil carbonate) showing an increasing trend throughout the entire interval. *Reticulofenestra pseudoumbilicus* is the second important carbonate producer with a contribution between 20 and 70 %. Especially in the lower part of the record and in the interval from 8.8 to 8.5 Ma, the reticulofenestrids produce a relatively high proportion of the nannofossil carbonate (up to 75 %). Generally, calcareous nannofossils are well preserved throughout the entire interval studied.

#### 4.3.2 Stable isotopic record of fraction < 20 µm

The isotopic record of the fraction < 20 µm (see Fig. 4.4), including the bulk nannofossil carbonate dominated by *Coccolithus pelagicus* and *Reticulofenestra pseudoumbilicus* (5-7 µm, 'medium') and *Reticulofenestra pseudoumbilicus* (> 7 µm, 'large'), follows the overall trends during the Middle to the Late Miocene (see global oxygen record of Zachos et al., 2002; Fig. 4.4). In general,  $\delta^{18}\text{O}_{<20\mu\text{m}}$  of ODP 1092 starts with values of about 2.6 ‰ at 12.5

Ma, followed by a slight decrease until 11.0 Ma, with the lowest value of 2.11 ‰ at the end of this interval.

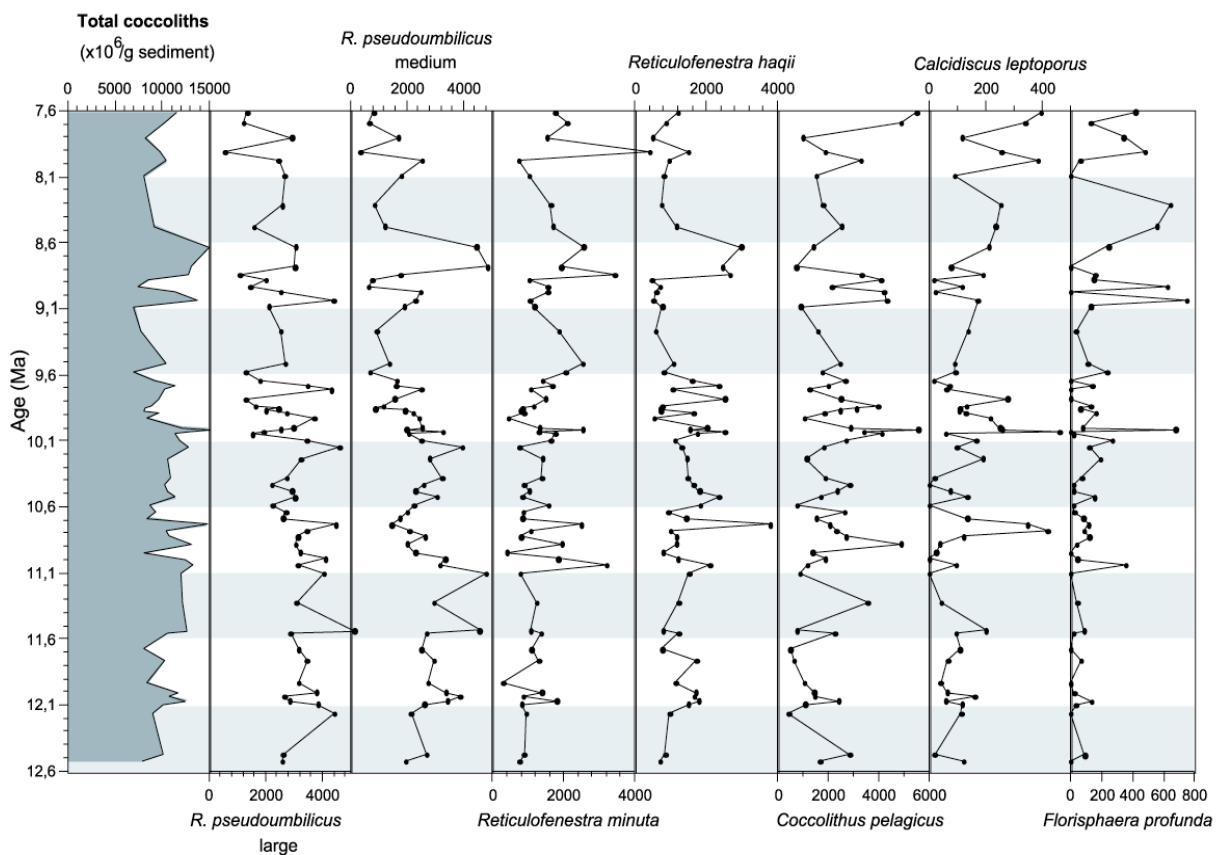


Fig. 4.3. Absolute numbers ( $\times 10^6/\text{g}$  sediment) of the total nannoplankton assemblage as well as of the most dominant species in Site 1092.

Between 11.0 and 10.2 Ma, the  $\delta^{18}\text{O}_{<20\mu\text{m}}$  record shows a positive shift up to highest values of 2.91 ‰. In the following interval up to 9.2 Ma, the  $\delta^{18}\text{O}$  record varies between minimum values around 2.2 ‰ and maximum values of 2.9 ‰. From 9.2 Ma to the top of the record, there is a trend towards progressively higher  $\delta^{18}\text{O}$  values at Site 1092 with most positive values around 3.5 ‰ at 7.7 Ma.

In the following interval to the top of the record, the amplitude increases up to 1.2 ‰. There are three peaks with most positive values. Compared to the hypothetical ‘ice-free’  $\delta^{18}\text{O}$  value of 2.75 ‰ which corresponds to a world without the presence of the Antarctic and Greenland ice sheets and with the same deep water temperatures as today (Shackleton and Kennett, 1975; Shackleton et al., 1995), the  $\delta^{18}\text{O}_{<20\mu\text{m}}$  record at Site 1092 shows similar values. A maximal offset of 0.6 ‰ appears during the Middle to Early Late Miocene, followed by an interval from 9.5 to 7.6 Ma with increased discrepancies between nannofossil carbonate  $\delta^{18}\text{O}$  and the hypothetical  $\delta^{18}\text{O}$  value for a situation without Antarctic ice.

The carbon isotope record of the fraction < 20  $\mu\text{m}$  starts with values of 2.6 ‰, followed by a sharp increase in  $\delta^{13}\text{C}_{<20\mu\text{m}}$  by 1‰ (Fig. 4.4). This highest values mark the beginning of an interval of decreasing  $\delta^{13}\text{C}_{<20\mu\text{m}}$  values, which ends around 9.5 Ma. At 9.3 Ma the  $\delta^{13}\text{C}_{<20\mu\text{m}}$  record reaches the lowest values in the entire interval. After this minimum, the  $\delta^{13}\text{C}$  values increase again, but still they do not reach the values from the base of the record. From 9.2 to the top of the interval, the  $\delta^{13}\text{C}_{<20\mu\text{m}}$  record shows a shift towards higher values, with a maximal amplitude of around 0.8 ‰.

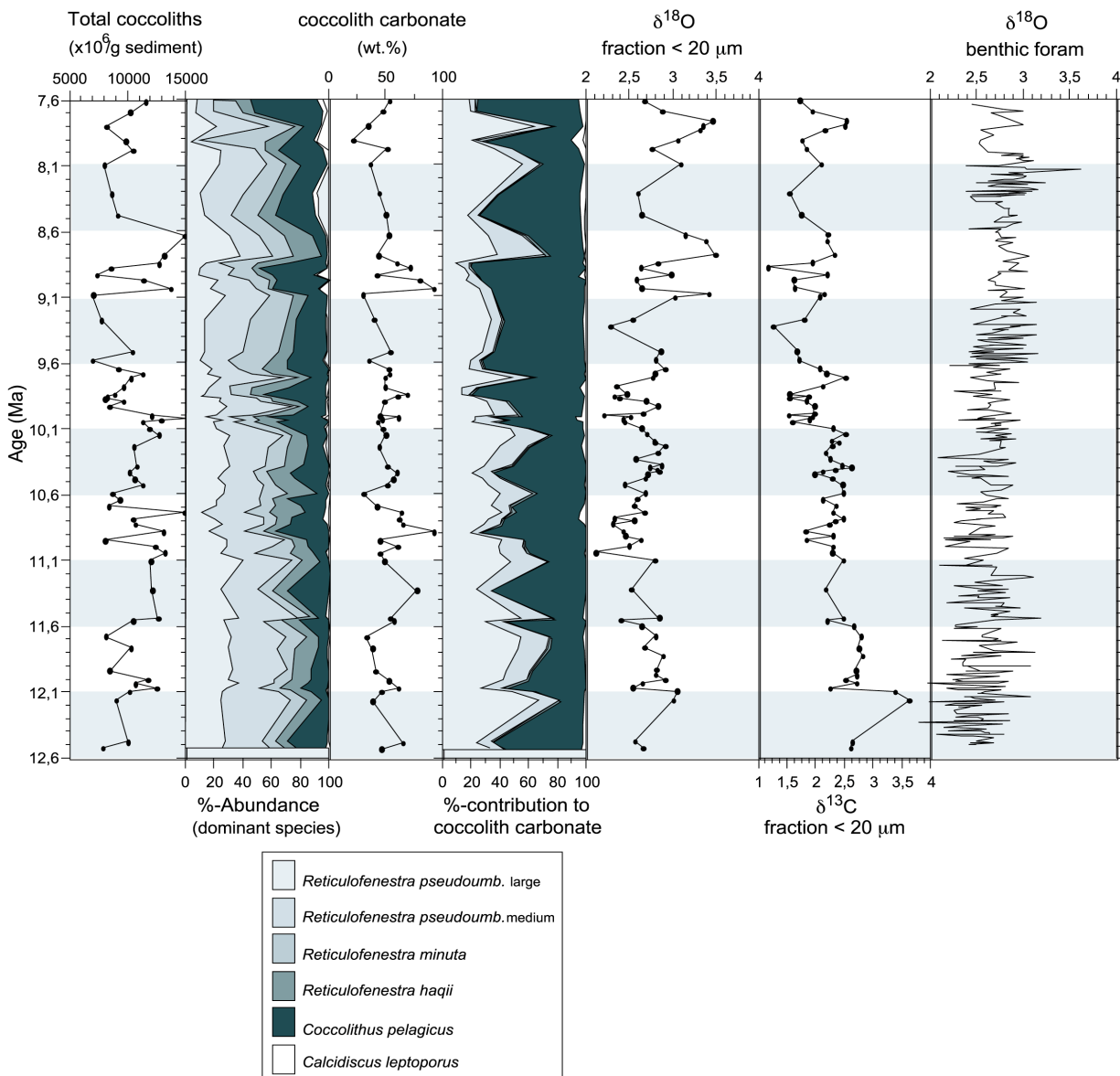


Fig. 4.4. Absolute numbers of nannofossils of the total assemblage, percent abundance of the dominant species, absolute nannofossil carbonate content, percent contribution of the dominant carbonate producers, stable isotopic data of the fraction < 20  $\mu\text{m}$  of Site 1092, and the global deep-sea oxygen isotope record derived from benthic foraminifers (from Zachos et al., 2001).

## 4.4 Discussion

### 4.4.1 Calcareous nannofossils and their paleoceanographic implications

In general, calcareous nannofossil assemblages found in the area of the Meteor Rise at Site 1092 are characterised by relatively low species diversity. The most dominant form is *Coccolithus pelagicus*, a species traditionally considered as a cold-water indicator (e.g., McIntyre and Bé, 1967; Winter et al., 1994), followed by cosmopolitan forms, such as *Reticulofenestra pseudoumbilicus* ('large' and 'medium'), *Reticulofenestra haqii* and *Reticulofenestra minuta*. *Calcidiscus leptoporus*, which is considered to be a warm-water species (Gard and Crux, 1991; Flores et al., 1999), is also recorded throughout the entire investigated interval, but with minor contributions.

*C. pelagicus* is well known as a modern cold-water species. Samtleben et al. (1995) have shown that its temperature-range includes even negative temperatures. Other authors have associated this form with increased productivity (Cachão and Moita, 1995). The recent distribution of *C. pelagicus* is restricted to high latitudes where it is known from the North Atlantic and the Subarctic area (McIntyre and Bé, 1967; Okada and McIntyre, 1977; Samtleben et al., 1995; Baumann et al., 1999). In the southern hemisphere, *C. pelagicus* is restricted to upwelling regions (McIntyre et al., 1970; Okada and McIntyre, 1977; Giraudeau et al., 1993; Baumann et al., 2000; Findlay and Giraudeau, 2000). Especially, the high values of *C. pelagicus* in the interval from 9.0 to 8.8 Ma and from 7.8 Ma to the end of the record may indicate increasing productivity associated with changes in nutrients. In the following interval from 8.8 to 8.6 Ma, taxa of the genus *Reticulofenestra* show higher values. Especially, 'small' placoliths, such as *R. minuta* and *R. haqii*, are of special interest, because their absolute and relative abundances increase in upwelling areas or episodes of high productivity (Wells and Okada, 1997; Flores et al., 1999; Bollmann et al., 1998) or high fertility (Biekart et al., 1989). Negri and Villa (2000) have also shown, that these forms are important paleo-ecological and paleoceanographic indicators for fertility changes in the superficial water masses.

*Florisphaera profunda* is the main contributor to the so-called deep-water assemblage (Okada and Honjo, 1973; Nishida, 1979; Reid, 1980). It has been shown that this form is a useful paleo-productivity indicator (e.g., Molfino and McIntyre, 1990; Bassinot et al., 1997). The nutrient availability is controlled by the depth of the nutricline, which can be monitored by the abundance of *F. profunda* (Molfino and McIntyre, 1990). At Site 1092, higher abundances of this form from 9.1 to 8.9 Ma and 8.6 to 8.2 Ma may be indicative for decreased productivity, which coincides with lower values of *R. minuta* and *R. haqii* in these intervals. Vice versa,

higher numbers of *R. haqii* and *R. minuta* correlate well with lower values of *F. profunda* in the time interval from 8.8 to 8.6 Ma.

#### 4.4.2 Fine-fraction stable isotopes

Stable isotopic measurements ( $\delta^{13}\text{C}$  and  $\delta^{18}\text{O}$ ) of biogenic carbonates from deep-sea sediments have been used to investigate past changes in oceanic productivity and shallow mixed-layer temperatures. In general, the oxygen isotopic ratio is used to reconstruct the temperature of ancient oceans. Additionally, the  $\delta^{18}\text{O}$  is a useful tool to trace changes in the oxygen isotopic ratio of seawater, which varies with global ice volume. The carbon isotope ratio reflects variations in the carbon isotopic composition of dissolved inorganic carbon in the ocean, which is controlled by organic matter production and respiration, but also by the exchange of carbon between different reservoirs. The paleoceanographic reconstructions of surface ocean conditions from stable isotopic measurements mostly relied on the analysis of planktic foraminifers because most foraminifers have a small or limited range of isotopic vital effects. Bulk carbonate has also been used for stable isotopic analysis, especially in sediments where foraminifers are sparse (e.g., Clarke and Jenkyns, 1999; Vonhof et al., 2000), to investigate past changes in oceanic productivity and shallow mixed-layer temperature.

Calcareous nannofossils depend on temperature, nutrients, and salinity. Additionally, the availability of sunlight is an important controlling factor (e.g., Giraudeau, 1992; Winter and Siesser, 1994). This phytoplankton group traces fluctuations in climate as well as changes in surface-water conditions. Because coccolithophores dwell and secrete coccolith plates within the photic zone (Okada and Honjo, 1973), their chemical composition are considered to record signals in the shallow mixed-layer (Goodney et al., 1980; Dudley et al., 1980, 1986). Coccoliths grown in culture experiments exhibit a nearly 5 ‰ array of interspecific ‘vital effects’ in both oxygen (Dudley and Goodney, 1979; Dudley et al., 1980, 1986; Ziveri et al., 2003) and carbon isotopes (Ziveri et al., 2003). Therefore, changes in the relative carbonate contribution of different calcareous nannofossil species may cause significant discrepancies in bulk or fine-fraction carbonate isotopic records, partially masking signals of changing environmental conditions. Therefore, changes in the relative carbonate contribution of different calcareous nannofossil species may cause significant discrepancies in bulk or fine-fraction carbonate isotopic records, partially masking signals of changing environmental conditions. Differences in the isotopic composition of different species of coccoliths may arise from different depth habitats within the water column or from species-specific ‘vital effects’ in isotopic fractionation.

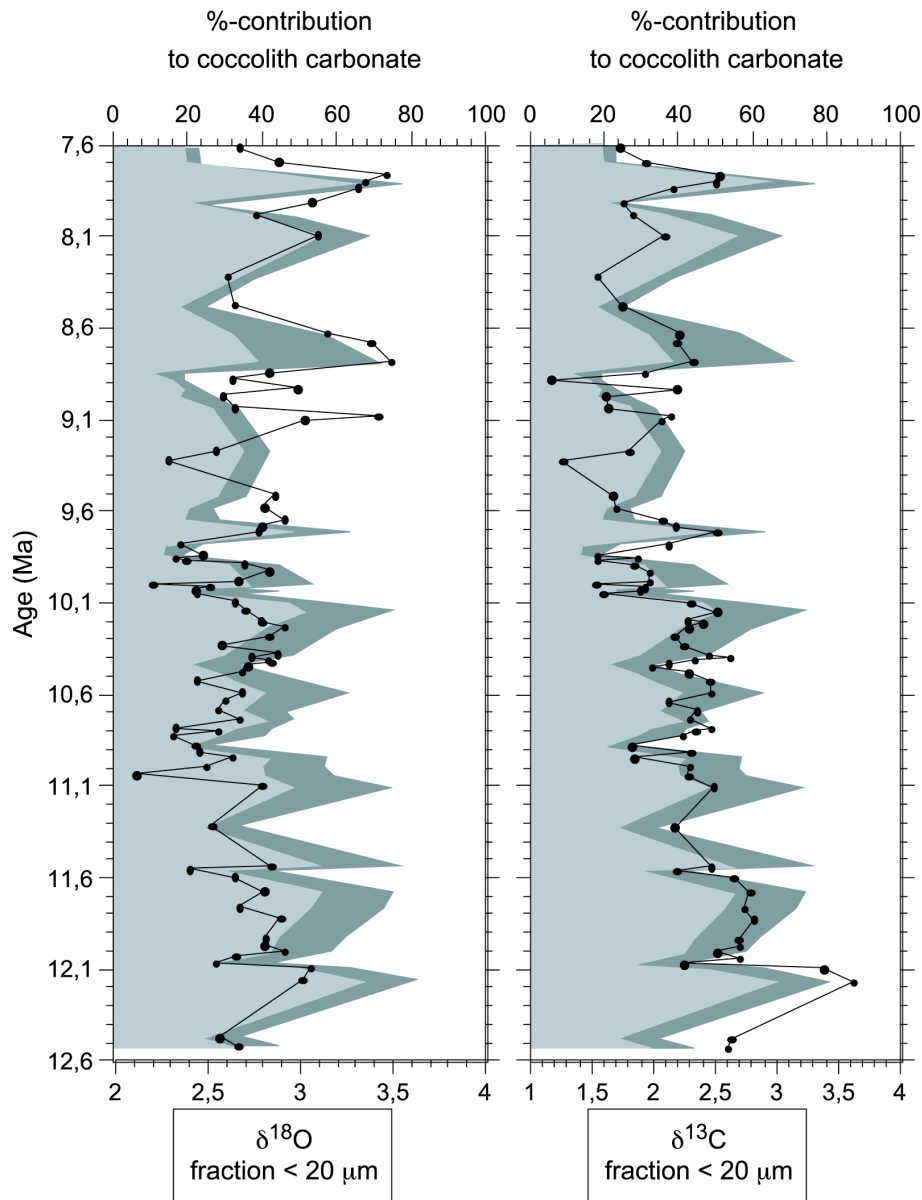


Fig. 4.5. Comparison of nannofossil oxygen and carbon isotopes (fraction < 20  $\mu\text{m}$ ) of ODP Sites 1092 (black lines) with percent contribution to coccolith carbonate produced by the species *R. pseudoumbilicus* 'large' (in light grey) and 'medium' (in dark grey).

Within one single species, vital effects are constant to within 1 ‰, with no strong response to growth rate variations (Ziveri et al., 2003). Therefore, to use nannofossil stable isotopes as a reliable proxy for paleoceanographic reconstruction of temperature and seawater chemistry, monospecific fractions are needed or, like in the current study, changes in nannofossil assemblages have to be taken into account.

At ODP Site 1092, the isotopic data of the bulk nannofossil carbonate (fraction < 20  $\mu\text{m}$ ) bear resemblance to the percent contribution of coccolith carbonate produced by both forms of *Reticulofenestra pseudoumbilicus* ('large' and 'medium'; see Fig. 4.5). These forms make

up between 20 and 70 % of the coccolith carbonate. Especially, the  $\delta^{13}\text{C}$  record resembles the carbonate contribution pattern of *R. pseudoumbilicus* (> 7  $\mu\text{m}$  in diameter, ‘large’). The  $\delta^{18}\text{O}$  data shows similarities with the carbonate content of the ‘larger’ reticulofenestrads particularly in the upper part of the investigated interval. For example, the positive shift in  $\delta^{18}\text{O}$  from 8.8 to 8.6 Ma and 7.9 to 7.7 Ma are easily comprehensible in a peak of the reticulofenestrad carbonate, when *R. pseudoumbilicus* produced more than 70% of the coccolith carbonate (Fig. 4.5). However, it is not clear whether the isotopic signals follow the pattern of reticulofenestrads, and thus show a ‘vital effect’ produced by isotopic fractionation of these nanoplankton species, or they indicate paleoceanographic conditions which go along with the changes in nannofossil assemblages. In order to answer this question we have compared the stable isotope data of the fine-fraction with those of the surface-dwelling planktic foraminifer *Globigerina bulloides* (Paulsen et al., manuscript in preparation: see Fig. 4.6). In general, the isotopic records of both the foraminiferal and the fine-fraction carbonate show similar trends, which contradicts the major influence of ‘vital effects’ of *R. pseudoumbilicus*. It seems likely that *R. pseudoumbilicus* responded very sensitive to changes in the surface-water conditions as also indicated by the fine-fraction isotopic record.

Previous studies have described an offset of more than 1 ‰ between surface-dwelling foraminifers and coccolith oxygen isotopes (e.g. Ennyu et al., 2002; Krammer et al., subm.) due to their different season of growth. Therefore, the difference between  $\delta^{18}\text{O}$  of surface-dwelling foraminifers and nannofossil carbonate allows the reconstruction of paleoseasonality. This offset in  $\delta^{18}\text{O}$  of Site 1092 is smaller, compared to data from Site 1085, ranging between 0.2 and 0.7 ‰. In the intervals from 10.0 to 9.8 Ma and 9.0 to 8.9 Ma, the coccolithophorid signals even converge with those of *G. bulloides*. It seems possible, that paleoseasonality was not the dominating factor in this study area. Carbon isotopic values of the fine-fraction also show a similar pattern to the foraminiferal signal, but they are on average depleted with respect to *G. bulloides* throughout the entire investigated interval. These results coincide with studies of Ennyu et al (2002) and Krammer et al. (subm.) where a clear offset between fine-fraction  $\delta^{13}\text{C}$  and surface-dwelling foraminifers was described.

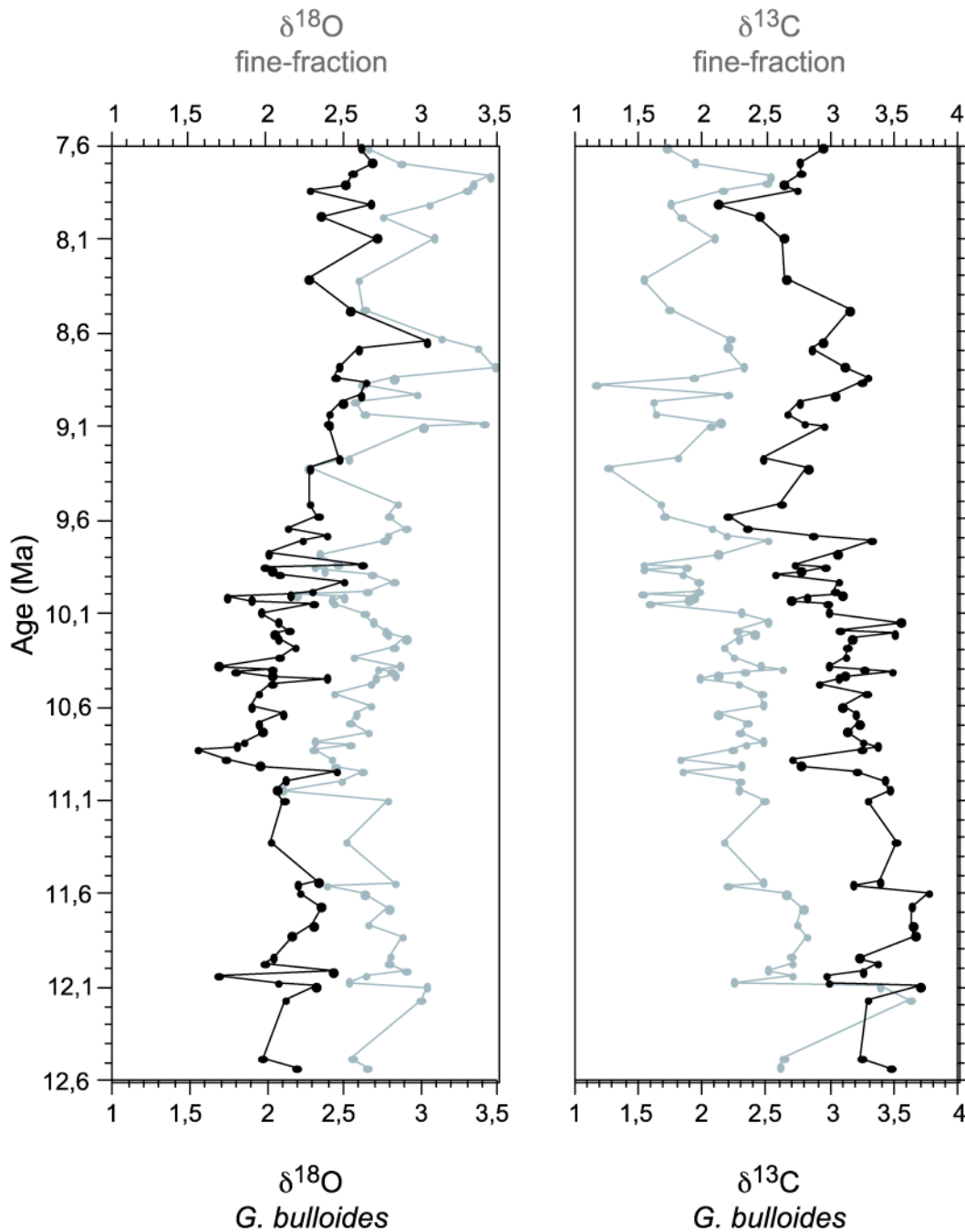


Fig. 4.6. Comparison of stable isotopes of both nannofossil and foraminiferal carbonate at ODP Site 1092. The grey line represents nannofossil carbonate isotopic records, the black line shows isotopes of the surface-dwelling planktic foraminifera *Globigerina bulloides* (data from Paulsen et al., manuscript in preparation).

Additionally, we compared the fine-fraction isotopic record of Site 1092 with the fine-fraction isotopic data set of different other ODP Sites (Krammer et al., subm.; Ennyu et al., 2002). Comparing the  $\delta^{18}\text{O}$  data with Site 1085 off SW-Africa, a distinct offset between these two records is recognizable (Fig. 4.7). This offset is even more pronounced, compared to the records of Sites 588 and 608 (Ennyu et al., 2002) in the oligotrophic open oceans. In general,

the  $\delta^{18}\text{O}$  values of Site 1092 are heavier, ranging between 2 and 3.5‰. This site-to-site offset in oxygen isotopes is probably due to difference in the temperature of the shallow mixed layer in which coccolithophores calcified. In general, the difference in the  $\delta^{18}\text{O}$  exhibits a slightly increasing trend during the entire interval with an average amplitude of  $\sim 1\text{‰}$ .

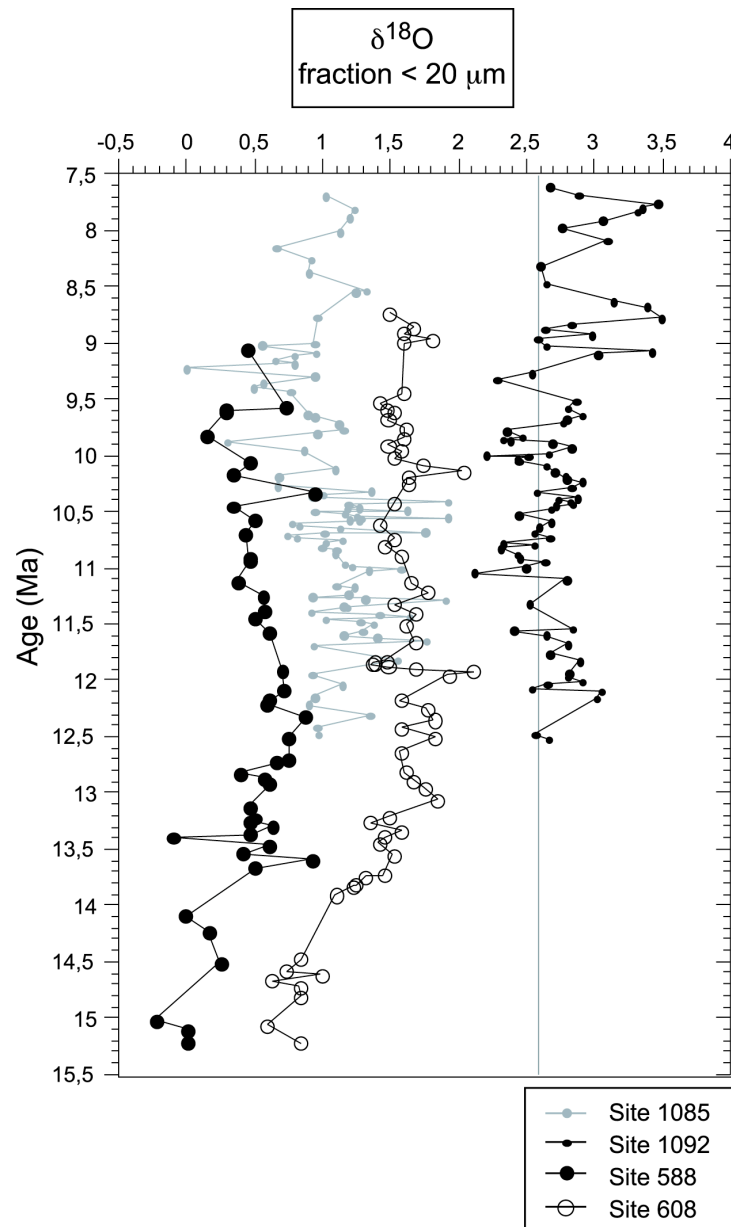


Fig. 4.7. Comparison of nannofossil oxygen isotopes (fraction < 20  $\mu\text{m}$ ) of ODP Sites 1085 (in light grey, from Krammer et al., subm.), 1092 (with black line), Site 588 (S-Pacific; Ennyu et al., 2002), and 608 (N-Atlantic; Ennyu et al., 2002). Grey vertical line indicates the  $\delta^{18}\text{O}$  value as it would be prior to the onset of Northern Hemisphere Glaciation and with no ice sheet present in Antarctica in the Southern Ocean.

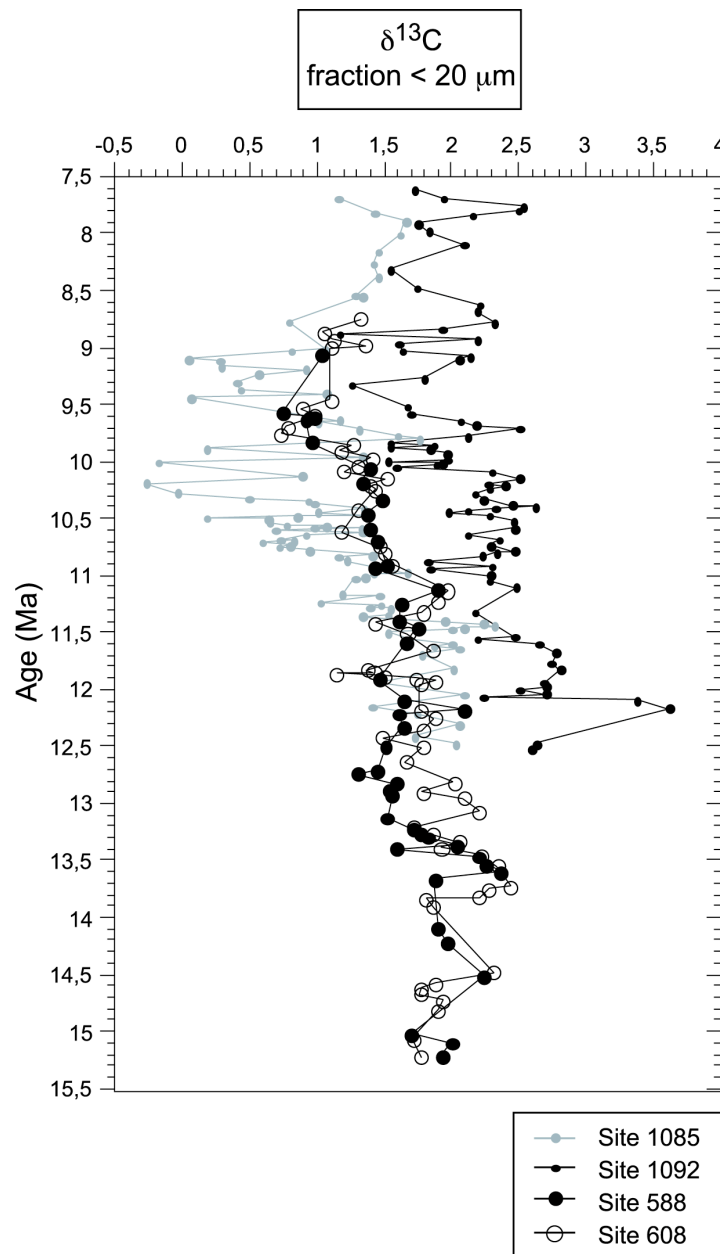


Fig. 4.8. Comparison of nannofossil carbon isotopes (fraction < 20  $\mu\text{m}$ ) of ODP Sites 1085 (in light grey, from Krammer et al., *subm.*), 1092 (with black line), 588 (S-Pacific, Ennyu et al., 2002), and 608 (N-Atlantic, Ennyu et al., 2002).

The  $\delta^{13}\text{C}$  values of the fine-fraction records from Sites 1092 and 1085 do not show such a distinct shift like the oxygen isotope data (see Fig. 4.8). This suggests that the  $\delta^{13}\text{C}$  of dissolved inorganic carbon (DIC) in surface waters in which coccolithophores calcified was relatively uniform through the Middle to Late Miocene in the Southern Atlantic. This coincides with data from Ennyu et al. (2002), who investigated fine-fraction stable isotopes in the Atlantic and the Pacific. In general, the  $\delta^{13}\text{C}$  values of Site 1092 are higher, showing less variation compared to Site 1085. Especially in the interval between 10.7 and 9.0 Ma, the  $\delta^{13}\text{C}$

record of 1085 exhibits the most depleted values, showing greater variations of  $\sim 1.5\text{‰}$ . The differences in  $\delta^{13}\text{C}$  between both sites increase up to  $2.5\text{‰}$  during this interval. One possible explanation for this stronger gradient is the initiation of the upwelling off Namibia at about 10 Ma (Krammer et al., 2005 in press) that influenced Site 1085. After 8.5 Ma, the  $\delta^{13}\text{C}$  data of both sites exhibit similar values again.

#### 4.5 Conclusion

We compared calcareous nanoplankton data with fine-fraction stable isotopes from the polyspecific nannofossil carbonate in the fraction  $< 20\ \mu\text{m}$  of ODP Site 1092 during the Middle to Late Miocene interval. The following conclusions and perspectives can be drawn from the present study:

- Analyses of calcareous nanoplankton give useful information about water masses and thus paleoceanographic developments in this region. The increase of *C. pelagicus* in the younger part of the investigated interval probably indicates a rise in productivity associated with changes in nutrient availability. Higher numbers of *R. haqii* and *R. minuta* between 8.8 and 8.6 Ma may also indicate increased productivity.
- The fine-fraction isotopic record of ODP Site 1092 shows similarities with the  $\%$ -contribution of coccolith carbonate which was produced by both forms of *R. pseudoumbilicus* ('large' and 'medium'). However, a comparison of fine-fraction stable isotopes with those of co-existing surface-dwelling foraminifers approved the assumption that fine-fraction isotopes represent conditions of the shallow mixed-layer. Thus, the isotopic record is not triggered by coccolithophorid 'vital effects'. The similar values in  $\delta^{18}\text{O}$  of both foraminifers and coccoliths show that paleoseasonality played a subordinate role at this location in the sub-Antarctic South Atlantic or, that both organism groups calcified in the same season.
- Comparing our isotopic signals of ODP Site 1092 with fine-fraction data of Sites 1085, 588 and 608 (Krammer et al., subm.; Ennyu et al., 2002), the  $\delta^{18}\text{O}$  record of Site 1092 shows a distinct offset towards heavier values due to difference in temperature between these locations. The difference in  $\delta^{18}\text{O}$  exhibits a slightly increasing trend during the entire interval probably associated with the expansion and establishment of the east Antarctic ice sheets and related cooling. The carbon isotopic records of both sites show more similar values suggesting that  $\delta^{13}\text{C}$  of dissolved inorganic carbon in

surface waters reflects the global  $\delta^{13}\text{C}$  trend during the Middle to Late Miocene in the investigated region of the sub-Antarctic South Atlantic.

### **Acknowledgements**

We thank H. Heilmann and B. Kokisch for laboratory assistance. We are indebted to M. Segl and her team for carefully supervising the stable isotope analyses. Discussions with M.-M. Kastanja, B. Beckmann, H. Paulsen, and T. Westerhold greatly increased the quality of the initial manuscript. This research used samples provided by the Ocean Drilling Program (ODP). Funding for this research was provided by Deutsche Forschungsgemeinschaft (DFG) (Research Center for Ocean Margins).

## **Chapter 5**

### **Conclusion and Perspectives**



## 5. Conclusion and Perspectives

In this thesis a data collection of calcareous nannoplankton and stable isotopic measurements in fine-fraction carbonate have been applied for reconstructing and understanding paleoenvironmental changes in Miocene sediments of the eastern South Atlantic. The geochemical reorganization in the world oceans across the Middle to Late Miocene transition and its impact on marine primary producers is documented in the obtained data.

This study showed that calcareous nannofossils were the major component in sediments of the eastern South Atlantic. Major oceanographic signals are preserved in the nannofossil sediment assemblages, and therefore reflect changes in surface-ocean circulation. It has been shown that some coccolithophorid species, such as *Reticulofenestra haqii* and *Reticulofenestra minuta*, reacted on the initiation of upwelling off Namibia at about 10 Ma. Nannoplankton data from different regions and latitudes (ODP Site 1085 off Namibia and ODP Site 1092 at Meteor Rise) allowed a detailed comparison of the different calcareous nannoplankton assemblages, the ecological implications and their contribution to the bulk carbonate content. A correlation between productivity and carbonate production by specific calcareous nannofossils, such as *Coccolithus pelagicus*, *Reticulofenestra minuta*, and *Reticulofenestra haqii*, seems reasonable.

Furthermore, we have measured polyspecific nannofossil carbonate stable isotopes of different size fractions at both sites to investigate the potential influence of changing nannofossil species composition on the isotopic record. At Site 1085 it has been shown that interspecific differences in isotopic fractionation of different nannoplankton species probably yielded to distinct offsets in the isotopic record. Additionally, we have shown the potential of nannofossil stable isotopes as indicators of conditions in the shallow mixed layer by comparing these records with those of coexisting planktic foraminifers. The results of this study have suggested that nannofossil carbonate isotopes at Site 1085 off SW-Africa reflect surface-water conditions of the late winter-early spring period when relatively cool, nutrient-rich subsurface water mass is entrained into surface-waters by vertical mixing. In contrast, foraminiferal stable isotopes reflect the post-deep-mixing, relatively warmer (late spring to fall) stratified surface waters. Therefore, it seems likely, that the isotopic offset between foraminiferal and nannofossil carbonate can be explained by the difference in the season of calcification. A comparison of foraminiferal and nannofossil oxygen isotopes allowed a reconstruction of the strength of paleoseasonality in the SE-Atlantic.

At Site 1092, located on the Meteor Rise at 29°S latitude, the difference between coccolithophorid and foraminiferal isotopic records is smaller, compared to Site 1085. It seems possible, that paleoseasonality was not the dominating factor in this study area.

A comparison of the isotopic fine-fraction signals of ODP Site 1085 and 1092 with other stable isotope records has shown distinct offsets in  $\delta^{18}\text{O}$  values, due to the difference in the temperature of the shallow mixed layer in which coccolithophores calcified. In contrast, the  $\delta^{13}\text{C}$  values of all sites show more similarities, suggesting that  $\delta^{13}\text{C}$  of dissolved inorganic carbon in surface waters reflects the global  $\delta^{13}\text{C}$  trend during the Middle to Late Miocene.

Since the role of isotopic ‘vital effects’ is not completely resolved yet, the need to extract single nanofossil species from sediments for isotopic measurements is still one big challenge that further investigations have to meet. Although new decanting and microfiltering techniques have achieved first auspicious results, future studies should focus on the development of less time-consuming, standardized techniques to extract single coccolithophorid species from sediments to establish correction factors for fossil coccolith stable isotopes. These methods would offer the possibility of using the organic and inorganic carbon phase of coccolithophores to calibrate temperature proxies, based on alkenone undersaturation ratios and species-specific  $\delta^{18}\text{O}$  of coccolith calcite.

Future studies should focus on one hand on major stable isotope excursions, e.g. the ‘Paleogene-Eocene Thermal Maximum’ (PETM) or the ‘Monterey Carbon Isotope Excursion’ (MCIE), and on the other hand on events marked by changing biological productivity, such as the ‘Biogenic Bloom’ in the Late Miocene to Early Pliocene. Investigations of nannoplankton assemblages and their stable isotopic composition could give useful information about the micropaleontological, environmental, and geochemical changes in surface waters during these time intervals.

## **Chapter 6**

### **References**



## 6. References

- Andruleit, H., 1996. A filtration technique for quantitative studies of coccoliths. *Micropaleontology* 42, 403-406.
- Bains, S., Corfield, R., Norris, R.D., 1999. Mechanisms of climate warming at the end of the Paleocene. *Science* 285, 724-727.
- Barker, P.F., Burrell, J., 1977. The opening of the Drake Passage. *Marine Geology* 25, 15-34.
- Barnola, J.M., Raynaud, D., Korotkevich, Y.S., Lorius, C., 1987. Vostok ice core provides 160 000-year record of atmospheric CO<sub>2</sub>. *Nature* 329, 408-414.
- Bassiot, F.C., Beaufort, L., Vincent, E., Labeyrie, L., 1997. Changes in the dynamics of western equatorial Atlantic surface currents and biogenic productivity at the "Mid-Pleistocene revolution" (930 ka). In: Shackleton, N.J., Curry, W.B., Richter, C., Bralower, T.J., et al. (Eds.), *Proc. ODP Sci. Res.* 154, 269-284.
- Baumann, K.-H., Freitag, T., 2004. Pleistocene fluctuations in the northern Benguela Current System as revealed by coccolith assemblages. *Mar. Micropaleontol.* 52, 195-215.
- Baumann, K.-H., Cepek, M., Kinkel, H., 1999. Coccolithophores as indicators of ocean water masses, surface-water temperature, and paleoproductivity – examples from the South Atlantic. In: Fischer, G., Wefer, G. (Eds.), *Use of proxies in Paleoceanography: Examples from the South Atlantic*. Springer, Berlin, pp. 117-144.
- Baumann, K.-H., Andruleit, H., Samtleben, S., 2000. Coccolithophores in the Nordic Seas: comparison of living communities with surface sediment assemblages. *Deep-Sea Res., II* 47, 1743-1772.
- Baumann, K.-H., Böckel, B., Frenz, M., 2004. Coccolith contribution to South Atlantic carbonate sedimentation. In: Thierstein, H.R., Young, J.R. (Eds.), *Coccolithophores. From Molecular Processes to Global Impact*. Springer-Verlag Berlin Heidelberg, pp. 367-402.
- Baumgartner, P.O., 1987. Age and genesis of Tethyan Jurassic radiolarites. *Eclogae Geol. Helv.* 80, 831-879.
- Berger, W. H., 1989. Global maps of ocean productivity. In: Berger, H. W., Smetacek, V. S., Wefer, G. (Eds.), *Productivity in the Ocean: Present and Past, Dahlem Conf.* John Wiley, Chichester, pp. 429-455.
- Berger, W.H., Roth, P.H., 1975. Oceanic micropaleontology: progress and prospect. *Rev. Geophys. Space Phys.* 13, 561-585.
- Berger, W.H., Fischer, K., Lai, C., Wu, G., 1987. Ocean productivity and organic carbon flux Part I. Overview and maps of primary productivity and export production. University of California, San Diego, SIO Ref. 87-30, 67pp.

- Berger, W. H., Leckie, R.M., Janecek, T. R., Stax, R., Takayama, T., 1993. Neogene Carbonate sedimentation on Ontong Java Plateau: Highlights and open questions, Proc. Ocean Drill. Program Sci. Results, 130, 711 – 744.
- Berger, W.H., Wefer, G., 1996. Expeditions into the past: Paleoceanographic studies in the South Atlantic. In: Wefer, G., Berger, W.H., Siedler, G., Webb, D.J. (Eds.), The South Atlantic: Present and Past Circulation. Springer-Verlag Berlin Heidelberg, pp. 363-410.
- Berner, R.A., 1994. GEOCARB II: a revised model of atmospheric CO<sub>2</sub> over Phanerozoic time. American Journal of Science 294, 56-91.
- Biekart, J.W, 1989. The distribution of calcareous nannoplankton in Late Quaternary sediments collected by the Snellius II Expedition in some southeast Indonesian basins. Proc. Koning. Ned. Akad. Wet. Ser. B 92, 77–141.
- Billard, C., 1994. Life cycles. In: Green, J.C., Leadbeater, B.S.C. (Eds.), The Haptophyte Algae. Systematics Assoc. Spec. Vol. 51, 167-186.
- Böckel, B., Baumann, K.-H., 2004. Distribution of coccoliths in surface-sediments of the south-eastern South Atlantic Ocean: ecology, preservation and carbonate contribution. Mar. Micropaleontol. 51, 301-320.
- Bolli, H. M., Ryan, W. B. F. et al., 1978. Initial reports of the Deep Sea Drilling Project vol. 40. US Government Printing Office, Washington, DC.
- Bollmann, L., Baumann, K.-H., Thierstein, H.R., 1998. Global dominance of *Gephyrocapsa* coccoliths in the Late Pleistocene: selective dissolution, evolution or global environment change. Paleoceanography 13, 517-529.
- Bown, P.R., 1998. Calcareous nannofossil biostratigraphy. British Micropalaeontological Society Publication Services, Chapman and Hall, London.
- Bown, P.R., Lees, J.A., Young, J.R., 2004. Calcareous nannoplankton evolution and diversity through time. In: Thierstein, H., Young, J.R. (Eds.), Coccolithophores: from molecular processes to global impact. Springer Verlag, pp. .
- Bralower, T.J., Bown, P.R., Siesser, W., 1991. Significance of Upper Triassic nannofossils from the Southern Hemisphere (ODP Leg 122, Wombat Plateau, NW Australia). Mar. Micropaleontol. 17, 119-154.
- Brassell, S.C., Eglinton, G., Marlowe, I.T., Pflaumann, U., Sarnthein, M., 1986. Molecular stratigraphy: A new tool for climatic assessment. Nature 320, 129-133.
- Broecker, W., 1971. A kinetic model for the chemical composition of seawater. Quaternary Res. 1, 188-207.
- Broecker, W.S., Peng, T.H., 1986. Global carbon cycle. Radiocarbon 28, 309-327.
- Cachão, M., Moita, M.T., 1995. Coccolithus pelagicus, a sort of productivity proxy? 6<sup>th</sup>

- International Nannoplankton Conference, Copenhagen, Abstracts, pp. 33-34.
- Censarek, B., Gersonde, R., 2002. Miocene diatom biostratigraphy at ODP Sites 689, 690, 1088, 1092 (Atlantic sector of the Southern Ocean). *Mar. Micropaleontol.* 45, 309-356.
- Clark, D.L., 1982. Origin, nature and world climate effect of Arctic Ocean ice-cover. *Nature* 300, 321-325.
- Clarke, L.J., Jenkyns, H.C., 1999. New oxygen isotope evidence for long-term Cretaceous climatic change in the Southern hemisphere. *Geology* 27, 699-702.
- Cortés, M.Y., 2000. Further evidence for the heterococcolith – holococcolith combination *Calcidiscus leptoporus* – *Crystallolithus rigidus*. *Mar. Micropaleontol.* 39, 35-37.
- Cortés, M.Y., Bollmann, J., Thierstein, H.R., 2001. Coccolithophore ecology at the HOT station ALOHA, Hawaii. *Deep-Sea Res. II*, 48, 1957-1981.
- Cortese, G., Gersonde, R., Hillenbrand, C.-D., Kuhn, G., 2004. Opal sedimentation shifts in the World Ocean over the last 15 Myr. *Earth Planet. Sci. Lett.* 224, 509-527.
- Cros, L., Kleijne, A., Billard, C., Young, J.R., 2000. New examples of holococcolith-heterococcolith combination coccospheres and their implications for coccolithophorid biology. *Mar. Micropaleontol.* 39, 1-34.
- Degens, E.T., 1989. *Perspectives on Biogeochemistry*. Springer, Berlin, Heidelberg, New York, 423pp.
- Deuser, W.G., 1986. Seasonal and interannual variations in the deep-water particle fluxes in the Sargasso Sea and their relation to surface hydrography. *Deep-Sea Res.* 33, 25- 246.
- Deuser, W.G., 1987. Seasonal variations in isotopic composition and deep-water fluxes of the tests of perennially abundant planktonic foraminifera of the Sargasso Sea: Results from sediment-trap collections and their paleoceanographic significance. *J. Foraminifer. Res.* 17, 14-27.
- Deuser, W.G., Ross, E.H., 1989. Seasonality abundant planktonic foraminifera of the Sargasso Sea: Succession, deep-water fluxes, isotopic compositions, and paleoceanographic implications. *J. Foraminifer. Res.* 19, 268-293.
- D'Hondt, S., Arthur, M.A., 1996. Late Cretaceous oceans and the cool tropics paradox. *Science* 271, 1838-1840.
- D'Hondt, S., Donaghay, P., Zachos, J.C., Luttenberg, D., Lindinger, M., 1998. Organic carbon fluxes and ecological recovery from the Cretaceous-Tertiary mass extinction. *Science* 282, 276-279.
- Dickens, G.R., 2001. Carbon addition and removal during the Late Paleocene Thermal Maximum: basic theory with a preliminary treatment of the isotope record at ODP Site 1051, Blake Nose. In: Kroon, D., Norris, R.D., Klaus, A. (Eds.), *Western North Atlantic*

- Paleogene and Cretaceous Paleooceanography. Geological Society of London Spec. Publ. 183, 293-305.
- Diekmann, B., Falkner, M., Kuhn, G., 2003. Environmental history of the south-eastern South Atlantic since the Middle Miocene: evidence from the sedimentological records of ODP Sites 1088 and 1092. *Sedimentology* 50, 511-529.
- Diester-Haass, L., Meyers, P. A., Rothe, P., 1990. Miocene history of the Benguela Current and Antarctic ice volumes: evidence from rhythmic sedimentation and current growth across the Walvis Ridge (DSDP Sites 632 and 532). *Paleoceanography* 5, 685-707.
- Diester-Haass, L., Meyers, P. A., Rothe, P., 1992. The Benguela Current and associated upwelling on the southwest African Margin: a synthesis of the Neogene-Quaternary record at DSDP sites 362 and 532. In: Summerhayes, C. P., Prell, W. L., Emeis, K. C. (Eds.), *Upwelling Systems: Evolution since the Early Miocene*. Geol. Soc. Lond. Spec. Publ. 64, 331-342.
- Diester-Haass, L., Meyers, P. A., Vidal, L., 2002. The late Miocene onset of high productivity in the Benguela Current upwelling system as part of a global pattern. *Mar. Geol.* 180, 87-103.
- Diester-Haass, L., Meyers, P.A., Bickert, T., 2004. Carbonate crash and biogenic bloom in the Late Miocene: Evidence from ODP Sites 1085, 1086, and 1087 in the Cape Basin, southeast Atlantic Ocean. *Paleoceanography*, 19, PA 1007, doi: 10.1029/2003PA000933.
- Di Nocera, S., Scandone, P., 1977. Triassic nannoplankton limestones of deep basin origin in the Central Mediterranean region. *Palaeogeography, Palaeoclimatology, Palaeoecology* 21, 101-111.
- Dudley, W.C., Goodney, D.E., 1979. Oxygen isotope analyses of coccoliths grown in culture. *Deep Sea Res., Part A*, 26, 495-503.
- Dudley, W.C., Duplessy, J.C., Blackwelder, P., Brand, L.E., Guillard, R.R.L., 1980. Coccoliths in Pleistocene-Holocene nannofossil assemblages. *Nature* 285, 222-223.
- Dudley, W.C., Blackwelder, P., Brand, L., Duplessy, J.C., 1986. Stable isotopic composition of coccoliths. *Mar. Micropaleontol.* 10, 1-8.
- Edwardsen, B., Eikrem, W., Green, J.C., Andersen, R.A., Moon-Van der Staay, S.Y., Medlin, L.K., 2000. Phylogenetic reconstructions of the Haptophyta inferred from 18S ribosomal DNA sequences and available morphological data. *Phycologia* 38, 149-155.
- Ennyu, A., Arthur, M.A., Pagani, M., 2002. Fine-fraction carbonate stable isotopes as indicators of seasonal shallow mixed-layer paleohydrography. *Mar. Micropaleontol.* 46, 317-342.

- Evans, H.F., Channell, J.E.T., 2003. Upper Miocene magnetic stratigraphy at ODP Site 1092 (sub-Antarctic South Atlantic): recognition of 'cryptochrons' in C5n.2n. *Geophysical Journal International* 153, 483-496.
- Evans, H.F., Westerhold, T., Channell, J.E.T., 2004. ODP Site 1092: revised composite depth section has implications for Upper Miocene 'cryptochrons'. *Geophys. J. Int.* 156, 195-199.
- Farrell, J. W., Raffi, I., Janecek, T. R., Murray, D. W., Levitan, M., Dadey, K. A., Emeis, K.-C., Lyle, M., Flores, J.-A., Hovan, S., 1995. Late Neogene sedimentation patterns in the eastern equatorial Pacific, *Proc. Ocean Drill. Program Sci. Results*, 138, 717– 756.
- Findlay, C.S., Flores, J.A., 2000. Subtropical Front fluctuations south of Australia (45°09'S, 146°17'E) for the last 130 ka years based on calcareous nannoplankton. *Mar. Micropaleontol.* 40, 403-416.
- Findlay, C.S., Giraudeau, J., 2000. Extant calcareous nannoplankton in the Australian sector of the Southern Ocean (austral summers 1994 and 1995). *Mar. Micropaleontol.* 40, 417-439.
- Findlay, C.S., Giraudeau, J., 2002. Movement of oceanic fronts south of Australia during the last 10 ka: interpretation of calcareous nannoplankton in surface sediments from the Southern Ocean. *Mar. Micropaleontol.* 893, 1-14.
- Flores, J.-A., Gersonde, R., Sierro, F. J., 1999. Pleistocene fluctuations in the Agulhas Current retroflexion based on the calcareous plankton record. *Mar. Micropaleontol.* 37, 1-22.
- Flower, B.P., Kennett, J.P., 1993. Relations between Monterey Formation deposition and middle Miocene global cooling: Naples Beach section, California. *Geology* 21, 877-880.
- Flower, B.P., Kennett, J.P., 1994. The middle Miocene climatic transition: East Antarctic ice sheet development, deep ocean circulation and global carbon cycling. *Palaeogeography, Palaeoclimatology, Palaeoecology* 108, 537-555.
- Flower, B.P., Kennett, J.P., 1995. Middle Miocene deepwater paleoceanography in the southwest Pacific: relations with East Antarctic Ice Sheet development. *Paleoceanography*, 10, 1095-1112.
- Fronval, T., Jansen, E., 1996. Late Neogene paleoclimates and paleoceanography in the Iceland-Norwegian Sea: evidence from the Iceland and Vøring Plateaus, ODP Leg 151 and 104. In: Thiede, J., Myhre, A.M., Firth, J., et al. (Eds.), *Proc. ODP, Sci. Results*, 151, College Station, TX (Ocean Drilling Program), 455-468.
- Gard, G., Crux, J.A., 1991. Preliminary results from Hole 704A: Arctic-Antarctic correlation through nannofossil biochronology. *Proc. ODP Sci. Res.* 114.
- Geisen, M., Billard., C., Broerse, A.T.C., Cros, L., Probert, I., Young, J.R., 2002. Life-cycle associations involving pairs of holococcolithophorid species: Intraspecific variation or cryptic speciation? *European Journal of Phycology* 37, 1-14.
- Gersonde, R., Hodell, D.A., Blum, P., et al., 1999. *Proc. ODP, Init. Rep.* 177. College Station,

TX.

- Gersonde, R., Hodell, D.A., 2002. Southern Ocean Paleoceanography – Insights from Ocean Drilling Program Leg 177. *Palaeogeogr. Palaeoclimat. Palaeoecol.* 182, 145-149.
- Gibbs, S.J., Young, J.R., Bralower, T.J., Sheckleton, N.J., 2005. Nannofossil evolutionary events in the mid-Pliocene: an assessment of the degree of synchrony in the extinctions of *Reticulofenestra pseudoumbilicus* and *Sphenolithus abies*. *Palaeogeogr. Palaeoclimatol. Palaeoecol.*, 217, 155-172.
- Giraudeau, J., 1992. Distribution of recent nannofossil beneath the Benguela system: southwest Africa continental margin. *Mar. Geol.* 108, 219-237.
- Giraudeau, J., Monteiro-Pedro, M.S., Nikodemus, K., 1993. Distribution and malformation of living coccolithophores in the northern Benguela upwelling system off Namibia. *Mar. Micropaleontol.* 22, 93-110.
- Giraudeau, J., Bailey, G.W., 1995. Spatial dynamics of coccolithophore communities during an upwelling event in the Southern Benguela System. *Cont. Shelf Res.*, 15, 1825-1852.
- Giraudeau, J., Rogers, J., 1994. Phytoplankton biomass and sea-surface temperature estimates from sea-bed distribution of nannofossils and planktonic foraminifera in the Benguela upwelling system. *Micropaleontology* 40 (3), 1825-1852.
- Goodney, D.E., Margolis, S.V., Dudley, W.C., Kroopnick, P., Williams, D.F., 1980. Oxygen and carbon isotopes of recent calcareous nannofossils as paleoceanographic indicators. *Mar. Micropaleontol.* 5, 31-42.
- Haidar, A.T., Thierstein, H.R., 2001. Coccolithophore dynamics off Bermuda (N. Atlantic). *Deep-Sea Res. II* 48, 1925-1956.
- Haidar, A.T., Thierstein, H.R., Deuser, W.G., 2000. Calcareous phytoplankton standing stocks, fluxes and accumulation in Holocene sediments off Bermuda (N. Atlantic). *Deep-Sea Res. II* 47, 1907-1938.
- Haq, B.U., 1980. Biogeographic history of Miocene calcareous nanoplankton and paleoceanography of the Atlantic Ocean. *Micropaleontol.* 26 (4), 414-443.
- Haq, B.U., Hardenbol, J., Hardenbol, J., 1987. Chronology of fluctuating sea level since the Triassic, *Science* 235, 1136-1167.
- Hart, M.B., 2003. The search for the origin of the planktic Foraminifera, *J. Geol. Soc.* 160, 341-343.
- Hart, T.J., Currie, R.T., 1960. The Benguela Current. *Discovery Rep.* 31, 123-298.
- Haug, G., Tiedemann, R., 1998. Effect of the formation of the Isthmus of Panama on Atlantic Ocean thermohaline circulation. *Nature* 393 (18), 673-676.
- Hay, B.J., Honjo, S., 1989. Particle sources in the present and Holocene Black Sea. *Oceanography* 2, 26-31.
- Hay, W.W., Brock, J.C., 1992. Temporal variation in intensity of upwelling off southwest

- Africa. In: Summerhayes, C.P., Prell, W.L., Emeis, K.C. (Eds.), *Upwelling Systems: Evolution since the Early Miocene*. Geol. Soc. Lond. Spec. Publ. 64, 463-497.
- Hay, W.W., Sibuet, J.-C. et al., 1984. *Initial Reports of the Deep Sea Drilling Project vol. 75*. US Government Printing Office, Washington, DC.
- Hodell, D.A., Ciesielski, P.F., 1990. Southern Ocean response to the intensification of Northern Hemisphere Glaciation at 2.4 Ma. In: Bleil, U., Thiede, J. (Eds.), *Geological History of the Polar Oceans: Arctic versus Antarctic*. NATO ASI Series, Series C: Mathematical and Physical Series. Kluwer, Dordrecht, pp. 707-728.
- Hodell, D.A., Gersonde, R., Blum, P., 2002. Leg 177 Synthesis: Insights into Southern Ocean Paleooceanography on Tectonic to Millennial Timescales. In: Gersonde, R., Hodell, D.A., Blum, P. (Eds.), *Proc. ODP, Sci. Res., 177*, 1-54.
- Holligan, P.M., Fernández, E., Aiken, J., Balch, W.M., Boyd, P., Burkill, P.H., Finch, M., Groom, S.B., Malin, G., Muller, K., Purdie, D.A., Robinson, C., Trees, C.C., Turner, S.M., van der Waal, P., 1993. A biogeochemical study of the coccolithophore *Emiliana huxleyi* in the North Atlantic. *Global Biogeochem. Cycles* 7, 879-900.
- Honjo, S., 1976. Coccoliths: Production, transportation and sedimentation. *Mar. Micropaleontol.* 1, 65-79.
- Jafar, A.S., 1983. Significance of Late Triassic calcareous nannoplankton from Austria and Southern Germany. *Neues Jahrbuch für Geologie und Paläontologie, Abhandlungen* 166, 218-259.
- Jansen, E., Sjøholm, J., 1991. Reconstruction of glaciation over the past 6 Myr from ice-born deposits in the Norwegian Sea. *Nature* 349, 600-603.
- Jasper, J.P., Hayes, J.M., 1990. A carbon isotope record of CO<sub>2</sub> levels during the late Quaternary. *Nature* 347, 462-464.
- Jordan, R.W., Zhao, M., Eglington, G., Weaver, P.P.E., 1996. Coccolith and alkenone stratigraphy and palaeoceanography at an upwelling site off NW Africa (ODP 658C) during the last 130,000 years. In: Whatley, R., Mognilevsky, A. (Eds.), *Microfossils and Oceanic Environments*. Univ. Wales, Aberystwyth Press, Aberystwyth, 111-130.
- Kastanja, M.M., Diekmann, B., Henrich, R., *subm.* Controls on carbonate versus terrigenous deposition in the incipient Benguela Upwelling system during the Middle to the Late Miocene (ODP Sites 1085 and 1087). Submitted to *Palaeogeogr. Palaeoclimatol. Palaeoecol.*
- Keller, G., Barron, J.A., 1983. Paleooceanographic implications of Miocene deep-sea hiatuses. *Geological Society of America Bulletin* 94, 590-613.
- Kennett, J.P., 1977. Cenozoic Evolution of Antarctic Glaciation, the Circum-Antarctic Ocean, and their Impact on Global Paleooceanography. *Journal of Geophysical Research* 82(27), 3843-3860.
- Kennett, J.P., 1982. *Marine Geology*. Prentice-Hall, Englewood Cliffs, New Jersey.
- Kennett, J.P., Shackleton, N.J., 1976. Oxygen isotopic evidence for the development of the

- psychrosphere 38 Myr ago. *Nature* 260, 513-515.
- Kennett, J.P., Hodell, D.A., 1993. Evidence for relative climate stability of Antarctica during the early Pliocene: A marine perspective. *Geogr. Ann.* 75, 205-220.
- Kennett, J.P., Houtz, R.E., Andrews, P.B., Edwards, A.R., Gostin, V.A., Hajos, M., Hampton, M., Jenkins, D.G., Margolis, S.V., Ovenshine, A.T., Perch-Nielsen, K., 1974. Development of the circum-Antarctic current. *Science* 186, 144-147.
- Kennett, J.P., Houtz, R.E., Andrews, P.B., Edwards, A.R., Gostin, V.A., Hajos, M., Hampton, M., Jenkins, D.G., Margolis, S.V., Ovenshine, A.T., Perch-Nielsen, K., 1975. Cenozoic paleoceanography in the southwest Pacific Ocean, Antarctic glaciation, and the development of the circum-Antarctic current. In: Kennett, J.P., Houtz, R.E. (Eds.), *Init. Rep. DSDP 29*, 1155-1169.
- King, T.A., Ellis, J., Murray, W.G., Shackleton, N.J., Harris, S., 1997. Miocene evolution of carbonate sedimentation at the Ceara Rise: a multivariate data/proxy approach. In: Shackleton, N.J., Curry, W.B., Richter, C., Bralower, T.J. (Eds.), *Proc. ODP, Sci. Res., 154: College Station, TX (Ocean Drilling Program)*, pp. 349-364.
- Kinkel, H., Baumann, K.-H., Cepek, M., 2000. Coccolithophores in the equatorial Atlantic Ocean: response to seasonal and Late Quaternary surface water variability. *Mar. Microplaeontol.* 39, 87-112.
- Knappertsbusch, M., Brummer, G.-J.A., 1995. A sediment trap investigation of sinking coccolithophorids in the North Atlantic. *Deep-Sea Res. I* 42, 1083-1109.
- Krammer, R., Baumann, K.-H., Henrich, R., 2005. Middle to Late Miocene fluctuations in the incipient Benguela Upwelling System revealed by calcareous nannofossil assemblages (ODP Site 1085A). *Palaeogeogr. Palaeoclimat. Palaeoecol.* In press.
- Krammer, R., Baumann, K.-H., Bickert, T., Henrich, R., *subm.* ODP Site 1085 nannofossil assemblages and fine-fraction carbonate stable isotopes as indicators for Middle to Late Miocene Benguela Upwelling initiation. Submitted to *Mar. Micropaleontology*.
- Larsen, H.C., Saunders, A.D., Clift, P.D., Beget, J., Wei, W., Spezzaferri, S., ODP Leg 152 Scientific Party, 1994. Seven million years of glaciation in Greenland. *Science* 264, 952-955.
- Lawver, L.A., Gahagan, L.M., Coffin, M.F., 1992. The Development of Paleoseaways around Antarctica. *The Antarctic Paleoenvironment: A Perspective On Global Change* 56, 7-30.
- Lawver, L.A., Gahagan, L.M., 1998. Opening of Drake Passage and its impact on Cenozoic ocean circulation. In: T.J. Crowley and K.C. Burke (Editors), *Tectonic boundary conditions for climate reconstructions. Oxford Monographs on Geology and Geophysics*, pp. 212-223.
- Lawver, L.A., Gahagan, L.M., 2003. Evolution of Cenozoic seaways in the circum-Antarctic region. *Palaeogeogr. Palaeoclimat. Palaeoecol.* 198, 11-37.
- Levitus, S., Boyer, T.P., 1994. *World Ocean Atlas 1994, Vol. 4: Temperature*. NOAA Atlas NESDIS 4. US Department of Commerce, Washington, DC.
- Levitus, S., Burgett, R., Boyer, T.P., 1994. *World Ocean Atlas 1994, Vol. 3: Salinity*. NOAA

- Atlas NESDIS 3. US Department of Commerce. Washington, DC.
- Lutjeharms, J.R.E., 1985. Location of frontal systems between Africa and Antarctica: some preliminary results. *Deep-Sea Res. Part A* 32, pp. 1499-1509.
- Lyle, M., 2003. Neogene carbonate burial in the Pacific Ocean, *Paleoceanography*, 18(3), 1059, doi:10.1029/2002PA000777.
- Lyle, M., Dadey, K.A., Farrell, J.W., 1995. The late Miocene (11 – 8 MA) eastern Pacific carbonate crash: evidence for reorganisation of deep-water circulation by the closure of the Panama gateway. *Proc. ODP, Sci. Res.* 138, 821-838.
- Lyle, M., Koizumi, I., Delaney, M.L., Barron, J.A., 2000. Sedimentary Record of the California Current System, Middle Miocene to Holocene: A Synthesis of Leg 167 Results. In: Lyle, M., Koizumi, I., Richter, C., Moore, T.C. Jr. (Eds.), *Proc. ODP, Sci. Res.* 167 [Online]. [http://www-odp.tamu.edu/publications/167\\_SR/167sr.htm](http://www-odp.tamu.edu/publications/167_SR/167sr.htm).
- Martin, R.E., 1995. Cyclic and secular variation in microfossil biomineralization—clues to the biogeochemical evolution of Phanerozoic oceans, *Glob. Planet. Change* 11, 1–23.
- McIntyre, A., 1967. Coccoliths as Paleoclimatic indicators of Pleistocene glaciation. *Science* 158, 1314-1317.
- McIntyre, A., Bé, A.W.H., 1967. Modern coccolithophoraceae of the Atlantic Ocean: I. Placoliths and cyrtoliths. *Deep-Sea Res.*, I 14, 561-597.
- McIntyre, A., Bé, A., Roche, M., 1970. Modern Pacific Coccolithophorida: a paleontological thermometer. *Transactions of the New York Academy of Science* II 32/6, 720-731.
- McIntyre, A., Ruddiman, W.R., Jantzen, R., 1972. Southward penetrations of the North Atlantic Polar Front: faunal and floral evidence of large-scale surface water mass movements over the last 225,000 years. *Deep-Sea Res.* 19, 61-77.
- Meyers, P.A., and Leg 75 Scientific Party, 1983. Organic geochemistry of Benguela Upwelling sediments recovered by DSDP/ IPOD Leg 75, in *Coastal Upwelling: Its Sediment Record, Part B*, edited by J. Thiede and E. Suess, pp. 453– 466, Plenum, New York.
- Michaels, A.F., Knap, A.H., 1996. Overview of the U.S. JGOFS Bermuda Atlantic Time-series Study and the Hydrostation S program. *Deep-Sea Res.* II 43, 157-198.
- Miller, K.G., Fairbanks, R.G., Mountain, G.S., 1987. Tertiary oxygen isotope synthesis, sea level history, and continental margin erosion. *Paleoceanography* 2, 1-19.
- Miller, K.G., Wright, J.D., Fairbanks, R.G., 1991. Unlocking the icehouse: Oligocene-miocene oxygen isotope, eustacy, and margin erosion. *Journal of Geophysical Research* 96, 6829-6848.
- Milliman, J.D., 1993. Production and accumulation of calcium carbonate in the ocean: budget of non steady state. *Global Biogeochemical Cycles* 7/4, 927-957.

- Molfino, B., MvIntyre, A., 1990. Precessional forcing of nutricline dynamics in the equatorial Atlantic. *Science* 249, 766-769.
- Negri, A., Villa, G., 2000. Calcareous nannofossil biostratigraphy, biochronology and paleoecology at the Tortonian/Messinian boundary of the Faneromeni section (Crete). *Palaeogeogr. Palaeoclimatol. Palaeoecol.* 156, 195-209.
- Nimer, N.A., Dixon, G.K., Merrett, M.J., 1992. Utilization of inorganic carbon by the coccolithophorid *Emiliania huxleyi* (Lohmann) Kamptner. *New Phytol.* 120, 153-158.
- Nimer, N.A., Merrett, M.J., 1995. calcification rates in relation to carbon dioxide release, photosynthetic carbon fixation and oxygen evolution in *Emiliania huxleyi*. *Bulletin de l'Institut Oceanographique (Monaco) Spec. Issue 14*, 37-42.
- Nimer, N.A., Iglesias-Rodriguez, M.D., Merret, M.J., 1997. Bicarbonate utilization by marine phytoplankton species. *J. Phycol.* 33, 625-631.
- Nishida, S., 1979. Atlas of Pacific nannoplankton. NOM, Spec. Paper 3, 1-23.
- Okada, H., Honjo, S., 1973. The distribution of oceanic coccolithophorids in the Pacific. *Deep-Sea Res.* 20, 355-374.
- Okada, H., McIntyre, A., 1977. Modern coccolithophores of the Pacific and North Atlantic Oceans. *Micropaleontology* 23, 1-55.
- Okada, H., Wells, P., 1997. Late Quaternary nannofossil indicators of climate change in two deep sea cores associated with the Leeuwin Current of western Australia. *Palaeogeogr. Palaeoclimatol. Palaeoecol.* 131, 413-432.
- Ortiz, J.D., Mix, A.C., Rugh, W., Watkins, J.M., Collier, R.W., 1996. Deep-dwelling foraminifera of the northeastern Pacific Ocean reveal environmental control of oxygen and carbon isotopic disequilibria. *Geochim. Cosmochim. Acta* 60, 4509-4523.
- Pagani, M., Arthur, M.A., Freeman, K.H., 2000. Variations in Miocene phytoplankton growth rates in the southwest Atlantic: Evidence for changes in ocean circulation. *Paleoceanography* 15(5), 486-496.
- Paull, C.K., Thierstein, H.R., 1987. Stable isotopic fractionation among particles in Quaternary coccolith-sized deep sea sediments. *Paleoceanography* 2, 423-429.
- Paull, C.K., Thierstein, H.R., 1990. Comparison of fine-fraction with monospecific foraminiferal stable isotopic stratigraphies from pelagic carbonates across the last glacial termination. *Mar. Micropaleontol.* 16, 207-217.
- Paulsen, H., Westerhold, T., Bickert, T., subm. Middle to Late Miocene cooling history of the subantarctic Atlantic (ODP 1092). Submitted to *Geology*.
- Perch-Nielsen, K., 1985. Cenozoic calcareous nannofossils. In: Bolli, H.M., Saunders, J.B., Perch-Nielsen, K. (Eds.), *Plankton Stratigraphy*. Cambridge University Press, Cambridge, pp. 427- 554.

- Peterson, R. G., Stramma, L., 1991. Upper-level circulation in the South Atlantic Ocean. *Prog. Oceanogr.* 26, 1-73.
- Peterson, L. C., Murray, D. W., Ehrmann, W. U., Hempel, P., 1992. Cenozoic carbonate accumulation and compensation depth changes in the Indian Ocean, in *Synthesis of Results From Scientific Drilling in the Indian Ocean*, Geophys. Monogr. Ser, vol. 70, edited by R. A. Duncan et al., pp. 311 –333, AGU, Washington, D. C.
- Petit, J.R., Jouzel, J., Raynaud, D., Barkov, N.I., Barnola, J.-M., Basile, I., Bender, M., Chappellaz, J., Davis, M., Delaygue, G., Delmotte, M., Kotlyakov, V.M., Legrand, M., Lipenkov, V.Y., Lorius, C., Pepin, L., Ritz, C., Saltzman, E., Stievenard, M., 1999. Climate and atmospheric history of the past 420,000 years from the Vostok ice core, Antarctica. *Nature* 399, 429-436.
- Pienaar, R.N., 1994. Ultrastructure and calcification of coccolithophores. In: Winter, A., Siesser, W.G. (Eds.), *Coccolithophores*. Cambridge University Press, Cambridge, pp. 13-38.
- Ravelo, A.C., Fairbanks, R.G., 1992. Oxygen isotopic composition of multiple species of planktic foraminifera: Records of the modern photic zone temperature gradient. *Paleoceanography* 7, 815-831.
- Raven, J.A., 1993. Limits on growth rates. *Nature* 361, 209-210.
- Reid, F.M.H., 1980. Coccolithophorids from the North Pacific central gyre with notes on their vertical and seasonal distribution. *Micropaleontology* 26, 151-176.
- Reid, J. R., 1996. On the circulation of the South Atlantic Ocean. In: Wefer, G., Berger, W. H., Siedler, G. and Webb, D. (Eds.), *The South Atlantic: Present and Past circulation*. Springer, Berlin, pp. 13-49.
- Renaud, S., Klaas, C., 2001. Seasonal variations in the morphology of the coccolithophore *Calcidiscus leptoporus* off Bermuda (N. Atlantic). *J. Plankton Res.* 23, 779-795.
- Ridgwell, A., Zeebe, R.E., 2005. The role of the global carbonate cycle in the regulation and evolution of the Earth system. *Earth Planet. Sci. Lett.* 234, 299-315.
- Riebesell, U., Wolf-Gladrow, D.A., Smetacek, V., 1993. Carbon dioxide limitation of marine phytoplankton growth rates. *Nature* 361, 249-251.
- Rost, B., Riebesell, U., 2004. Coccolithophores and the biological pump: responses to environmental changes. Thierstein, H.R., Young, J.R. (Eds.), *Coccolithophores. From Molecular Processes to Global Impact*. Springer-Verlag Berlin Heidelberg, pp. 99-125.
- Rost, B., Zondervan, I., Riebesell, U., 2002. Light-dependent carbon isotope fractionation in the coccolithophorid *Emiliania huxleyi*. *Limnol. Oceanogr.* 47, 120-128.
- Roth, P.H., 1987. Mesozoic calcareous nannofossil evolution: relation to paleoceanographic events. *Paleoceanography* 6, 601-611.

- Roth, P.H., 1989. Ocean circulation and calcareous nannoplankton evolution during Jurassic and Cretaceous. *Palaeogeogr. Palaeoclimat. Palaeoecol.* 74, 111-126.
- Roth, P.H., 1994. Distribution of coccoliths in oceanic sediments. In: Winter, A., Siesser, W.G. (Eds.), *Coccolithophores*. Cambridge University Press, Cambridge, pp. 199-218.
- Roth, P.H., Mullin, M.M., Berger, W.H., 1975. Coccolith sedimentation by faecal pellets: Laboratory experiment and field observations. *Geol. Soc. Amer. Bull.* 86 (8), 1079-1084.
- Roth, M. J., Droxler, A. W., Kameo, K., 2000. The Caribbean Carbonate Crash at the Middle to Late Miocene Transition: linkage to the establishment of the Modern Global Ocean Conveyor. In: Leckie, R. M., Sigurdsson, H., Acton, G. D., Draper, G. (Eds.), *Proc. ODP, Sci. Res.*, 165: College Station, TX (Ocean Drilling Program), pp. 249-273.
- Samtleben, C., Bickert, T., 1990. Coccoliths in sediment traps from the Norwegian Sea. *Mar. Microplaeontol.* 16, 39-64.
- Samtleben, C., Schäfer, P., Andrulleit, H., Baumann, A., Baumann, K.-H., Kohly, A., Matthiessen, J., Schroeder-Ritzrau, A., 1995. Plankton in the Norwegian-Greenland Sea: From living communities to Sediment Assemblages – an actualistic approach. *Geol. Rundschau* 84, 108-136.
- Sarmiento, J.L., Gruber, N., Brzezinski, M.A., Dunne, J.P. 2004. High-latitude controls of thermocline nutrients and low latitude biological productivity. *Nature* 427, 56-60.
- Shackleton, N.J., Kennett, J.P., 1975. Paleotemperature history of the Cenozoic and the initiation of Antarctic glaciation: Oxygen and carbon isotope analyses in DSDP Sites 277, 279, and 281. Initial Rep. Deep Sea Drill. Project 29, 743-755.
- Shackleton, N.J., Hall, M.A., 1997. The late Miocene stable isotope record, Site 926. In: Shackleton, N.J., Curry, W.B., Richter, C., Bralower, T.J., et al. (Eds.), *Proc. ODP Sci. Res.* 154, 367-373.
- Shackleton, N.J., Hall, M.A., Pate, D., 1995. Pliocene stable isotope stratigraphy of Site 846. In: Pisias, N.G., Mayer, L.A., Janecek, T.R., Palmer-Julson, A., van Andel, T.H. (Eds.), *Proc. ODP Sci. Results* 138, 337-355.
- Shannon, L.V., Pillar, L.C., 1986. The Benguela ecosystem Part III. Plankton. *Oceanography and Marine Annual Review* 24, 65-170.
- Shannon, L.V., Nelson, G., 1996. The Benguela: large scale features and processes and system variability. In: Wefer, G., Berger, W. H., Siedler, G. and Webb, D. (Eds.), *The South Atlantic: Present and Past circulation*. Springer, Berlin, pp. 163-210.
- Siesser, W.G., 1980. Late Miocene origin of the Benguela upwelling system off northern Namibia, *Science* 208, 283–285.
- Sikes, C.S., Fabry, V.J., 1994. Photosynthesis, CaCO<sub>3</sub> Deposition, Coccolithophorids, and the Global Carbon Cycle. In: Tolbert, N.E., Preiss, J. (Eds.), *Regulation of Atmospheric CO<sub>2</sub> and O<sub>2</sub> by Photosynthetic Carbon Metabolism*. Oxford University Press, New York, Oxford.

- Steinberg, D.K., Carlson, C.A., Bates, N.R., Johnson, R.J., Michaels, A.F., Knap, A.H., 2001. Overview of the U.S. JGOFS Bermuda Atlantic Time-series Study (BATS): a decade-scale look at ocean biology and biogeochemistry. *Deep-Sea Res. II* 48, 1405-1447.
- Steinmetz, J.C., 1991. Calcareous nannoplankton biocoenosis: Sediment trap studies in the equatorial Atlantic, central Pacific and Panama Basin. In: Honjo, S. (Ed.), *Ocean Biocoenosis Series No. I*. Woods Hole Oceanogr. Inst. Press, 85 pp.
- Steinmetz, J.C., 1994. Sedimentation of coccolithophores. In: Winter, A., Siesser, W.G. (Eds.), *Coccolithophores*. Cambridge University Press, Cambridge, pp. 179-198.
- Stoll, H.M., 2005. Limited range of interspecific vital effects in coccolith stable isotopic records during the Paleocene-Eocene thermal maximum. *Paleoceanography*, 20, PA 1007, doi: 10.1029/2004PA001046.
- Stoll, H.M., Schrag, D.P., 2000. Coccolith Sr/Ca as a new indicator of coccolithophorid calcification and growth rate. *Geochem. Geophys. Geosys.* 1:1999GC000015.
- Stoll, H., Ziveri, P., 2002. Methods for separation of monospecific coccolith samples from sediments, *Mar. Micropaleontol.* 46, 209-221.
- Stoll, H.M., Ziveri, P., 2004. Coccolithophorid-based geochemical paleoproxies. In: Thierstein, H.R., Young, J.R. (Eds.), *Coccolithophores. From Molecular Processes to Global Impact*. Springer-Verlag Berlin Heidelberg, pp. 529-562.
- Stramma, L., Peterson, R.G., 1989. Geostrophic transport in the Benguela Current region. *J. Phys. Oceanogr.* 19, 1440-1448.
- Thiede, J., Winkler, A., Wolf-Welling, T., Eldholm, O., Myhre, A.M., Baumann, K.-H., Henrich, R., Stein, R., 1998. Late Cenozoic history of the polar North Atlantic: Results from Ocean Drilling. *Quat. Science Reviews*, 17, 185-208.
- Van Zinderen Bakker, E.M., 1984. Palynological evidence of late cenozoic arid conditions along the Namibia Coast from Holes 532 and 530A, Leg 75, Deep Sea Drilling Project. In: Hay, W.W., Sibuet, J.-C. (Eds.), *Init. Repts. DSDP, 75: Washington (U.S. Government Printing Office)*, pp. 763-766.
- Vonhof, H.B., Smit, J., Brinkhuis, H., Montanari, A., Nederbragt, A.J., 2000. Global cooling accelerated by early late Eocene impacts?. *Geology* 28, 687-690.
- Wefer, G., Fischer, G., 1993. Seasonal pattern of vertical particle flux in equatorial and coastal upwelling areas of the eastern Atlantic. *Deep-Sea Res.* 40, 1613-1645.
- Wefer, G., Berger, W.H., Bickert, T., Donner, B., Fischer, G., Kemle-von-Mücke, S., Meinecke, G., Müller, P.J., Mulitza, S., Niebler, H.-S., Pätzold, J., Schmidt, H., Schneider, R. R., Segl, M., 1996. Late Quaternary surface circulation of the south Atlantic: The stable isotope record and implications for heat transport and productivity. In: Wefer, G., Berger, W.H., Siedler, G., Webb, D. (Eds.), *The South Atlantic: Present and Past circulation*. Springer, Berlin, pp. 461-502.
- Wefer, G., Berger, W.H., Richter, C., Shipboard Party, 1998. Proceedings of the Ocean Drilling Program Initial Reports 175, <http://odsun3.tamu.edu/publications/prelim/175->

- prelim/.
- Wells, P., Okada, H., 1997. Response of nannoplankton to major changes in sea-surface temperature and movements of hydrological fronts over Site DSDP 594 (south Chatham Rise, southeastern New Zealand), during the last 130 kyr. *Mar. Micropaleontol.* 32, 341-363.
- Westbroek, P., Young, J.R., Linschooten, K., 1989. Coccolith production (biomineralization) in the marine alga *Emiliana huxleyi*. *J. Protozool.* 36, 368-373.
- Westbroeck, P., Brown, C.W., van Bleijswijk, J., Brownlee, C., Brummer, G.J., Conte, M., Egge, J., Fernández, E., Jordan, R., Knappertsbusch, M., Stefels, J., Veldhuis, M., van der Waal, P., Young, J.R., 1993. A model system approach to biological climate forcing. The example of *Emiliana huxleyi*. *Global and Planetary Change* 8, 27-46.
- Westerhold, T., 2003. The Middle Miocene carbonate Crash: Relationship to Neogene Changes in Ocean Circulation and Global Climate. Dissertation, University of Bremen. [http://elib.suub.uni-bremen.de/publications/dissertations/E-Diss728\\_CC\\_West.pdf](http://elib.suub.uni-bremen.de/publications/dissertations/E-Diss728_CC_West.pdf).
- Westerhold, T., Bickert, T., Röhl, U., 2005. Middle to late Miocene oxygen isotope stratigraphy of ODP Site 1085 (SE Atlantic): new constraints on Miocene climate variability and sea-level fluctuations. *Palaeogeogr. Palaeoclimatol. Palaeoecol.* 217, 205-222.
- Westerhold, T., Bickert, T., Röhl, U., 2005. Miocene evolution of carbonate sedimentation in the eastern South Atlantic: High-resolution XRF – scanning records of ODP Sites 1085 and 1087. Submitted to *Marine Geology*.
- Winter, A., Martin, K., 1990. Late quaternary history of the Agulhas Current. *Paleoceanography* 5, 479-486.
- Winter, A., Siesser, W., 1994. *Coccolithophores* Cambridge University Press, Cambridge, 242p.
- Winter, A., Reiss, Z., Luz, B., 1979. Distribution of living coccolithophore assemblages in the Gulf of Elat (Aqaba). *Mar. Micropaleontol.* 4, 197-223.
- Winter, A., Jordan, R.W., Roth, P., 1994. Biogeography of living coccolithophores in ocean waters. In: Winter, A., Siesser, W.G. (Eds.), *Coccolithophores*. Cambridge University Press, Cambridge, pp. 161-177.
- Wolf, T.C.W., Thiede, J., 1991. History of terrigenous sedimentation during the past 10 my in the North Atlantic (ODP Legs 104, 105, and DSDP 81). *Marine Geology*, 101, 83-102.
- Wolf-Welling, T.C.W., Cremer, M., O'Connell, S., Winkler, A., Thiede, J., 1996. Cenozoic Arctic Gateway paleoclimate variability: indications from changes in coarse-fraction composition (ODP Leg 151). In: Thiede, J., Myhre, A.M., Firth, J., et al. (Eds.), *Proc. ODP, Sci. Results, 151*, College Station, TX (Ocean Drilling Program), 515-567.
- Wood, R.A., Grotzinger, J.P., Dickson, J.A.D., 2002. Proterozoic modular biomineralized metazoan from the Nama Group, Namibia, *Science* 296, 2383–2386.

- Woodruff, F., Savin, S.M., 1989. Miocene deep water oceanography. *Paleoceanography* 4, 87-140.
- Wright, J.D., Miller, K.G., 1993. Southern Ocean influences on late Eocene to Miocene deepwater circulation. In: Kennett, J.P., Warnke, D.A. (Eds.), *The Antarctic Paleoenvironment: A Perspective on Global Change*. *Antarct. Res. Ser.* 60, 1-25.
- Wright, J.D., Miller, K.G., 1996. Control of the North Atlantic Deep Water. *Paleoceanography* 11, 157-170.
- Wright, J.D., Miller, K.G., Fairbanks, R.G., 1992. Early and Middle Miocene Stable Isotopes: Implications for Deepwater Circulation and Climate. *Paleoceanography* 7(3), 357-389.
- Young, J., 1994. Function of coccoliths. In: Winter, A., Siesser, W.G. (Eds.), *Coccolithophores*. Cambridge University Press, Cambridge, pp. 63-82.
- Young, J.R., 1998. Chapter 9: Neogene. In: Bown, P.R. (Ed.), *Calcareous Nannofossil Biostratigraphy*. Kluwer Academic Publishers, Dordrecht, pp. 225– 265.
- Young, J.R., Ziveri, P., 2000. Calculation of coccolith volume and its use in calibration of carbonate flux estimates. *Deep-Sea Res., II* 47, 1679-1700.
- Zachos, J.C., Arthur, M.A., Dean, W.E., 1989. Geochemical evidence for suppression of pelagic marine productivity at the Cretaceous/Tertiary boundary. *Nature* 337, 61-64.
- Zachos, J.C., Stott, L.D., Lohmann, K.C., 1994. Evolution of early Cenozoic marine temperatures. *Paleoceanography* 9, 353-387.
- Zachos, J., Pagani, M., Sloan, L., Thomas, E., Billups, K., 2001. Trends, rhythms, and aberrations in global climate 65 Ma to present, *Science*, 292, 686–693.
- Zeebe, R.E., Westbroek, P., 2003. A simple model for the CaCO<sub>3</sub> saturation state of the ocean: the „Strangelove,“ the „Neritan,“ and the „Cretan“ Ocean, *Geochem. Geophys. Geosyst.* 4, [doi:10.1029/2003GC000538](https://doi.org/10.1029/2003GC000538).
- Zhisheng, A., Kutzbach, J.E., Prell, W.L., Porters, S.C., 2001. Evolution of Asian monsoon and the phased uplift of the Himalaya-Tibetan plateau since Late Miocene times. *Nature* 411, 62-66.
- Ziveri, P., Stoll, H., Probert, I., Klaas, C., Geisen, M., Ganssen, G., Young, J., 2003. Stable isotope ‘vital effects’ in coccolith calcite. *Earth Planet. Sci. Lett.* 210, 137-149.



## **Chapter 7**

### **Acknowledgements**



Mein Dank gilt:

... Herrn Prof. Rüdiger Henrich für die Vergabe der Doktorarbeit und deren Betreuung.

... Herrn Prof. Gerhard Bohrmann für die freundliche und prompte Übernahme des Zweitgutachtens.

... Dr. Karl-Heinz Baumann und Dr. Torsten Bickert für ihre wissenschaftliche Unterstützung und Hilfe. Ich kann mich glücklich schätzen, 'rechtzeitig' unter ihre fachlichen Fittiche genommen worden zu sein.

... Renate Henning, Brit Kokisch und Helga Heilmann für die Unterstützung im Labor. Bei Helga habe ich auch auf persönlicher Ebene eine wertvolle Gesprächspartnerin gefunden. Dafür ein ganz großes Dankeschön, Helga!

... meinen Projektkollegen Mia Maria Kastanja, Thomas Westerhold und Harald Paulsen für zahlreiche Diskussionen und Anregungen. Bei Harald Paulsen bedanke ich mich zusätzlich für die Freigabe von noch nicht publizierten Daten, bei Mia für das Erlernen 'unnützer' indonesischer Vokabeln mit enormem Unterhaltungswert.

... meinen derzeitigen Kollegen und Kolleginnen in der Arbeitsgruppe Sedimentologie/ Paläo-Ozeanographie, aber auch allen 'Ehemaligen' im Fachbereich Geowissenschaften, sowohl für das nette Arbeitsklima und die fachliche Unterstützung, als auch für die eine oder andere amüsante Anekdote. Anne, Babette, Bastian, Dorit, Elisa, Fanni, Hanni, Heiko, Helge, Henning, Jörg, Julius, Käthe, Martin 'Kö', Mia, Micha, Ralph, Rebecca, Roberto, Sadat, Stefan, Till und Ulli und einige andere werde ich immer in Erinnerung behalten.

... vor allem Britta Beckmann, Jens Holtvoeth, Christine Holz, Aggeliki 'Aggie' Georgiopolou und Meral Köbrich für unzählige fachliche bis völlig absurde Diskussionen, hunderte gemeinsame Kaffeehaus-Besuche und andere 'interessante' Abende. Ihre Wärme und Offenheit, ihr umwerfender Sinn für Humor und ihre Leidenschaft für Skurriles gepaart mit unerschrockener Ehrlichkeit verblüffen mich immer wieder.

... all meinen Freunden in Deutschland, allen voran Frank Slotke, Hendrik Laue, Tina Klebeck, Ronald Bormann, Christian Heidkamp und - last, but not least - Mark Zander, für seelische Unterstützung, Korrekturlesen und Anregungen - aber auch für nette Ablenkung, das In-den-Armennehmen und das gemeinsame Sich-die-Nächte-um-die-Ohren-schlagen.

... Sascha Lange für die moralische Unterstützung in den letzten 'harten' Monaten. Seine Aufmunterung und Nähe haben mir Kraft und Zuversicht gegeben.

... meinen Freunden zuhause in Österreich dafür, dass sie mich bei jedem Besuch empfangen haben, als wäre ich nie weg gegangen. Jessi, Bertl, Eddl, Muri, Andi, Jürgen, Bitsch, Zitzi, Bernd, Roswitha und Fritz - Daunkschean!

... meiner Familie, allen voran meiner Schwester Maria – der stärksten und leidenschaftlichsten Mitkämpferin – für Unterstützung aus der Ferne ... und manchmal auch aus der Nähe.

Wir stehen immer noch vor der Tür, hinter der die großen Antworten warten. Arthur Miller